UTILIZATION OF DROSOPHILA HSP70 GENE FOR IDENTIFICATION OF GENUINE POL II ELONGATION FACTORS: IDENTIFICATION OF SPT6 AS A FACTOR THAT ENHANCES THE ELONGATION RATE OF POL II IN VIVO

A Dissertation

Presented to the Faculty of the Graduate School

of Cornell University

In Partial Fulfillment of the Requirements for the Degree of

Doctor of Philosophy

by

Mohammad Behfar Mohseni Ardehali

May 2010

UTILIZATION OF DROSOPHILA HSP70 GENE FOR IDENTIFICATION OF GENUINE POL II ELONGATION FACTORS; IDENTIFICATION OF SPT6 AS A FACTOR THAT ENHANCES THE ELONGATION RATE OF POL II IN VIVO

Mohammad Behfar Mohseni Ardehali

Cornell University 2010

Transcription by RNA polymerase II is a multistep process that requires orchestrated function of multiple transcription factors. Several eukaryotic transcription factors have been shown to modulate the elongation rate of RNA polymerase II (Pol II) on naked or chromatin-reconstituted templates *in vitro*. However, none of the tested factors have been shown to directly affect the elongation rate of Pol II *in vivo*. In the work presented here, I will show that complementary molecular and imaging techniques, in combination with utilization of the *Drosophila Hsp70* gene, provides an attractive and suitable model for identification of *bona fide* transcription elongation factors *in vivo*. Through ChIP assays of the first wave of Pol II after heat shock in S2 cells I show that KD of Spt6 reduces the rate of Pol II elongation. Also, fluorescence recovery after photobleaching assays of GFP-Pol II in salivary gland cells show that this Spt6-dependent effect on elongation rate persists during steady-state-induced transcription, reducing the elongation rate from approximately 1100 to 500 bp/min. This drop in the rate of transcription elongation results in accumulation of less *Hsp70* mRNA after heat shock induction. I also demonstrate that Spt6 plays a critical role in

recruitment of the Paf1 complex and Spt5 to the heat shock loci. RNAi knock-down of Spt6 also decreases the global levels of Ser2-P CTD. Furthermore, RNAi depletion of Spt6 reveals its broad requirement during different stages of development.

In summary, this work shows that in combination with complementary molecular and imaging techniques, the *Drosophila Hsp70* gene provides an attractive model system for analyzing the role of suspected transcription factors in transcription elongation.

In a separate project, I also report that a previously uncharacterized SET domain-containing *Drosophila* nuclear protein, CG40351 (dSet1), and not the other putative histone H3K4 methyltransferases, is predominantly responsible for trimethylation of bulk histone H3K4 and histones at the 5'-end of tested transcriptionally-active genes. Polytene staining and live cell imaging results also show widespread association of dSet1 with transcriptionally-active loci, including activated *Hsp70* gene. I also show that dSet1 is required for maximal accumulation of *Hsp70* and *Hsp26* mRNA during the steady state of transcription activation.

BIOGRAPHICAL SKETCH

Behfar was born on a sunny day on July 25th 1976 in Shiraz, Iran. He attended elementary school on 3 different continents and returned back to his hometown to finish his middle and high school education. He attended the college of science at Shiraz University and obtained his B.Sc. degree in general biology in 1999. During his years at Shiraz University, playing basketball kept him away from doing any research. However, he did develop a profound interest in biochemistry and molecular biology, thanks in part to his professor's enthusiasm and style of teaching (Dr. Ali Moradshahi). Upon graduation, he started his master's degree in molecular and cellular biology in 1999 at Razi University, but withdrew after a year to pursue his M.Sc degree at Ball State University. He was admitted into the genetics and development graduate program in the department of molecular biology and genetics at Cornell University in September 2003, where he completed his Ph.D in March of 2010.

To my Parents

تقدیم به پدر و مادرم

ACKNOWLEDGMENTS

The work described here in this dissertation would not have been complete without the help and contribution of numerous people. First and foremost, I would like to thank my Ph.D. adviser, Dr. John Lis for his insights, guidance and support throughout these years. His enthusiasm and passion for science has always been a source of inspiration for me. I am also grateful that during my training he gave me the opportunity and freedom to explore topics and subject that I have been interested in. I consider myself very fortunate to have had him as my adviser.

I would also like to thank Dr.Lee Kraus for his insightful comments and suggestions during our joint group and committee meetings. I am also grateful to Dr. Sylvia Lee for giving me the opportunity to rotate in her lab and her helpful suggestions during my committee meetings. I would also like to extend my gratitude towards Dr. Karen Adelman, a former postdoctoral associate in John's lab. Karen was my mentor and guided me though my rotation project and helped me start my graduate research once I joined the Lis lab.

Many thanks to current and past members of the Lis lab for their help with experiments as well as stimulating conversations, I have learned immensely from all of them. Insightful discussions with these lab members throughout the years have made me more prepared for carrying out research. I am also thankful to the members of the Kraus lab for helpful suggestions and discussions during our joint group meetings.

I would also like to thank Dr. Teresa Gunn for allowing me to rotate in her lab during my first year. My special thanks also go to Drs. Nancy and Mohammad Behforouz for providing me the opportunity to continue my education at Ball State University.

TABLE OF CONTENTS

LIST OF FIGURES

LIST OF TABLES

LIST OF ABBREVIATIONS

Ash1- Absent, small, or homeoticdiscs 1

Ash2- Absent, small, or homeoticdiscs 2

CCC-Chromosome conformation capture

CDK-Cyclin dependent kinase

ChIP-Chromatin Immunoprecipitation

CTD- C-terminal domain of Rpb1 subunit of Pol II

dsRNA- double stranded RNA

FACT-facilitates chromatin transcription

FRAP-fluorescence recovery after Photobleaching

GFP-green fluorescent protein

GTF- general transcription factors

HS-Heat shock

HSF-Heat shock factor

IP-Immunoprecipitation

KD-knock-down

MPM- multiphoton microscopy

ORF-Open reading frame

PARP- Poly (ADP-ribose) polymerase

PIC-Preinitiation complex

Pol II- RNA polymerase II

P-TEFb- Positive transcription elongation factor b

RNAi- RNA interference

TBP-TATA binding factor

TSS-transcription start site

CHAPTER 1

INTRODUCTION[1]

Development, growth and formation of a mature multicellular organism from a single cell is contingent on coordinated spatial and temporal expression of specific genes at the right level. This process is primarily controlled at the transcriptional level by regulating production of messenger RNA (mRNA) and non-translated regulatory RNA molecules such as microRNA (miRNA) from the DNA template. The burden of transcription from nuclear DNA templates in eukaryotic organisms is divided between 3 distinct complexes: RNA polymerase I, II and III. While RNA polymerase I (Pol I) is responsible for generation of more than 75% of cellular RNA, the transcriptional repertoire of Pol I is predominantly limited to generation of the three largest ribosomal RNA (rRNA) molecules (Werner et al, 2009). RNA polymerase III (Pol III) is also primarily responsible for transcription of transfer RNA (tRNA), the smaller ribosomal RNA subunit, U6 small nuclear RNA (RNA) and a subset of other structural RNA molecules (Dieci et al, 2007). Overall, these Pol III transcripts comprise about 15% of the total cellular RNA (Werner et al, 2009). The third class of RNA transcription machinery, RNA polymerase II (Pol II), is responsible for transcription of mRNA and the majority of miRNA molecules. While less than 10% of the total cellular RNA is transcribed by RNA polymerase II, the Pol II transcriptome is the most diverse and highly regulated of all classes of RNA polymerases. All the protein coding genes with their vastly diverse expression patterns and functions are transcribed by Pol II and

[1] Parts of this chapter have been published in Fuda *et al.*, 2009 and Ardehali & Lis, 2009

their expression is subject to a sophisticated regulation mechanism that involves many different transcription factors. In fact, it has been predicted that about 4.5% of genes in *Drosophila* encode factors that are implicated in the process of transcription (Tupler et al, 2001), underlining the significance and complexity of this process. The focus of this thesis is regulation of transcription by RNA polymerase II. Therefore, what follows is an introduction to different stages of Pol II transcription as well as transcription factors that facilitate this process.

The RNA polymerase II is a massive complex (larger than 500 KDa) comprised of 12 subunits (Bushnell & Kornberg, 2003). The largest subunit, Rpb1, contains an unstructured C terminal domain (CTD) comprised of a canonical YSPTSPS heptapeptide repeat. The number of repeats varies from 17 to 52 in different eukaryotic species. There are 45 repeats in *Drosophila.* However, only a few of them have the conserved canonical sequence (Chapman et al, 2008, Corden, 1990). The Serine (Ser) residues at position 2 and 5 of this heptapeptide repeat are subject to phosphorylation by different protein kinase complexes during different stages of transcription. The details of the stages at which these residues are phosphorylated is described in the upcoming sections.

1.1 Different stages of transcription by RNA polymerase II

The transcription cycle by Pol II could be dissected into 8 distinct steps: chromatin opening, preinitiation complex (PIC) formation, initiation, promoter escape/clearance, escape from pause, productive elongation, termination and recycling (Fuda et al, 2009). However, in this chapter, I will combine some steps and describe the transcription cycle in three steps: initiation, productive elongation and termination,

with specific focus on the productive elongation step, which is the subject of this thesis in Chapter 3.

1.1.1 Transcription Initiation

Genes that are regulated by recruitment of Pol II to their promoter often have promoters that are covered with nucleosomes. Nucleosome, the building block of chromatin is a 147 bp DNA sequence wrapped 1.65 turn around the core histone octamer. The histone octamer is comprised of two histone H3:H4 and two H2A:H2B dimers (Campos & Reinberg, 2009). Nucleosomes could block access to the regulatory elements on the DNA sequence, including those required for proper transcription initiation; therefore it is essential to have the nucleosome structure disassembled at the promoter region prior to transcription initiation. The *Saccharomyces cerevisiae* acid phosphatase *PHO5* gene is one of the best studied genes that are regulated at the level of activator recruitment and eviction of 4 positioned nucleosomes over the promoter (Fuda et al, 2009). Nucleosome remodelers and factors that covalently modify histones are also important for efficient removal of nucleosomes. For example, it has been shown that both human and yeast activators interact with the SWI/SNF remodeling complexes (Swi/Snf complex in yeast) and positively stimulate transcription from nucleosome-containing templates (Peterson & Workman, 2000). Moreover, recruitment of histone-modifying enzymes such as the histone acetyltransferase Gcn5 to galactose-inducible genes by the yeast activator Gal4 provides another means through which activators influence and alter the outcome of transcription by modulating the chromatin state at the promoter (Larschan & Winston, 2001).

The 35 bp region upstream and downstream of the transcription initiation site is defined as the core promoter region. This region harbors a number of cis regulatory elements that are recognized by different basal transcription factors. Some more prominent core promoter elements include: TATA box, initiator (Inr), BRE (TFIIB recognition element), DPE (downstream promoter element) and MTE (motif ten element). It must be noted that core promoter regions possess a large degree of structural diversity in terms of element composition and this diversity is a contributing factor to the diversity of transcription regulation mechanisms (Smale & Kadonaga, 2003). On its own, Pol II is unable to directly recognize the target promoter regions and core promoter element recognition and PIC formation is mainly mediated through a subset of transcription factors known as general transcription factors (GTFs) that include: TFIID, TFIIA, TFIIB, TFIIF, TFIIE and TFIIH (Müller et al, 2007). Our understanding of the intricacies and mechanism of transcription initiation is mostly based on extensive *in vitro* studies that were carried out on TATA-containing promoters (Smale & Kadonaga, 2003). Therefore, here I will describe the events that lead to PIC formation and transcription initiation on a TATA-containing promoter. In the first step of the process, the TATA-binding protein (TBP), a subunit of TFIID basal transcription machinery (or SAGA) recognizes and binds to the TATA-box, which lies 25-30 bp upstream of the transcription start site (in yeast the TATA-box is present further upstream, -40 to -120 away from the transcription start site (Struhl, 1989). Upon binding of TBP to the TATA box, two other GTFs, TFIIB and TFIIA are recruited to the core promoter region and through interactions with both DNA (BRE element in case of TFIIB) and TBP (Geiger et al, 1996) they stabilize the TBP/TATA-

box interaction and confer directionality to the to-be assembled PIC (Deng & Roberts, 2007). The stabilized TFIIB-TBP-TFIIA complex provides the platform for recruitment and association of the TFIIF associated Pol II to the core promoter region. Formation of the pre-initiation complex is subsequently completed upon addition of TFIIE and TFIIH (Müller et al, 2007).

Following PIC formation, XPB, the DNA-dependent DNA-helicase subunit of the TFIIH complex facilitates melting of 11-15 bps of DNA around the transcription start site and this structural transition allows entrance of the single-stranded DNA template into the active site of Pol II (Cramer, 2004). Pol II enters promoter escape after transcribing about 20 bps. During this stage, the Pol II molecule breaks contact with the core promoter elements and some basal transcription machinery. In addition to the helicase activity, the TFIIH complex phosphorylates Ser5 residue of Rpb1 CTD during the initiation phase and this is thought to facilitate dissociation of Pol II from promoter-associated transcription factors (Liu et al, 2004).

1.1.2 Transcription elongation

Transcription elongation is generally defined as the stage during which the Pol II molecule and its associated factors traverse through the body of the gene. Until recently, the general consensus among researchers in the field of transcription was that the majority of eukaryotic genes are regulated at the stage of Pol II recruitment to the promoter. However, emerging evidence suggest that in fact most genes are regulated at a step between recruitment and productive elongation that is known as promoter-proximal pausing (Core et al, 2008, Muse et al, 2007). Promoter-proximal paused Pol II molecules are transcriptionally engaged molecules that are paused at the 5'-end of

the transcription unit after transcribing between 20 to 40 bps of DNA downstream of the transcription start site. Upon reception of the appropriate stimulation signal, paused pol II molecules enter productive elongation mode and complete the transcription cycle (Saunders et al, 2006). In addition to providing the means for a more rapid response to transcription induction, promoter proximal pausing is believed to serve as a check point before the Pol II molecule becomes fully committed to productive elongation. Moreover, recent results indicate that promoter-proximal pausing is associated with synchronous expression of developmentally regulated genes in all cells of the embryonic tissue (Boettiger & Levine, 2009).

Phosphorylation of Ser2 is an important step in transition of Pol II into productive elongation. Release of the Pol II molecule from the pause site is concurrent with phosphorylation of Ser2 residue of Rpb1 CTD by the P-TEFb kinase complex (Saunders et al, 2006). In addition to facilitating maturation of Pol II molecules into productive elongation, Phosphorylation of the Ser2 residue also increases the affinity of many factors that associate with elongating Pol II including but not limited to: the elongation factor Spt6 (Yoh et al, 2007), the termination factor pcf11 (Sadowski et al, 2003)and the histone H3K36 methyltransferase Set2 (Li et al, 2002).

1.1.2.1 Elongation rate and processivity of Pol II

Elongation rate and processivity (ability to traverse through the entire length of the transcription unit) are two distinct and key features of elongating Pol II molecules (Mason & Struhl, 2005). Dissociation of Pol II anywhere along the body of the gene prior to completion of transcription would result in abortive transcription. This could be extremely unfavorable and costly from the bioenergetics standpoint, especially

during transcription of very large genes such as the 2300 kb human dystrophin gene (Tennyson et al, 1995).In fact, transcription elongation is a highly processive event i*n vivo*, and in vitro results have shown that isolated elongating Pol II complexes can withstand high salt concentrations and remain transcriptionally engaged (Uptain et al, 1997).

In the Past 30 years researchers have carried out experiments using a wide array of biochemical, molecular and imaging techniques to determine the elongation rate of RNA polymerase II (Pol II) *in vivo* (Table 1.1).

Table 1.1 Comparison of Pol II elongation rate estimates derived from different studies (adapted from Ardehali & Lis, 2009).

Gene (length)	Organism/cell line	Elongation rate	Method	Reference
galactose-inducible hybrid gene (8kb)	yeast	2 kb/min	Pol II ChIP	Mason and Struhl. 2005
E74 (60kb)	drosophila	1.1 kb/min	Northern Blot	Thummel et al. 1990
Ubx (78kb)	drosophila	1.4 kb/min	*in situ* Hybridization	Shermoen et al. 1981
Hsp70 (2.4kb)	drosophila	1.2 kb/min	nuclear run on & Live cell imaging	O'Brien and Lis. 1993
murine mammary tumor virus (7.8kb)	rat HTC cells	1.5 kb/min	nuclease protection assay	Ucker and Yamamoto, 1984
engineered HIV reporter (3.8kb)	human U2OS cells	1.9 kb/min	live cell imaging	Boireau et al. 2007
dystrophin (2300kb)	human myogenic cells	2.4 kb/min	RT-PCR	Tennyson et al. 1995
engineered gene cassette (3.3kb)	human U2OS cells	4.3 kb/min	live cell imaging	Darzacq et al. 2207
heterogeneous nuclear RNA	HeLa cells	3-6kb/min	radioisotope pulse labelling	sehgal et al. 1976
Beta-Actin (3 kb)	normal rat kidney cells	1.1kb/min	FISH	emino et al. 1998
10 native genes (~100-580 kb)	human Tet-21 cells	3.8 kb/min	RT-PCR	Singh and Padgett. 2010

To measure the elongation rate of transcription *in vivo*, previous studies have focused on developmentally regulated or stimuli-responsive genes and measured the time that it takes for the "first wave" of Pol II molecules to reach the 3'-end of the transcription unit (O'Brien & Lis, 1993, Shermoen & O'Farrell, 1981, Thummel et al, 1990), or the time required for the "last wave" of Pol II molecules to leave the body of

the gene upon transcription shutdown (Mason & Struhl, 2005). These measurements, which were mostly done in *drosophila* and yeast, have estimated elongation rates to be 1.1 to 2 kb/min. Measurement of Pol II elongation rate in mammals has been associated with a large degree of variation, with estimates anywhere between ~1.3 to 4.3 kb/min (Boireau et al, 2007, Darzacq et al, 2007, Femino et al, 1998, Tennyson et al, 1995, Ucker & Yamamoto, 1984). The highest rate, unlike with other estimates, was obtained by modeling calculations that removed probabilistic pausing to derive a rate for pure 'rapid elongation' (Darzacq et al, 2007), therefore, it was generally believed that the average elongation rate of Pol II in eukaryotic systems was in the range of 1.5-2 kb/min. A recent study has measured the elongation rate of Pol II at a subset of relatively long native human genes (~100-580 kb) to be around 3.8 kb/min with relatively small variation in the genes tested(Singh & Padgett, 2009). This average value is closer to the higher estimates derived from previous studies.

Comparison of Pol II elongation rate in *drosophila* and yeast with that of human cells(higher elongation rate estimates derived from more recent studies (Darzacq et al, 2007, Singh & Padgett, 2009) suggest that the elongation rate is as much as 3 times faster in human cells). The state of chromatin at the transcribed loci may influence the rate at which Pol II traverses through a gene. In other words, the more compact chromatin landscape of a non-transcribed gene might pose a greater barrier to Pol II passage through nucleosomes, leading to an overall slower apparent elongation rate. This provides an explanation for why the rate of transcription at the transcriptionally active genes is higher than previous measurement at mostly inducible genes. Separate biochemical and imaging measurements at the major *Drosophila* heat

shock gene, *Hsp70*, suggested that elongation rates are comparable during the first wave of heat shock-induced transcription, when chromatin is in a more compact state (Petesch & Lis, 2008) and steady-state of transcription at a fully-activated *Hsp70* (O'Brien & Lis, 1993, Yao et al, 2007). However, it should be noted that *Hsp70* even under non-heat shock conditions is known to be still not truly virgin chromatin and is at least modestly transcribed. In addition, a measurement of elongation rate at the inducible human *PKR* gene estimates the elongation rate to be 3.3 kb/min, which is only slightly lower than the calculated 3.8 kb/min average (Singh & Padgett, 2009). Therefore, the rate of elongation may be comparable for both the first induced and the steady-state transcribing Pol II.

This difference in elongation rates between different species might be understood from an evolutionary standpoint. The average length of mRNA-coding genes in yeast and *drosophila* is 1.45 and 3.05 kb respectively (Adams et al, 2000), whereas, due to presence of many lengthy introns, the average human gene is 27 kb long (Venter et al, 2001)(Adams et al, 2000). At the extreme, at a rate of 3.8 kb/min transcription from the longest gene in human, dystrophin (2,300 kb), would still take10 hours. Therefore, it is tempting to speculate that mammals have developed mechanisms that allow Pol II to transcribe their correspondingly larger genes at higher rates.

1.1.2.2 Nucleosomes pose an obstacle to efficient transcription elongation

A major challenge facing the elongating RNA polymerase II molecule is transcription through the arrayed nucleosomes present on the body of the gene. Results from a number of studies have shown that Pol II and GTFs are not sufficient for

transcription through nucleosome-assembled templates *in* vitro (Owen-Hughes & Workman, 1994). These experiments have shown that high salt concentration (250-400 mM KCl), or presence of the transcription elongation factor complex, FACT (facilitates chromatin transcription), could alleviate this repression (Izban & Luse, 1991, Izban & Luse, 1992, Orphanides et al, 1998). Results from *in vivo* experiments in eukaryotic organisms as diverse as yeast and *Drosophila* have revealed that robust transcription results in loss of nucleosomal structure and partial loss of histone occupancy on the body of the genes (Lee et al, 2004, Petesch & Lis, 2008, Schwabish & Struhl, 2004, Zhao et al, 2005). *In vitro* biochemical studies geared toward addressing the changes in nucleosome structure during Pol II passage has revealed that Pol II displaces a H2A/H2B dimer, leading to formation of an intermediate sub-nucleosomal hexamer, which reassembles into an octamer upon passage of Pol II (Kireeva et al, 2002, Kulaeva et al, 2007). In addition, it was shown that this H2A/H2B displacement is facilitated by the FACT complex (Belotserkovskaya et al, 2003). Factors that facilitate passage of Pol II molecule through transcriptional units on chromatin are discussed in the following sections.

1.1.2.3 Transcription elongation factors

Traditionally, the criteria for defining a factor as a transcription elongation factor come from at least one of the following observations: a) detection of that particular factor on the body of transcriptionally-active genes by ChIP (Kim et al, 2004a, Saunders et al, 2003), b) Its stimulation of transcription elongation from *in vitro* templates and (Gerber et al, 2001, Rondon et al, 2003a, Rondon et al, 2004, Wada et al, 1998) c) in the case of yeast transcription factors, sensitivity of the mutant

yeast strains to 6-azauracil (6AU), a drug that depletes the intracellular levels of GTP and UTP (Arndt & Kane, 2003). While all these assays provide, invaluable and informative information, which suggest that a factor may be an elongation factor, none are direct evidence for involvement of a factor in stimulation of transcription elongation rate or processivity *in vivo*.

Many factors including the FACT, DSIF, Paf1 and THO/TREX complexes as well as TFIIS, IWS1 and Spt6 have been shown to be present on the body of transcriptionally active genes during the elongation stage of transcription in different model systems (Kim et al, 2004b, Saunders et al, 2003, Sims et al, 2004). Although many of these elongation factors have been shown to stimulate the catalytic activity of Pol II *in vitro* (Endoh et al, 2004, Gerber et al, 2001, Gerber et al, 2004, Rondon et al, 2003b, Rondon et al, 2004, Wada et al, 1998), surprisingly mutation in none of these factors has resulted in detectable elongation rate defects at an inducible gene *in vivo* (Mason & Struhl, 2005). This lack of observed defect in elongation could be due to redundancy among transcription elongation factor or that these factors have a role only for certain genes or under particular conditions. In some cases the effects may not be detectable with an assay that examines the rate of clearance of the last wave of Pol II following glucose repression. Using the native major *Drosophila* heat shock gene, *Hsp70*. Interestingly, in the above study the authors found CTDK-1, TFIIS and SPT4 to only be required for processivity at a galactose inducible 8kb yeast gene (Mason & Struhl, 2005).

Spt6

Spt6 was identified in a genetic screen for factors that suppress transcription

defects caused by insertion of a transposable Ty element in the promoter region of yeast *HIS4* and *LYS2* genes (Winston et al, 1984) and Later on, the same lab showed that null *spt6* yeast strains are not viable (Clark-Adams & Winston, 1987). In *Drosophila*, available Spt6 mutants are recessive lethal at the embryonic stage (Peter et al, 2002), and in zebra fish, animals encoding a homozygous truncated version of Pandora (Spt6 homolog) suffer from a multitude of developmental defects (Keegan et al, 2002). The *C. elegans* ortholog of Spt6, *emb-5*, is also an essential gene, which was identified in a screen for genes that cause embryonic lethality (Nishiwaki et al, 1993). All this data point to the fact that Spt6 is an essential gene plays a critical role in organisms as diverse as yeast and zebra fish.

The dSpt6 protein is an 1831 amino acid peptide with a mass of 208.5 KDa. It is highly acidic (net charge of -55) and it contains 5 distinguishable domains: A tex homology region resembling a prokaryotic class of proteins involved in transcription, a helix loop helix domain adjacent to the Tex domain, RNA binding S1 domain, Src homology domain 2 (SH2) and a serine, threonine, glycine rich C-terminal domain (Kaplan et al, 2000). The SH2 domain of Spt6 has been shown to interact with the Ser2 phosphorylated CTD of Rpb1 during transcription elongation (Yoh et al, 2007) (Figure 1.1). In general Spt6 is a highly conserved transcription factor; at the amino acid level as it shares a significant level of identity with budding yeast (23%), C. elegans (34%), Zebra fish (50%) and human (50%) orthologs.

A plethora of evidence has demonstrated presence of physical and genetic interaction between Spt6, Pol II and other well-known transcription factors. In yeast,

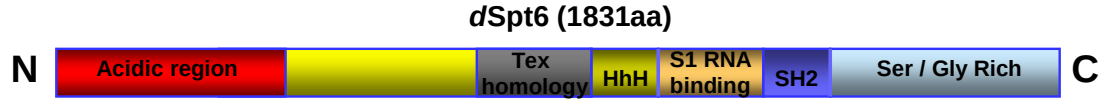

Figure 1.1 Schematic representation of *Drosophila* Spt6 domains. The SH2 domain interacts with Ser2 phosphorylated Pol II

Spt6 mutants enhance the mutant phenotypes of some well characterized transcription factors involved in elongation, including TFIIS, Spt4-Spt5 and components of the Paf1 complex (Costa & Arndt, 2000, Squazzo et al, 2002), which suggests that these factors may be functioning in the same process.

Physical interaction of Spt6 with the pol II, especially the transcriptionally active form has been documented in different organisms. In addition to interacting with SPT4, SPT5, IWS1 and the FACT complex, the yeast preferentially interacts with the hyperphosphorylated form of Pol II (Pol IIo) (Krogan et al, 2002, Lindstrom et al, 2003a). Through its SH2 domian, the human Spt6 also interacts with Ser2 phosphorylated form of CTD, providing further support for involvement of Spt6 in transcription elongation (Yoh et al, 2007). Moreover, Spt6 also shows weak physical interaction with the third subunit of RNA polymerase II, Rpb3 (Endoh et al, 2004). The dSpt6 also shows physical interacts with components of the exosome complex (Andrulis et al, 2002), a complex having a role in processing of rRNA and small nucleolar RNA (snoRNA) as well as degrading pre-mRNA species that are not properly spliced. Through its interaction with IWS1, the human Spt6 also interacts with the nuclear RNA export factor Aly and exosome components (Yoh et al, 2007)

In *Drosophila*, kinetic analysis of Spt6 recruitment by polytene staining shows that this factor is recruited to heat shock loci 87A and 87C two minutes after heat

shock stress (Andrulis et al, 2000, Kaplan et al, 2000). High resolution kinetic analysis of dSpt6 distribution on heat shock genes revealed that prior to HS, Spt6 is not present at the promoter proximal pause site, but it is detected as early as 75 sec after HS on the body of the gene. Its spatial and temporal distribution resembles that of the FACT complex and both factors show greater occupancy in the nucleosome occupied region of *hsp70,* as revealed by ChIP analysis (Saunders et al, 2003). A recent study from our lab also showed that association of Spt6 with the *Hsp70* is dependent on presence of productively elongating Pol II (Ni et al, 2007).

Many studies have also reported interaction with histones and histone chaperone activity for Spt6. Initial experiments carried out in yeast showed that overexpression of a histone H3, truncated at the N-terminal tail, suppresses the *spt6* phenotypes. However, overexpression of a H3 protein truncated in the globular domain fails to suppress the spt6$^-$ phenotypes, suggesting that Spt6 and H3 may be interacting and that this interaction is via the globular domain of H3. GST-Spt6 pull-down assay provided evidence for physical interaction between Spt6 and a proteolytic fragment of histone H3 that was missing the first 23 amino acids (Bortvin & Winston, 1996). Interaction of Spt6 with histone H3 has also been reported in higher eukaryotes. In a pulldown assay, it was shown that the C-terminus of Spt6 physically interacts with histone H3 (Winkler et al, 2000). However, structural studies suggest that the Tex HtH domain has structural similarity with the nucleosome-binding SLIDE domain of ISWI, suggesting that the Tex domain close to the N-terminus may be the domain involved in histone binding and chaperone activity (Johnson et al, 2008). Spt6 has been shown to possess ATP-independent nucleosome assembly activity, as shown

by *in vitro* plasmid supercoiling assays (Bortvin & Winston, 1996). In yeast, a mutation in Spt6 results in the loss of normal chromatin structure and the emergence of cryptic transcription from within the open reading frame (ORF) of the gene (Kaplan et al, 2003). In support of this finding, it was recently shown that Spt6 facilitates reassembly of nucleosomes at inducible genes upon repression of transcription (Adkins & Tyler, 2006).

FACT

The heterodimeric FACT complex (facilitates chromatin transcription) was identified as a factor that facilitates transcription elongation on nucleosome-assembled templates *in vitro* (Orphanides et al, 1998), by facilitating eviction of a H2A/H2B dimer and leaving behind a hexameric histone structure, which the Pol II can elongate through . The FACT complex in higher eukaryotes is comprised of two subunits, Spt16 and SSRP1 (Pob3 and Nhp6a;b in yeast). Components of the yeast FACT complex show physical interaction with Spt4, Spt5, Spt6 and the hyperphosphorylated form of Pol II (Pol IIo). In addition, mutation in components of FACT complex confers sensitivity to 6AU, an indirect mark of involvement in transcription elongation (Belotserkovskaya & Reinberg, 2004). Mutation in yeast FACT components leads to spurious transcription initiation from cryptic sites within the coding region of transcriptionally active genes, indicating that FACT is required for maintenance of chromatin structure on the body of genes (Kaplan et al, 2003). Multiple studies in organisms as diverse as yeast, *Drosophila* and human have shown association of FACT with the body of Pol II transcribed genes. FACT has also been implicated in transcription of Pol I and Pol III transcribed genes in human cells (Birch et al, 2009,

Kim et al, 2004a, Saunders et al, 2003). While all the above studies indicate that FACT is involved in transcription elongation, a number of studies have demonstrated that FACT is also required for proper DNA replication in *Xenopus laevis* (Okuhara et al, 1999). Moreover, Pob3 the small subunit of FACT was initially identified as a factor that physically interacts with DNA polymerase α (Wittmeyer & Formosa, 1997). These studies underscore the diverse function that FACT plays during both RNA transcription and DNA replication.

Paf1

Paf1 is a multi-subunit transcription elongation complex comprised of 5 subunits in yeast and human cells (Jaehning, Kim et al, 2010). In yeast, Paf1 is required for proper methylation of histone H3 K4, K36 and K79 by separate methyltransferases (Shilatifard, 2004). Paf1 has also been implicated in RNA processing and transcription termination in yeast (Mueller et al, 2004). In *Drosophila* Paf1 encodes an essential gene and recent studies from our lab has shown that it is recruited to heat shock loci after HS induction. Paf1 depletion by RNAi leads to defects in induction of *hsp70* gene. Moreover, high resolution ChIP analysis showed that its recruitment pattern is similar to Spt6 and FACT, suggesting that it is involved in the process of elongation. In *Drosophila* any other studied eukaryotic organisms, Paf1 is also required for proper trimethylation of histone H3K4 at the 5'-end region of Hsp70 and a subset of other transcriptionally active genes (Adelman et al, 2006).

1.2 The *Drosophila* heat shock gene *Hsp70* as a model for studying inducible gene induction

The Drosophila Hsp70 gene has been used as an attractive gene system for shedding light on mechanisms and factors that govern transcription from inducible genes. Rapid inducibility, robust induction (more than 100-fold induction for *hsp70*), and synchronous activation of this gene has made the *Drosophila Hsp70* gene an attractive and powerful tool for studying transcription (Lis, 2007).

Studies that date back to late 1970s have shown that the 5'-end of the heat shock genes, including *Hsp70*, are DNase I hypersensitive even prior to gene activation (Keene & Elgin, 1981, Wu, 1980, Wu et al, 1979), which suggested open chromatin structure may be required for rapid response to heat stress. Later on, it was shown that GA-rich sequences upstream of the start site serve as a platform for binding of the GAGA factor (GAF), which in cooperation with the ATP-dependent chromatin remodeling factor, NURF facilitates remodeling of the nucleosomes in this region (Tsukiyama & Wu, 1995). The *Hsp70* gene also contains a transcriptionally engaged, but paused Pol II at the 5'-promoter proximal region (+20 to +45 downstream of the transcription start site) the short nascent transcript has also been shown to be capped at the pause site (Rasmussen & Lis, 1993, Rougvie & Lis, 1988). Upon thermal stress, the heat shock transcription activator, heat shock factor (HSF), trimerizes and binds to a tandem array of heat shock elements (HSE) that reside upstream of the transcription initiation site (Fernandes et al, 1995). Binding of HSF to the HSE is followed by recruitment of the Mediator complex that serves as a coactivator (Park et al, 2001). In addition, recruitment of *Drosophila* P-TEFb kinase,

the only CTD Ser2 kinase in flies, to the 5'-promoter proximal region of *Hsp70* coincides with the rapid release of polymerase from the paused state (Boehm et al, 2003, Lis et al, 2000, Ni et al, 2004). Biochemical experiments (nuclear run-on assay) have estimated the elongation rate of the first wave of Pol II molecules that reach the 3'-end of *Hsp70* at 1.2 kb/min (O'Brien & Lis, 1993). In addition, imaging techniques have also shown that during the steady state of transcription from the *Hsp70* gene, the elongating rate is about 1.5 kb/min (Yao et al, 2007). These elongation rates are consistent with other elongation rate estimates for other genes in *Drosophila* (Shermoen & O'Farrell, 1981, Thummel et al, 1990). During transcription elongation when the Pol II encounters the nucleosomal barrier (starting at ~ +350 downstream of transcription start site) well known transcription elongation factors such as Spt6, FACT and Paf1 are recruited to the elongating Pol II molecule (Adelman et al, 2006, Saunders et al, 2003). RNA processing and surveillance factors also join the elongating Pol II complex to facilitate downstream processing tasks (Andrulis et al, 2002, Ni et al, 2007).

Gene activation results in nucleosome eviction and chromatin decompaction at the transcriptionally active locus and this process is thought to be facilitated by elongating Pol II and the transcription factors that are associated with it(Li et al, 2007). A recent report from our lab has revealed that histone eviction and loss of nucleosome structure over *Hsp70* happens in two distinct steps. As early as 30 seconds after heat shock induction a decrease in nucleosome density could be detected at the 3'-end of *Hsp70* (it takes the first wave of Pol II molecules 120 sec to reach the 3'-end of *Hsp70*). This initial loss is independent of elongating Pol II, but dependent on HSF

and PARP. While a second wave of loss in nucleosome density occurs concurrent with the passage of the elongating Pol II molecules (Petesch & Lis, 2008).

The rapid transition from an almost transcriptionally-silent state with a compact chromatin to a decondensed and transcriptionally-active state, where Pol II reaches the 3'-end of the gene in 120 sec makes the *Hsp70* gene an attractive model system for finding factors that contribute to the process of transcription elongation. In Chapter 2 of this thesis, I will describe how the Hsp70 gene can be used as an attractive system for identification of *bona fide* transcription elongation factors.

1.3 The role of covalent histone modification in transcription

Different residues of core histones within the nucleosome are subject to various covalent modifications that could modulate accessibility to the underlying DNA sequence, and thus alter the transcriptional output at that locus. Different classes of modification such as acetylation, methylation, phosphorylation, ubiquitination and sumoylation have been reported for different residues that are mostly closer to the accessible N-terminal tail of histones. Certain modifications are associated with transcription repression and are considered to be heterochromatic modifications (e.g., histone H3K27 methylation), whereas some are hallmarks of active transcription and are sometimes described as euchromatic modifications (e.g., histone H3K4 methylation and H3 & H4 Acetylation) (Li et al, 2007). From the functional perspective, histone modifications that are associated with active transcription are postulated to have two major roles: a) modify the compactness of chromatin by disrupting the contact between adjacent nucleosomes as well as loosening the contact between the core histone and the DNA, b) providing a platform for chromatin-

interacting factors that interact with modified histones through specialized domains that recognize those modification marks (Kouzarides, 2007). As an example, acetylation of histone H4 at lysine 5 and 12 residues neutralizes the positive charge of the lysine residues and this facilitates formation of a more open chromatin structure at the promoter region that could help to activate of transcription (Kouzarides, 2007). This modification also provides a platform for a factor like Brd4, which binds to these modifications through its double bromodomain and facilitates transcription activation through its association with P-TEFb (Wu & Chiang, 2007).

Histone methylation is another modification that marks different nucleosomes on chromatin. Methylation of histones at the lysine or arginine residues is associated with transcriptionally active or repressed chromatin domains. While this modification does not alter the net charge of the nucleosome residues, it is well established that many chromatin interacting factors associate with these modifications via a subset of domains on factors that "Read" these modifications (Campos & Reinberg, 2009). Methylation marks offer more diversity than acetylation marks as methylated lysine residues could be found in mono, di or trimethylated states and each could be recognized by different factors (Ruthenburg et al, 2007). As a prelude to what will be discussed in chapter 3, in the following section I will focus on histone methylation marks that are associated with active transcription (H3K4, H3K36; H3K79 methylation) with specific focus on H3K4 trimethylation, a modification that is tightly associated with the 5'-end of actively-transcribed genes.

1.3.1 Histone H3K4 trimethylation and its role in transcription elongation

Methylation of Histone H3 at the lysine 4 residue was first reported in 1975 as

a minor methylation site on histone H3 compared to K9 and K27, which were found to comprise the majority of H3 methylation sites in trout testis (Honda et al, 1975). Methylation of histone H3 at the lysine 4 residues takes place on the ζ-amine group and it could be found in mono, di or trimethylated states (Martin & Zhang, 2005). Genomic-scale analyses in the past decade have shed light on different chromatin regions that are associated with these three different states of H3K4 methylation and the correlation between having these marks and the level of gene expression from the associated gene. In yeast H3K4me1 is primarily found at the 3'-end of coding regions whereas H3K4me2 is mostly uniform throughout the gene with a peak observable in the middle of the transcription unit. Histone H3K4me3 shows a less dispersed localization pattern and it predominantly localizes to the 5'-end region of the gene (Ng et al, 2003, Pokholok et al, 2005). In contrast to what has been described in yeast, histone H3K4 di and trimethylation marks in *Drosophila*, mouse and human show a high degree of colocalization and are present together at the 5'-end/promoter region of transcriptionally-active genes (Bernstein et al, 2005, Schübeler et al, 2004b). Histone H3K4me3 has been shown to provide a platform for a number of factors that are implicated in transcription activation. This modification is recognized by the chromodomain subunits of CHD1 ATPase, and TAF3 a component of TFIID basal transcription machinery (Pray-Grant et al, 2005, Sims III et al, 2007, Vermeulen et al, 2007). These interactions and their implication for transcription is described in further detail in Chapter 3.

Histone H3K36me is another histone modification that is associated with actively-transcribed regions of chromatin in eukaryotic cells (Workman, 2006). H3K36me2 is mainly present on the middle of the gene, whereas H3K36me3 is predominantly present closer to the 3'-end of active genes in organisms as diverse as yeast, *Drosophila*, chicken and human (Bannister et al, 2005, Barski et al, 2007, Bell et al, 2007, Pokholok et al, 2005). From the functional perspective, it has been shown that histone H3K36 methylation is critical for suppression of cryptic transcription initiation from within the body of genes. Through association of the EAF3 subunit of the Rpd3S deacetylase complex with H3K36 methylation mark, the deacetylase complex co-transcriptionally removes acetylation marks that were placed on the body of the gene upon transcription activation. Removal of histone acetylation marks induces formation of a more closed chromatin state that prevents access to cryptic intragenic promoters and spurious transcription initiation from within the body of the genes (Carrozza et al, 2005). In *Drosophila* the responsibility for H3K36 methylation is divided between two factors. The dMes-4 is responsible for dimethylation of H3K36, while trimethylation is carried out by dHypb. Both factors are associates with transcriptionally active genes (Bell et al, 2007). It has been shown that Set2 the sole yeast H3K36 methyltransferase preferentially associates with Ser2 phosphorylated Pol II through its Set2 Rpb1 interacting domain (SRI) and as expected, it predominantly associates with the body of transcriptionally-active genes (Kizer et al, 2005, Krogan et al, 2003). In addition Spt6 has been shown to be required for H3K36 methylation by Set2 (Carrozza et al, 2005, Youdell et al, 2008). Therefore, it is likely that emergence

of cryptic intragenic transcription in mutant *spt6* cells in yeast, is partly due to lack of Rpd3S recruitment to the genes.

Another modification that has been shown to be associated with active transcription is H3K79 methylation. Unlike most other methylated histone residues, histone H3K79 is positioned within the globular domain of histone H3. In yeast this modification is carried out by DOT1 an enzyme that does not contain the SET domain. In yeast, similar to H3K36 methylation, H3K79me3 is more prevalent on the body of transcriptionally active genes and while a correlation exists between H3K79 methylation and gene expression levels, the dynamic range is not as wide as the correlation observed for H3K4 or H3K36 methylation (Pokholok et al, 2005). The H3K79me2 mark has also been reported to associate with the body of actively transcribed genes in *Drosophila* and human (Okada et al, 2005, Schübeler et al, 2004a). Interestingly in a separate report and in contrast to previous findings, ChIP-seq experiments on human T cells revealed that H3K79me3 is mainly present at the promoter region of genes and it shows higher correlation with transcriptionally repressed genes, while H3K79me1 shows association with transcription activation (Barski et al, 2007). In *Drosophila*, mutation in the sole H3K79 methyltransferase, Grappa, leads to phenotypes characteristic of both Trithorax group as well as polycomb group proteins (Shanower et al, 2005). Consistent with the contradictory reports associating H3K79 methylation with transcription activation and repression, this latter study suggest that H3K79 methylation may play role in both gene activation and repression .

CHAPTER 2

UTILIZATION OF *DROSOPHILA HSP70* GENE SYSTEM FOR IDENTIFICATION OF GENUINE RNA POLYMERASE II ELONGATION FACTORS; IDENTIFICATION OF SPT6 AS A FACTOR THAT ENHANCES THE ELONGATION RATE OF RNA POLYMERASE II IN VIVO

2.1 Introduction[2]:

In eukaryotic organisms, production of mature mRNA by RNA Polymerase II (Pol II) is an orchestrated, multi-step process facilitated by a plethora of factors. Transcription by Pol II can be categorized into three main stages: initiation, elongation and termination (Svejstrup, 2004). Transcription elongation is increasingly emerging as a stage that contains rate-limiting steps in transcription of many metazoan genes (Guenther et al, 2007, Muse et al, 2007). During transcription elongation, Pol II must contend with nucleosomes, the repeating units of chromatin, which act as a barrier to elongation (Izban & Luse, 1992, Workman, 2006). To facilitate the processivity and elongation rate of Pol II for transcription through nucleosomes, factors broadly known as elongation factors interact with Pol II and track through the body of the gene along with the Pol II complex (Saunders et al, 2006b). Several eukaryotic transcription factors have been shown to modulate the elongation rate of RNA Polymerase II (Pol II) on naked or chromatin-reconstituted templates *in vitro*. However, none of the tested factors have been demonstrated to directly affect the elongation rate of Pol II *in*

[2] Sections of this chapter have been published in Ardehali et al., 2009

vivo. Past attempts to address whether a transcription factor facilitates the normal elongation rate of Pol II *in vivo* have focused on tracking the dissociation kinetics of the "last wave" of Pol II molecules at an engineered galactose-inducible gene after cells were shifted to a glucose rich medium (Mason & Struhl, 2003, Mason & Struhl, 2005). Surprisingly, none of the mutations in any of the elongation factors led to detectable elongation rate defect (Mason & Struhl, 2005, Schwabish & Struhl, 2006, Schwabish & Struhl, 2007).

The *Drosophila Hsp70* heat shock (HS) gene is a well-suited gene model for studying inducible genes that are regulated at the elongation step (Lis, 2007). Prior to induction, the gene is prepared for activation with a Pol II molecule that is paused 20-40 bp downstream of the transcription start site (TSS) (Gilmour & Lis, 1986, Rasmussen & Lis, 1993, Rougvie & Lis, 1988). Thermal induction results in recruitment of the P-TEFb kinase, which releases the Pol II molecule from the pause site to begin its progression into productive elongation (Boehm et al, 2003, Lis et al, 2000, Ni et al, 2004, Ni et al, 2007). Nuclear run on and *in vivo* crosslinking assays revealed that these pioneering Pol II molecules that leave the pause site transcribe at a rate of ~1.2 kb/min (O'Brien & Lis, 1993), consistent with what has been reported for other genes in other systems (Thummel et al, 1990, Ucker & Yamamoto, 1984). In addition, recent multiphoton microscopy (MPM) imaging data has confirmed the previously reported elongation rate at the *Hsp70* gene (Yao et al, 2007).

Past studies have revealed that the FACT and Paf1 elongation complexes along with the elongation factor Spt6 are recruited to the nucleosome-containing regions of *Hsp70* upon heat shock induction (Adelman et al, 2006, Andrulis et al, 2000, Saunders

et al, 2003), raising the possibility that these factors may influence the elongation properties of RNA polymerase II. The unique molecular characteristics of *Hsp70* described above encouraged me to design experiments to address the requirement of different elongation factors, specifically Spt6, during the elongation phase of transcription.

Previous experiments from our lab and other groups have shown that the transcription elongation factor Spt6 is present on the body of genes in various model systems in a transcription-dependent manner (Adelman et al, 2006, Kaplan et al, 2005, Kim et al, 2004b, Saunders et al, 2003). Further evidence for its implication in transcription elongation come from observations that yeast Spt6 predominantly interacts with the hyperphosphorylated form of Pol II (Lindstrom et al, 2003b, Wada et al, 1998), and that human Spt6 physically interacts with Pol II by binding to the Ser-2 phosphorylated form of CTD through its SH2 domain (Yoh et al, 2007). Recent results suggest that Spt6 also provides a link to processing, export and RNA surveillance by physically associating with Iws1 and components of the exosome complex (Andrulis et al, 2002, Kaplan et al, 2005, Yoh et al, 2007). Spt6 also physically interacts with histones, predominantly with histone H3 in both yeast and human and possesses nucleosome assembly activity *in vitro* (Bortvin & Winston, 1996, Winkler et al, 2000). Mutation in Spt6 has also been reported to result in cryptic transcription initiation from within the open reading frame (ORF) (Kaplan et al, 2003). Therefore, based on available data, the in vivo function of Spt6 in transcription could be divided into two categories: first, reassembly of nucleosomes on the gene behind the transcribing Pol II enzyme; second, providing a link to concurrent and down-

stream processing and export events. However, the contribution of this factor in directly facilitating transcription elongation by Pol II *in vivo* remains largely unexplored.

In this chapter I have examined the involvement of these aforementioned elongation factors on transcription elongation from *Hsp70* with a specific focus and emphasis on Spt6. In the result section I have discussed the experiments that were carried out to determine if Spt6 influences different aspects of transcription elongation from *Hsp70* and how and through which mechanisms it may be doing so.

2.2 Results

2.2.1 Spt6 is required for Optimal Induction of Heat Shock Genes *in vivo*

To identify factors that are required for transcription of the induced *Hsp70* gene, we carried out a functional RNAi screen on a subset of known and suspected *Drosophila* transcription factors in S2 cells. These factors were selected based on present literature on transcription in all eukaryotic organisms. In total, we knocked-down 141 potential targets implicated in different aspects of transcription and assessed the level of *Hsp70* mRNA after a 20 min HS induction. Knock-down (KD) of 33 of these factors resulted in 33% or more decrease in accumulation of Hsp70 transcript (Table I). One of the factors that emerged from this screen was Spt6 (Table 1.1). Spt6 KD resulted in a 43% reduction in the level of induced *Hsp70* RNA when Spt6 protein levels were decreased 70% in comparison to that of the control RNAi-treated (bacterial β-galactosidase LacZ RNAi) cells (Figure 2.1A).

In previous studies we have reported recruitment of Spt6 to nucleosome-containing regions of *Hsp70* upon induction (Andrulis et al, 2000, Saunders et al, 2003), as well as its physical association with components of the exosome complex (Andrulis et al, 2002). However, the exact mechanism through which Spt6 participates in transcription from heat shock genes *in vivo* remained unanswered.

To gain a more mechanistic insight into how Spt6 facilitates transcription I examined *Hsp70* transcript accumulation following a 5, 10 and 20 min instantaneous heat shock. Results from Northern Blot analysis revealed that Spt6 KD decreases the induction and accumulation of *Hsp70* mRNA (Figure 2.1B, 2.1C). This defect in mRNA accumulation is more prominent at earlier stages of the thermal stress (3-fold defect at 5 min compared to a 2-fold decrease by 20 min). Moreover, as shown in Figure 2.1D, Spt6 KD also results in almost a 2-fold decrease in the levels of *Hsp83* mRNA 20 min after HS induction. These results suggest that Spt6 is necessary for optimal induction of heat shock genes *in vivo*. It is worth pointing out that I did not observe any cryptic transcription emanating from upstream of the probe hybridization site (~+1700) in Spt6 KD cells. This allowed me to investigate different aspects of transcription elongation at this rapidly-inducible heat shock gene.

2.2.2 Spt6 positively stimulates the rate of productive elongation of the 'first wave' of Pol II molecules after heat shock induction

Although sensitivity to the cellular nucleotide-depleting drug, 6-azauracil in yeast (Hartzog et al, 1998), and in vitro transcription assays on naked templates (Endoh et al, 2004, Yoh et al, 2007) have implicated Spt6 in transcription elongation, no direct analysis has been carried out to address the requirement for this

Table 2.1 RNAi screen result showing factors that stimulate transcription from induced *Hsp70* gene

Targeted Factor (RNAi)	CG number	% Hsp70 mRNA (+/- Error*)	Function
Art4/CARM1	*CG5358*	65 (4)	Histone Modification
Cdk7	*CG3319*	49 (1)	Kinase, Initiation, Elongation
Cdk8	*CG10572*	60 (1)	Coactivator
CKIIa	*CG17520*	54 (4)	Kinase
Cpsf30	*CG3642*	64 (12)	Processing, Termination
CstF50	*CG2261*	56 (10)	Processing, Termination
CycT	*CG6292*	20 (5)	Kinase, Elongation
Elf1	*CG40228*	66 (7)	Elongation
ElonginA	*CG6755*	28 (6)	Elongation
ElonginC	*CG9291*	52 (7)	Elongation
Ell	*CG32217*	65 (16)	Elongation
ERCC3	*CG8019*	61 (3)	Initiation & Elongation
Fcp1	*CG12252*	48 (3)	CTD Phosphatase
GAF	*CG33261*	58 (6)	Core Transcription
Gcn5	*CG4107*	66 (3)	Coactivator
HDAC3	*CG2128*	67 (2)	Histone Modification
HSF	*CG5748*	5 (3)	Activator
Med15	*CG4184*	54 (8)	Coactivator
Med31	*CG1057*	60 (9)	Coactivator
NELF-D	*CG9984*	67 (16)	Elongation
Paf1	*CG2503*	66 (8)	Elongation
PARP	*CG40411*	43 (11)	Chromatin Modification
pk92B	*CG4720*	61 (9)	Upstream Signaling
Pros45	*CG1489*	54 (5)	Proteosome
Rrp6	*CG7292*	59 (4)	Exosome
Spt2	*CG5815*	61 (3)	Elongation, Processing
Spt4	*CG12372*	61 (12)	Elongation
Spt6	*CG12225*	57 (1)	Elongation
TFIIB	*CG5193*	44 (3)	General Transcription, Initiation
TFIIFa	*CG10281*	39 (4)	General Transcription, Initiation
UAP56	*CG7269*	62 (6)	Export
UbcD6	*CG2013*	44 (8)	Histone Modification
Upb8 (not)	*CG4166*	49 (1)	Coactivator

Table shows relative *Hsp70* mRNA levels after a 20 min heat shock (HS) induction.
mRNA levels are shown as % of untreated or mock treated (LacZ) controls.
*Error denotes the range of at least two independent expeirments.

Figure 2.1 Spt6 RNAi decreases the accumulation of *Hsp70* and *Hsp83* mRNA upon induction.
A) Immunoblot on lysates from LacZ (mock treatment) and Spt6 RNAi treated cells with Spt6 and TFIIS (loading control) antibodies. 1 corresponds to 4.0×10^5 cells. Serial dilution of the untreated extract was also loaded to quantify the efficiency of RNAi KD. **B)** Time course analysis of *Hsp70* mRNA accumulation in RNAi treated samples. Cells were heat shocked (HS) for the indicated time. The level of *Hsp70* transcript was analyzed by Northern Blot. Pol III-transcribed U6 snRNA was used as an internal standard from normalization (each set represents three biological replicates). **C)** Graph depicts the normalized values of *Hsp70* transcripts (error bars represent SEM). **D)** Levels of *Hsp83* mRNA accumulation after a 20 min HS induction (error bars denote standard deviation).

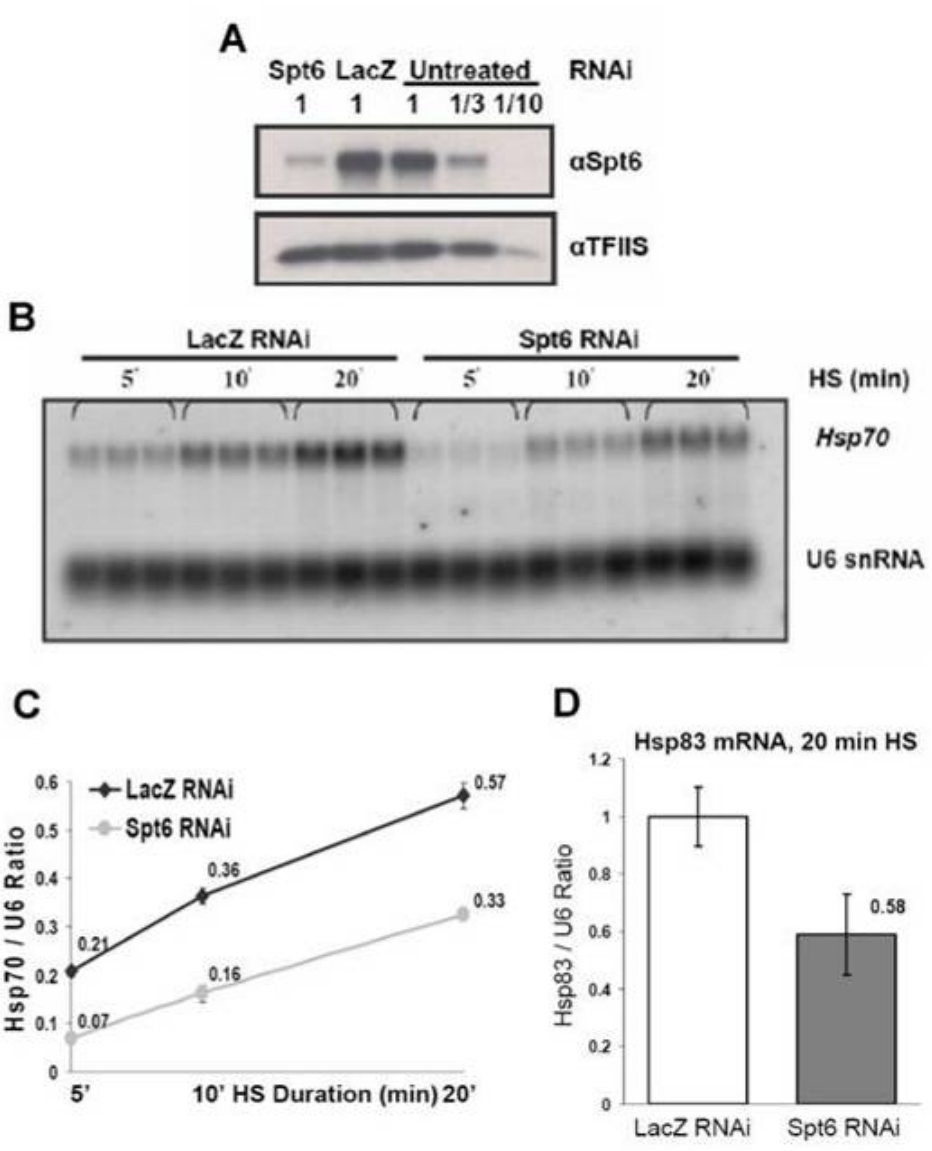
A
Spt6 LacZ Untreated RNAi
1 1 1 1/3 1/10
αSpt6
αTFIIS
B
LacZ RNAi
Spt6 RNAi
5' 10' 20' 5' 10' 20'
HS (min)
Hsp70
U6 snRNA
C
LacZ RNAi
Spt6 RNAi
Hsp70 / U6 Ratio
0.6
0.5
0.4
0.3
0.2
0.1
0
0.21
0.36
0.57
0.07
0.16
0.33
5'
10' HS Duration (min)
20'
D
Hsp83 mRNA, 20 min HS
Hsp83 / U6 Ratio
1.2
1
0.8
0.6
0.4
0.2
0
0.58
LacZ RNAi
Spt6 RNAi

factor in transcription elongation in the context of a native chromatin template *in vivo*. Therefore, I first sought to examine the effect of Spt6 KD on the elongation rate and processivity of Pol II at transcriptionally active heat shock genes. This was carried out in a kinetic analysis by taking "snapshots" of the density and distribution of Pol II, on heat shock genes at different time points after HS induction. First, to check that Spt6 levels were reduced on the body of *Hsp70* in Spt6 RNAi cells, I performed ChIP with antibody against Spt6. Figure 2.2A shows that in addition to the global reduction in the levels of Spt6 (Figure 2.1A), Spt6 KD also decreases association of Spt6 with the body of induced *Hsp70* 18 min after HS induction in Spt6 KD cells. I next analyzed the status of Rpb3 (a subunit of Pol II) after an 18 min HS induction, when steady state transcription from the *Hsp70* gene has been established (Boehm et al, 2003), and did not observe any drop in Spt6 RNAi cells throughout the body of the gene. In fact, I noticed higher levels of Pol II on the body of *Hsp70* with the Spt6 KD samples in comparison to LacZ dsRNA treated cells (Figure 2.2D), a result expected if the transcription elongation rate decreased relative to rate of initiation and entry of Pol II molecules into elongation.

Upon transcription induction, heat shock genes in both yeast and Drosophila undergo rapid nucleosome disassembly (Petesch & Lis, 2008, Zhao et al, 2005), making the chromatin architecture of the gene more permissive for passage of Pol II. Given that Spt6 physically interacts with histones and has histone chaperone activity (Adkins & Tyler, 2006, Bortvin & Winston, 1996, Winkler et al, 2000), I sought to investigate the role of this factor in transcription elongation of the first wave of RNA Polymerase II molecules that have to negotiate with the nucleosomal-barrier during

the early stages of heat shock activation. As shown in Figure 2.2B, Spt6 KD, followed by a short 2 min HS induction, does not negatively affect the density of Rpb3 at the 5'-proximal region of *Hsp70*, a region where Spt6 is not strongly recruited after induction (Andrulis et al, 2000, Saunders et al, 2003). However, I noticed that the density of Pol II molecules gradually decreases as I surveyed the middle (+946) and 3'-end (+2210) of the gene relative to the LacZ KD (Figure 2.2B). This loss of signal suggests that in the context of chromatin *in vivo,* KD of Spt6 reduces the elongation rate of the initial Pol II molecules that enter the productive elongation mode. I also included an intermediate 6 min HS time point in my analysis when the density of Pol II and transcription factors on the body of *Hsp70* are near the peak level (Boehm et al, 2003). At this time point in the Spt6 RNAi cells, the density of Pol II molecules at the 5' and middle region of the gene is comparable to that of the LacZ RNAi sample. However, the fact that Pol II molecules are not transcribing at normal rate is noticeable, as the density of Pol II at the 3'-end (+2210) of the gene was still not restored to levels similar to that of the control cells (Figure 2.2C).

Hsp83 is another heat shock gene that also recruits Spt6 (Andrulis et al, 2000). This gene is transcribed at relatively high levels prior to HS induction, and its expression only increases a few fold upon thermal stress (Xiao & Lis, 1989). I also observed a slower transcription elongation rate at this gene in Spt6-depleted S2 cells. Six min after HS induction, the time at which we expect to detect the induced Pol II molecules at the 3'-end of this gene, the Rpb3 density is about 2-fold less at the +3680 region of the gene in Spt6 RNAi samples compared to LacZ RNAi treated control (Figure 2.2E). Therefore Spt6 not only facilitates elongation when a repressed gene

becomes active (*Hsp70*), but it is also essential for efficient elongation rate of genes that are constitutively active and are slightly upregulated upon induction (*Hsp83*). The kinetics of Pol II elongation at a constitutively active *Hsp83* gene in Spt6 KD cells also suggests that this factor is also critical for elongation during the steady state of transcription. These results indicate that Spt6 is required for efficient transcription elongation at both the *Hsp70* and *Hsp83* genes, which each have distinct transcription regulatory profiles.

2.2.3 Spt6 is required for transcription elongation at normal rates during the steady state of *Hsp70* transcription

After an 18 min HS, the density of Pol II molecules on the body of the *Hsp70* are slightly higher all across the gene in the Spt6 RNAi cells when compared to the LacZ RNAi samples (Figure 2.2D). It is tempting to speculate that slower Pol II elongation rates at this gene lead to an increase in Pol II density on the body of *Hsp70*. However, as a result of saturation of the Pol II signal after prolonged gene inductions, it is not possible to address whether these polymerase molecules are traveling at normal rates during the steady state of HS induction by ChIP assay.

To overcome this technical obstacle and to determine the kinetics of Pol II elongation during the steady state of transcription in absence of Spt6, I took advantage of the recently described multiphoton microscopy (MPM)-based Fluorescence Recovery after Photobleaching (FRAP) technique that was adapted and optimized by Jie Yao, a former graduate student in our Laboratory (Yao et al, 2006, Yao et al, 2007). This technique allows monitoring the recovery rate of fluorescent-tagged transcription factors at the distinctive heat shock loci 87A and 87C of living salivary gland cells. I

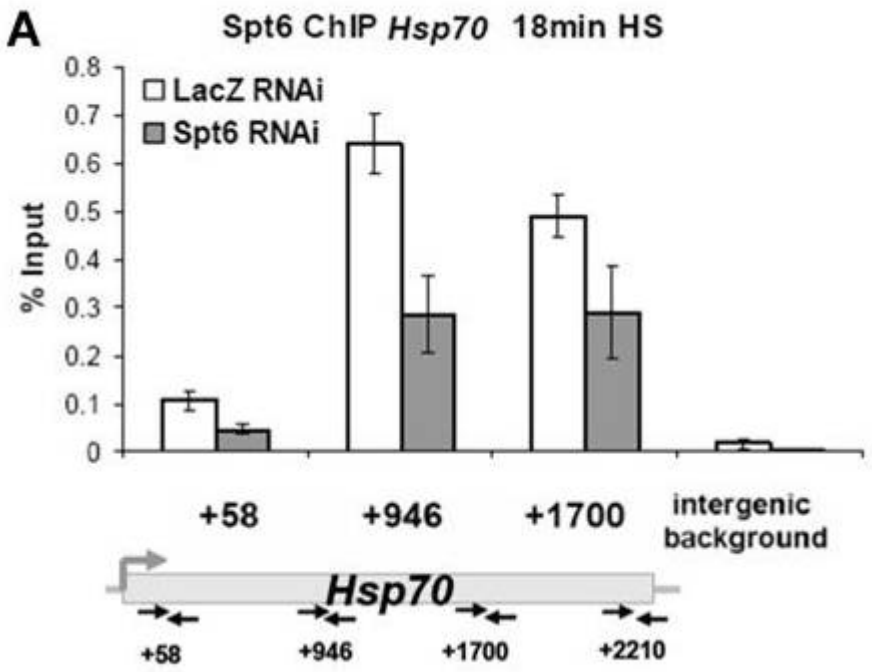

Figure 2.2 Depletion of Spt6 reduces the elongation rate of RNA polymerase II immediately after HS induction.
A) ChIP results showing association of Spt6 with different regions of the *Hsp70* transcript in both Spt6 and LacZ RNAi treated samples. Time course analysis of Pol II (α-Rpb3) density and distribution at *Hsp70* by 2 min **(B)**, 6 min **(C)**; 18 min **(D)** after heat shock induction in Spt6 and LacZ RNAi samples. Numbers below each bar represents the position of real-time PCR primers relative to the Hsp70 transcription start site, as depicted at the bottom of panel A. E) Rpb3 occupancy on the body of *Hsp83* at different time points after heat shock induction. The grey box downstream of the +62 primer denotes the relative position of *Hsp83* intron. Error bars denote SEM of at least three biological replicates. The intergenic background primer pair targets a region 32 Kb downstream of the last Hsp70 gene at the 87C genomic loci.

Figure 2.2 (continued)

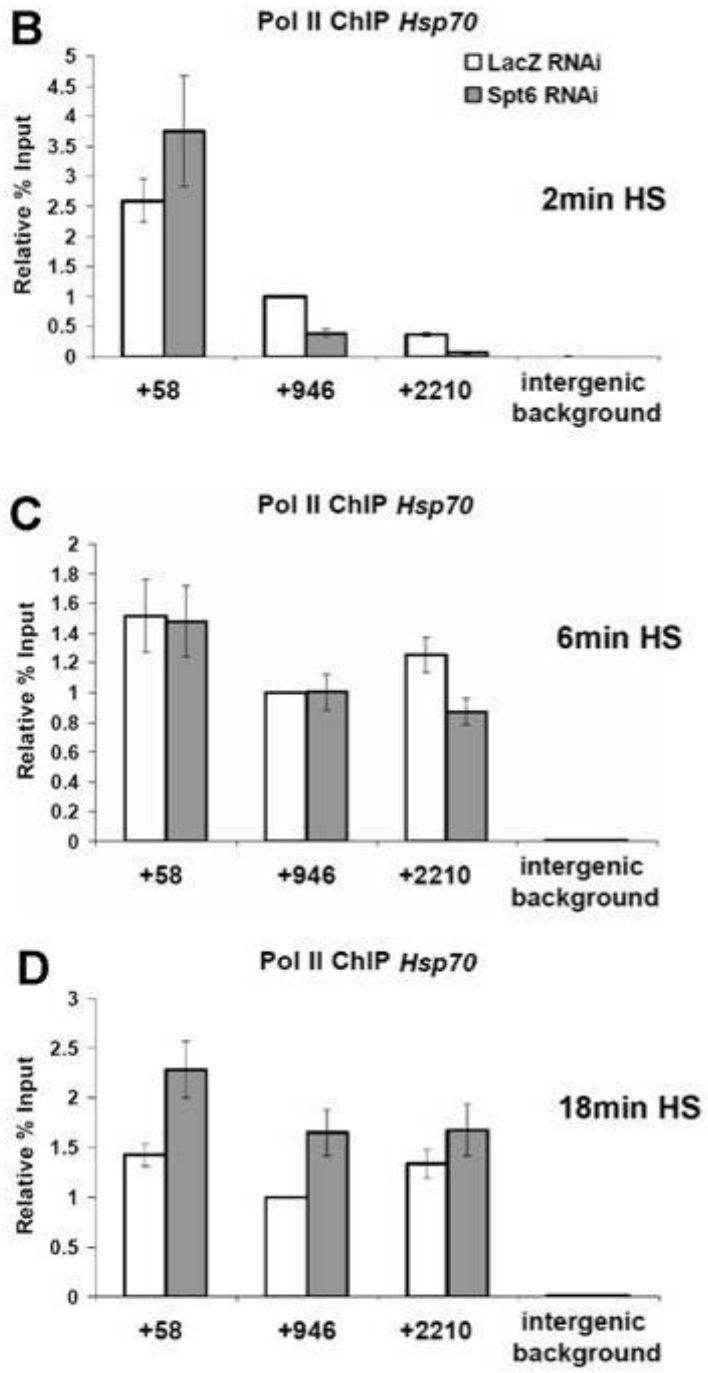

Figure 2.2 (continued)

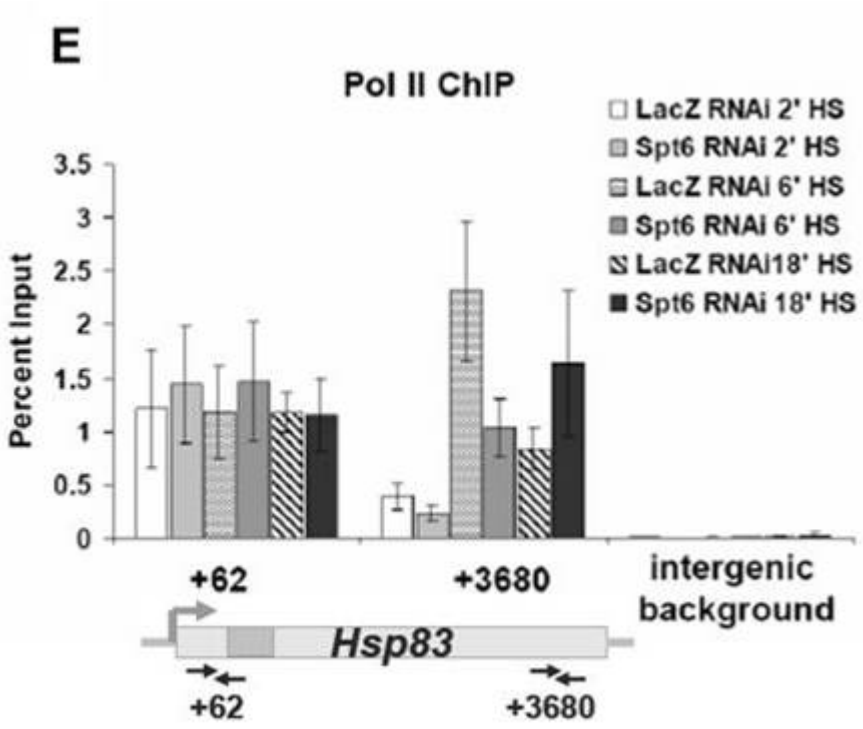

generated a knock-down UAS-Spt6^{RNAi} fly line that transcribes a 670bp Spt6-dsRNA and Jie Yao compared the recovery rate (elongation rate) of EGFP-Rpb3 molecules at the HS loci in the salivary gland of these larvae with that of the wild type animals.

I checked that the Spt6 RNAi construct is effective in the third instar larvae by crossing the UAS-Spt6^{RNAi} line to a line that ubiquitously and constitutively expresses GAL4 under the control of the Actin5C promoter (Figure 2.3A). Moreover, Spt6 KD in the salivary glands of these flies was also confirmed by comparing the fluorescence intensity of transgenically-expressed YFP-Spt6 molecules in control and Spt6^{RNAi} animals (Figure 2.3B).

By 10 min after heat shock induction, high levels of EGFP-Rpb3 molecules localize to the two adjacent 87A and 87C loci, making the two HS puffs easily distinguishable from other genomic loci (Yao et al, 2006) (Figure 2.3C, prebleach). In addition, 10 min after heat shock activation the native *Hsp70* genes are at the steady state level of transcription (Yao et al, 2007). We (The FRAP experiment and analysis of the data was carried out by Jie Yao) photobleached these loci and monitored the recovery of EGFP-Rpb3 fluorescent signal for more than 5 min in both wild type and Spt6^{RNAi} salivary glands (Figure 2.3C). Interestingly, FRAP results revealed that recovery rate of EGFP-Rpb3 in the Spt6^{RNAi} glands is almost twice as slow as wild type glands ($t_{1/2}$ of ~80 sec compared to $t_{1/2}$ of~ 41 sec Figure 2.3D). Given that the EGFP-Rpb3 signal reaches plateau in Spt6 RNAi glands almost ~300 sec after Photobleaching (Figure 2.3D), we estimate the rate of transcription by Pol II at the 2.4 kb *Hsp70* to be about 480 bp/min in the Spt6-depleted glands. This is more than 2-fold slower than the elongation rate in control glands (~1100 bp/min).

Figure 2.3 FRAP analysis of Pol II at 87A; 87C heat shock loci upon full heat shock activation in Spt6 RNAi and control animals.
A) Western Blot analysis showing general KD of Spt6 in the 3rd instar larvae of actin5C-GAL4/ UAS-Spt6^{RNAi} (RNAi +) and TM6/UAS-Spt6^{RNAi} (RNAi -). TFIIS staining served as a loading control. Dilution of the lysates was also loaded to quantify the KD efficiency. **B)** KD of Spt6 in the salivary glands of Spt6^{RNAi} animals was assessed by examining the fluorescent intensity resulting from expression of UAS-YFP-Spt6 insert in YFP-Spt6/+; 6983-GAL4/+ (RNAi -) or YFP-Spt6/+;6983-GAL4/UAS-Spt6^{RNAi} (RNAi +)lines. **C)** Images of EGFP-Rpb3 at heat shock loci after full gene activation in control (upper panel) or RNAi + glands (bottom panel) prior and post photobleaching. Time after the start of photobleaching is shown on the upper corner of each image in seconds. Genotypes are UAS-EGFP-Rpb3/CyO; 6983-GAL4/Ubx (RNAi -) and UAS-EGFP-Rpb3/+; 6983-GAL4/UAS-Spt6^{RNAi} (RNAi+). **D)** Normalized fluorescence intensity plots of the FRAP analysis for the 87A and 87C loci in control (green) and Spt6 RNAi (red) samples. Dotted lines denote the line from which $t_{1/2}$ is derived.

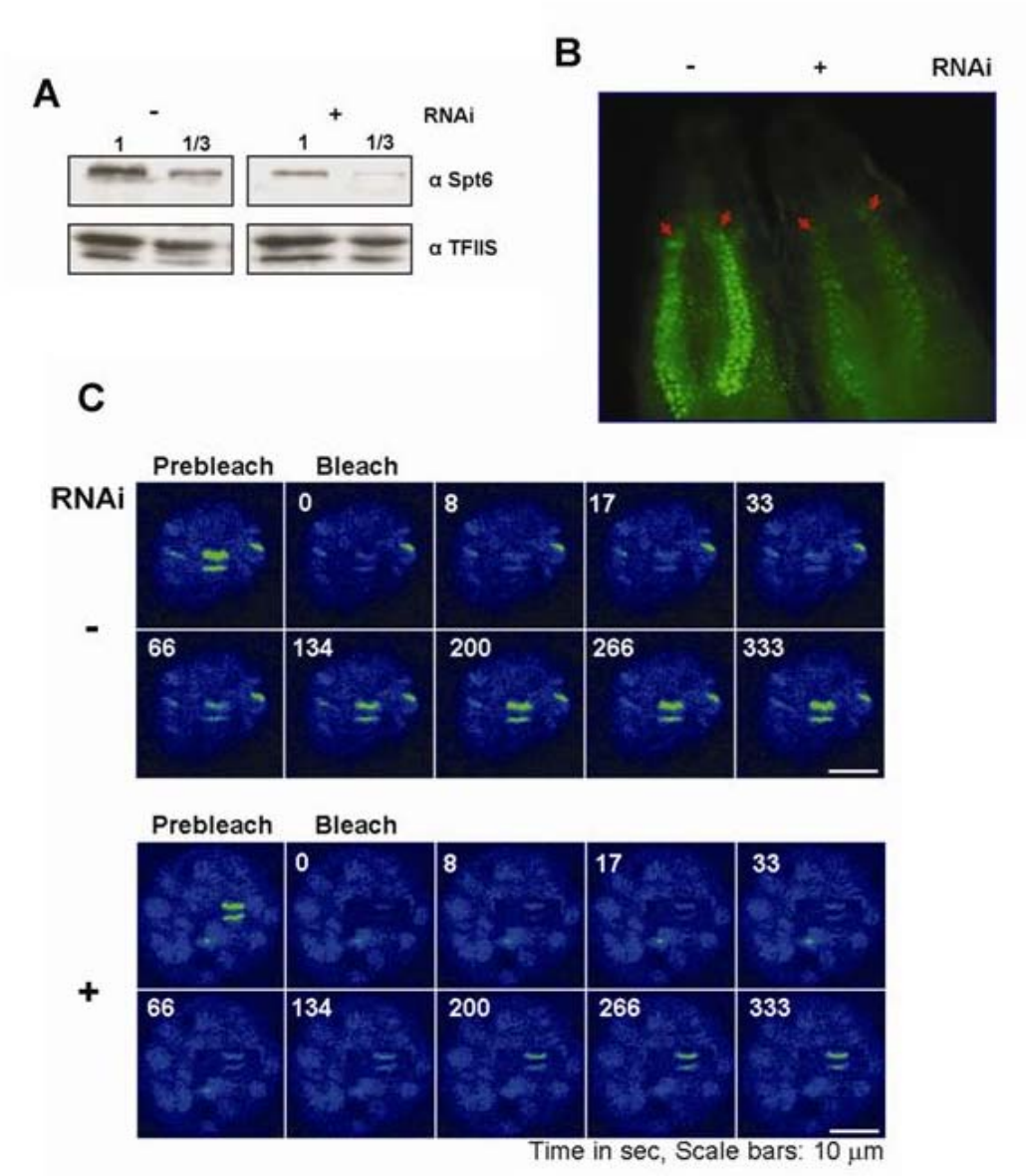
A
-
+
RNAi
1
1/3
1
1/3
α Spt6
α TFIIS
B
-
+
RNAi
C
RNAi
Prebleach
Bleach
0
8
17
33
-
66
134
200
266
333
Prebleach
Bleach
0
8
17
33
+
66
134
200
266
333
Time in sec, Scale bars: 10 μm

Figure 2.3 (continued)

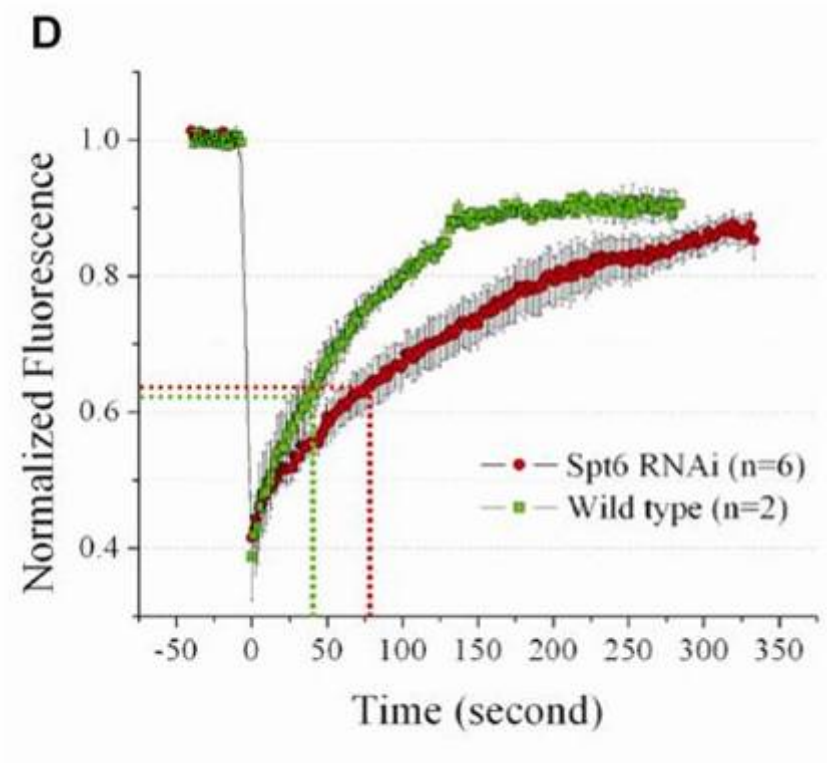

Results from this FRAP experiment led me to draw two major conclusions: First, in addition to playing a critical role in facilitating productive transcription elongation during the initial stage of heat shock induction, Spt6 is also required for transcription elongation at normal rates during the steady state of transcription from *Hsp70* at which time the nucleosome architecture of *Hsp70* is in a more permissive transcriptional state (Petesch & Lis, 2008). Second, the role of Spt6 in stimulating transcription elongation could be demonstrated beyond cultured cells to living animal tissue.

2.2.4 Histone H3-K36 trimethylation does not detectably stimulate Pol II elongation rate

To provide a possible mechanistic explanation for how Spt6 stimulates the elongation rate of transcription, I first checked the density of histone H3 over *Hsp70* in S2 cells. In yeast, mutation in Spt6 results in a decrease in the density of histones on the body of transcriptionally active genes, exposing the cryptic transcription initiation sites within the gene (Kaplan et al, 2003). Interestingly, and in contrast to what has been reported in yeast, I noted that Spt6 RNAi treatments produced either no change or a small increase in the density of histone H3 on the body of the induced *Hsp70* (Figure 2.4A).

Actively transcribed genes show enrichment of histone H3K36 trimethylation, and the extent of this modification correlates with the level of transcription (Li et al, 2007). Previous studies have shown that Spt6 is required for H3-K36 methylation of nucleosomes at actively transcribed genes as well as H3-K36 trimethylation of chromatin in *in vitro* assays (Carrozza et al, 2005, Youdell et al, 2008). I examined the status of H3-K36 trimethylation at *Hsp70* and observed a small decrease in the density

of H3-K36 trimethylation on the body of *Hsp70* during the steady state of HS induction in Spt6 KD cells (Figure 2.4B). To determine if this small drop in trimethylation of H3-K36 is accountable for the transcription elongation defect seen at this gene, I knocked down the *Drosophila* H3-K36 trimethyltransferase, Hypb (dHypb) (Bell et al, 2007), and measured the elongation rate of Pol II early after heat shock induction at *Hsp70*. Knock-down of dHypb results in 60% or more decrease in the cellular level of H3-K36 methylation (Figure 2.4C), as well as ~70% decrease in the H3-K36 trimethylation mark on the body of *Hsp70* (Figure 2.4E). However, we did not observe any decrease in the elongation rate of Pol II molecules at *Hsp70* as detected by ChIP 2min after HS induction (Figure 2.4D), These results suggest that stimulation of elongation rate at

Hsp70 by Spt6 is not mediated through H3-K36 methylation and that trimethylation of H3-K36 by dHypb is not critical for efficient transcription elongation at *Hsp70*.

2.2.5 Spt6 Knock-down leads to accelerated termination at transcriptionally active heat shock genes

Although the density of Pol II throughout the body of the HS genes in the Spt6 RNAi cells is comparable to or even higher than LacZ RNAi cells during the steady state of transcription (Figure 2.2D, 2.2E), we noticed that the density of Pol II molecules sharply drops immediately after the polyadenylation signal (polyA) in the Spt6 RNAi treated cells 18 min after HS activation (Figure 2.5A, 2.5B). This reduction in the density of Pol II downstream of the polyA site during the steady state of HS induction was observed at both *Hsp70* and *Hsp83* genes and is reminiscent of recently described results where Spt6 mutation or depletion, leads to decreased read-through transcription

Figure 2.4 H3-K36 trimethylation does not positively stimulate the elongation rate of Pol II at *Hsp70*.
A) ChIP experiment showing the density of histone H3 throughout the body of *Hsp70* 18min after HS induction in LacZ (white) and Spt6 (gray) RNAi treated cells. N≥3, error bars denote SEM. **B)** H3-K36 trimethylation levels at different regions of *Hsp70* 18min after HS were normalized to histone H3 density at the respective regions in LacZ(white) and Spt6 (gray) RNAi samples. N=3, error bars denote SEM. **C)** Western Blot of lysates from LacZ, Spt6 and dHypb RNAi treated cells were probed for H3-K36 trimethylation mark. TFIIS antibody was used as a loading control. **D)** ChIP experiment showing the first wave of Pol II molecules traversing through *Hsp70* 2min after HS induction in LacZ (white), dHypb (gray) and Spt6 (dark gray) RNAi treated cells. N=2 for LacZ and dHypb error bars denote range. N=1 for Spt6 (Spt6 RNAi was included as a positive control for elongation rate defects. Results from this single experiment are consistent with what has been described in Figure 2.2B). **E)** Tandem RNAi ChIP showing the K36 trimethylation level of histone H3 over the *Hsp70* gene 2min after HS induction in LacZ(white) and dHypb(gray) KD cells. N=2, error bars denote range.(values normalized to the histone H3 levels at the corresponding regions). Lack of any observable defect in the H3-K36 trimethylation signal in dHypb samples at the +2210 region is probably due to the fact that only a small fraction of Pol II molecules have reached this region 2min after HS. Not long enough for the possible cotranscriptional trimethylation of H3-K36 to occur. **F)** dHypb does not alter the histone H3 density over the *Hsp70* gene. Tandem RNAi ChIP showing the density of Histone H3 over the Hsp70 gene 2min after HS induction. The numbers below the gene map denotes the center of primer pairs that were used in the real-time PCR assay.

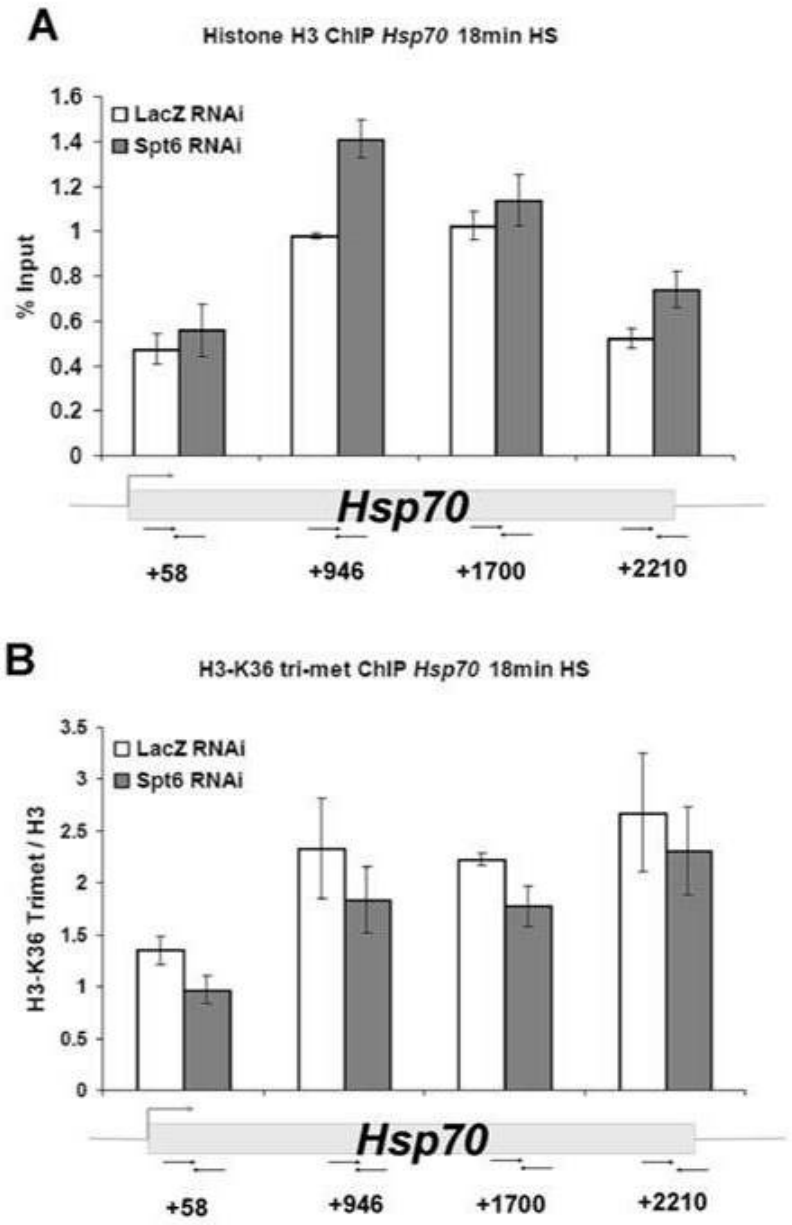
A
Histone H3 ChIP Hsp70 18min HS
LacZ RNAi
Spt6 RNAi
% Input
1.6
1.4
1.2
1
0.8
0.6
0.4
0.2
0
Hsp70
+58
+946
+1700
+2210
B
H3-K36 tri-met ChIP Hsp70 18min HS
LacZ RNAi
Spt6 RNAi
H3-K36 Trimet / H3
3.5
3
2.5
2
1.5
1
0.5
0
Hsp70
+58
+946
+1700
+2210

Figure 2.4 (continued)

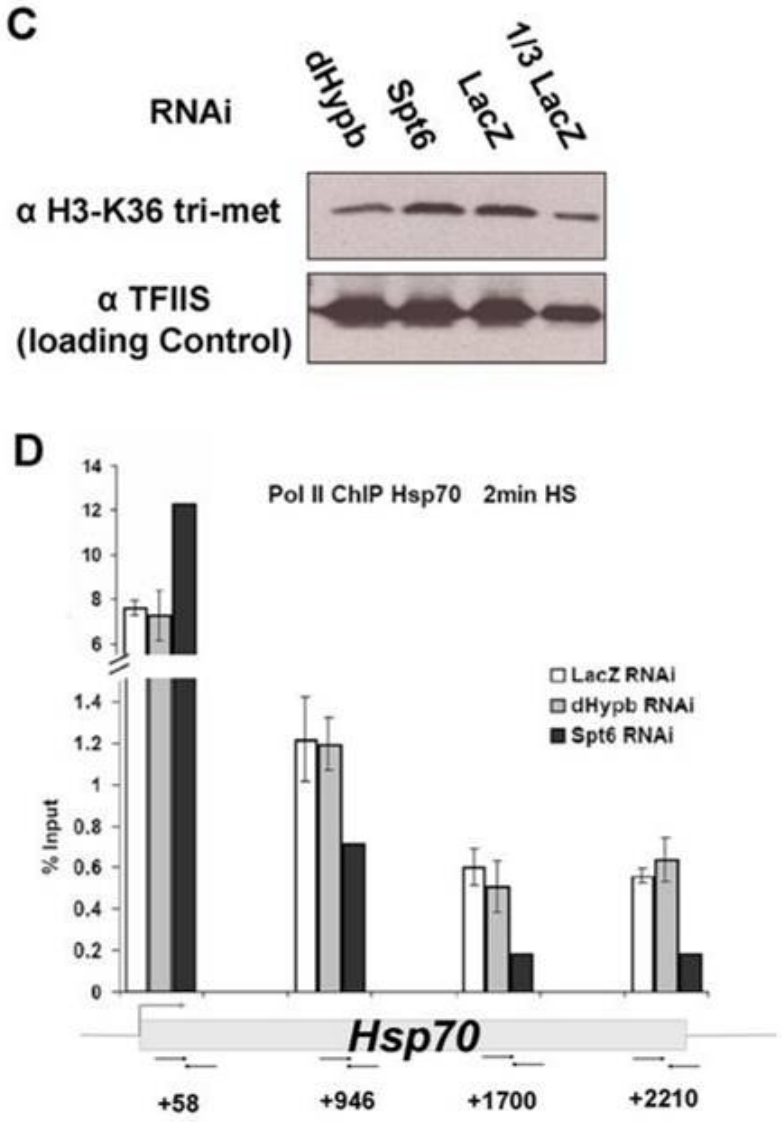

Figure 2.4 (continued)

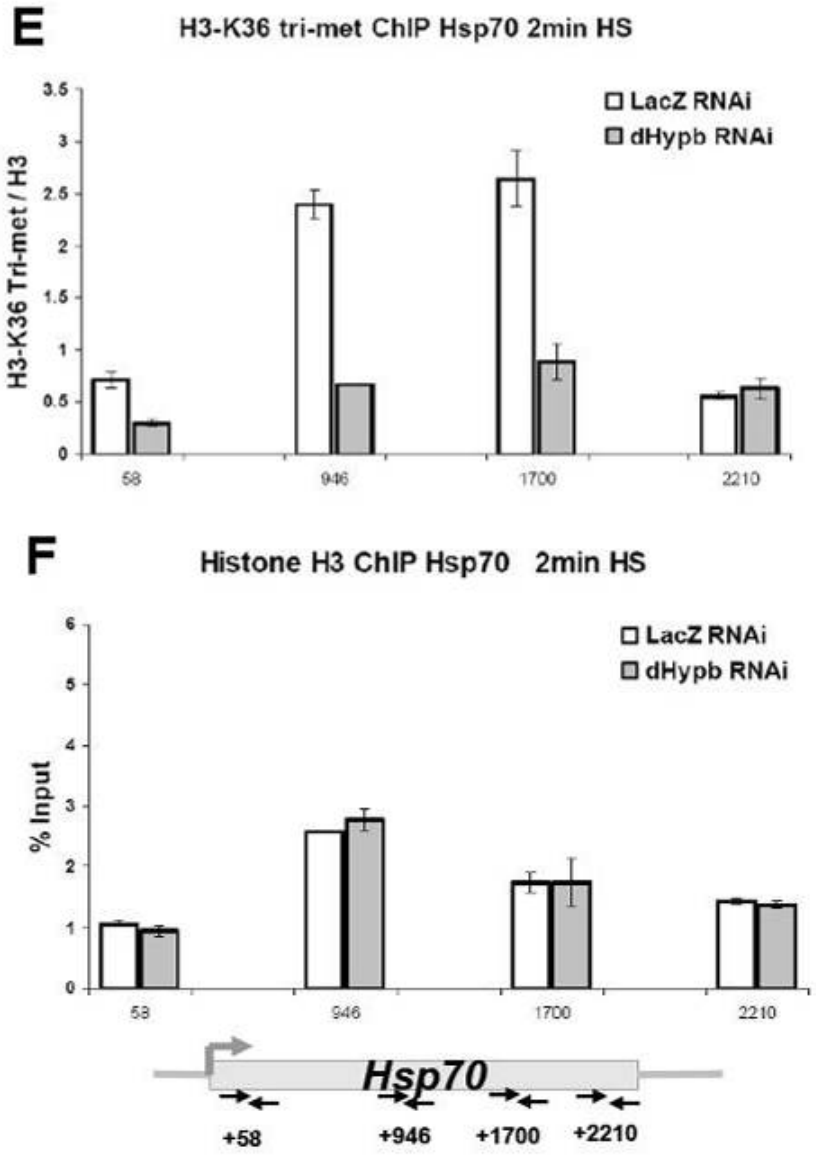

at two tandem genes in yeast and decreased utilization of downstream polyadenylation sites (Kaplan et al, 2005, Yoh et al, 2007).

2.2.6 Examining the status of Ser2 phosphorylation of CTD in Spt6 KD cells

Here I showed that the positive influence of Spt6 on transcription elongation is not mediated through histone H3K36me3, as RNAi KD of Spt6 does not notably decrease the levels of this modification on the body of the gene, moreover, depletion of the *Drosophila* histone H3K36 methyltransferase, dHypb, does not decrease the elongation rate of the first wave of Pol II molecules upon transcription induction. As noted earlier, recent results have shown that Spt6 binds to the CTD of Rpb1 through the interaction of its SH2 domain with Ser2 phosphorylated form of CTD (Yoh et al, 2007). I hypothesized that possible loss of this interaction in Spt6 RNAi samples may expose the CTD of Rpb1 to phosphatases and therefore, removal of this mark could lead to a decrease in the elongation rate of Pol II on the body of *Hsp70*. To test this idea I first checked the global levels of Ser2 phosphorylation in Spt6 RNAi and control cells and interestingly enough, loss of Spt6 results in about a 2-fold decrease in the cellular levels of Ser-2 phosphorylated CTD (Figure 2.6.A). I also tested to see if the global loss of Ser2-P that I observe by Western Blot is also visible on the body of the gene by ChIP. Therefore, I performed ChIP using an indirect immunoprecipitation technique with a secondary antibody (described in Appendix C). Results show that loss of Spt6 does not lead to a significant decrease in the levels of Ser2 or Ser5 phosphorylation, ruling out the possibility that Spt6 KD results in loss of Ser2-P signal on the body of *Hsp70* gene (Figure 2.6B). I also did not see any drop in the density of Ser5-P CTD (Figure 2.6B).

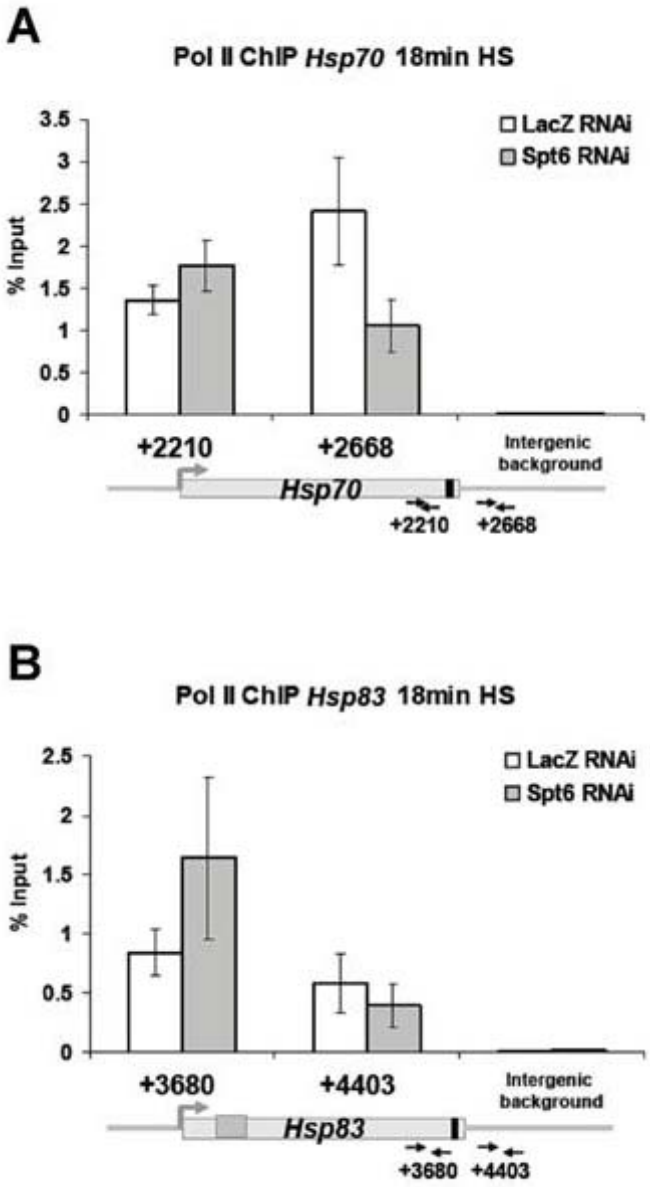

Figure 2.5 Spt6 is required for proper transcription termination at the transcriptionally active heat shock genes
A) Rpb3 (Pol II) density upstream (+2210) and downstream (+2668) of the polyadenylation signal in Spt6 and LacZ RNAi samples 18min after HS induction (n=4, error bars denote SEM). The black box between the two primer pair regions represents the relative position of the polyadenylation signal. **B)** Same as in A showing the Hsp83 gene (n=3, error bars denote SEM).

2.2.7 Stimulation of Pol II elongation rate by Spt6 is not mediated through TFIIS

Recent work has revealed that depletion of *Drosophila* TFIIS leads to reduction in recruitment of Pol II and defects in the elongation rate of polymerase, plausibly through Pol II backtracking and arrest early after heat shock induction (Adelman et al, 2005). I sought to test whether the elongation rate defect that we observe immediately after heat shock induction in Spt6 KD cells is due to a defect in recruitment of TFIIS. Apart from a 25% decrease in the density of TFIIS at the +58 region of *Hsp70* in the Spt6 depleted cells, we observed no difference in the density of TFIIS on the body of *Hsp70* in Spt6 RNAi treated cells in comparison to LacZ RNAi cells (Figure 2.7A). While TFIIS KD decreases the density of paused Pol II prior to induction, it also results in a larger drop in the density of Pol II at the 3'-end of the gene 2min after HS induction (Adelman et al, 2005). Here we show that this gradual drop in the density of Pol II on the body of the gene 2min after HS induction in Spt6 RNAi is not an indirect consequence of the deficiency in recruitment of TFIIS (Figure 2.6A).

2.2.8 Spt6 is required for maximal recruitment of Paf1 and Spt5 to transcriptionally active *Hsp70*

In yeast, Spt6 is required for association of Ctr9, a component of the Paf1 complex, with the body of transcriptionally active galactose-inducible genes (Kaplan et al, 2005). We have tested the requirement of Spt6 for association of Paf1 with transcriptionally active genes in a metazoan organism. Spt6 RNAi results in a similar reduction in association of Paf1 with the nucleosome-containing regions (+946 and

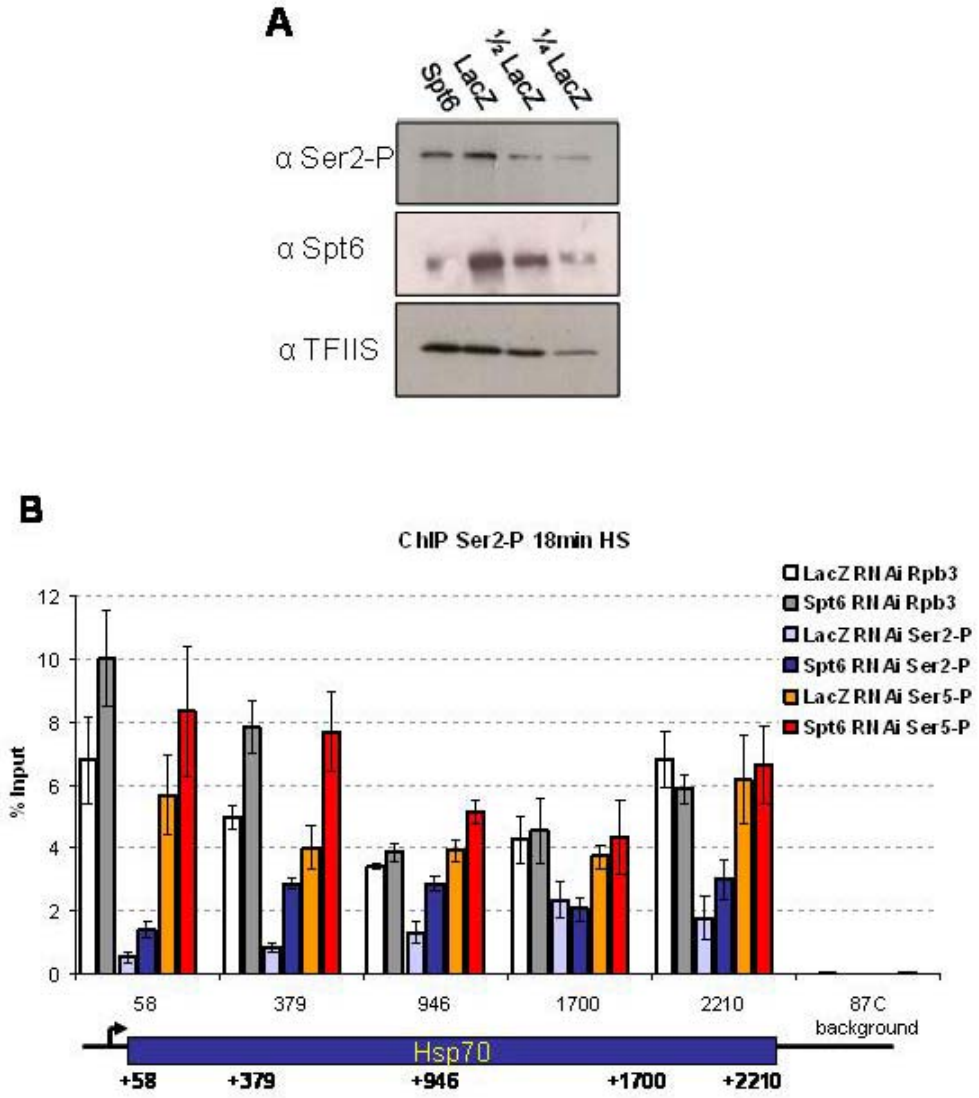

Figure 2.6 Spt6 RNAi decreases the global level of CTD Ser2 phosphorylation
A) A representative Western Blot showing the levels of CTD Ser2 phosphorylation in LacZ and Spt6 RNAi cells in S2 cells. **B)** Ser2P and Ser5P ChIP experiment showing the density of this mark as well as the overall density of Pol II (Rpb3) on the body of Hsp7o during the steady state of transcription elongation, 18 min after HS induction. N=3 for all samples except LacZ Ser2P (n=2), error bars denote SEM.

+1700) of activated *Hsp70* (Figure 2.7B). The *Drosophila* Rtf1 is another transcription elongation factor, which unlike the yeast ortholog, does not appear to be a stable component of the Paf1 complex (Adelman et al, 2006). However, this factor requires Paf1 for association with transcriptionally active HS genes (Adelman et al, 2006, Mueller et al, 2004). We find that Spt6 RNAi also leads to a significant decrease in association of this factor with the nucleosome-occupied regions (+946 and +1700) of *Hsp70* (Figure 2.7C). This defect in recruitment of Rtf1 is possibly an indirect consequence of Paf1 absence from the coding region of the *Hsp70* gene.

Zhuoyu Ni, a former graduate student in our lab has observed that Spt5 KD by RNAi results in accelerated dissociation of Pol II molecules from downstream of the polyA signal site at *Hsp70*. Similar observations have been reported in yeast where, yeast strains mutant for Spt5 preferentially utilize the upstream polyA signals (Cui & Denis, 2003), or that Spt5 prevents premature RNA dissociation from the transcription machinery at the terminator sequences *in vitro* (Bourgeois et al, 2002). To test whether the accelerated dissociation of Pol II downstream of the polyA signal site that we detect at *Hsp70* in Spt6 RNAi cells is a consequence of defect in association of Spt5 with active *Hsp70*, I also quantified the levels of Spt5 by ChIP during the steady state of heat shock induction. Unlike Spt6, Spt5 is strongly present at the 5'-proximal region of *Hsp70* ORF both prior to and after heat shock activation (Saunders et al, 2003). Interestingly, while the density of Spt5 is comparable in both Spt6 and LacZ RNAi samples at the 5'-proximal region of the *Hsp70* gene during the steady state of HS activation, a modest decrease in association of Spt5 with the middle and 3'-end (+946 and +1700) of the *Hsp70* gene was observed in Spt6 RNAi samples (Figure

Figure 2.7 Spt6 is required for maximal recruitment of Paf1, Rtf1 and spt5 to *Hsp70*.
(A-D) Association of TFIIS **(A)**, Paf1 **(B)**, Rtf1 **(C)** and Spt5 **(D)** with different regions of the *Hsp70* gene 18 min after full heat shock activation as detected by ChIP. The X-axis denotes the center of primer pairs used in the real-time PCR experiment. The Y-axis refers to the Percent inputs values for each factor normalized to the level of Pol II (Rpb3) present at the same region (error bars denote SEM of three independent experiments)**.(G)** Cellular levels of each of the indicated proteins in Spt6, LacZ RNAi treated and untreated samples. Other RNAi treatments included to show the specificity of antibody for each experiment.

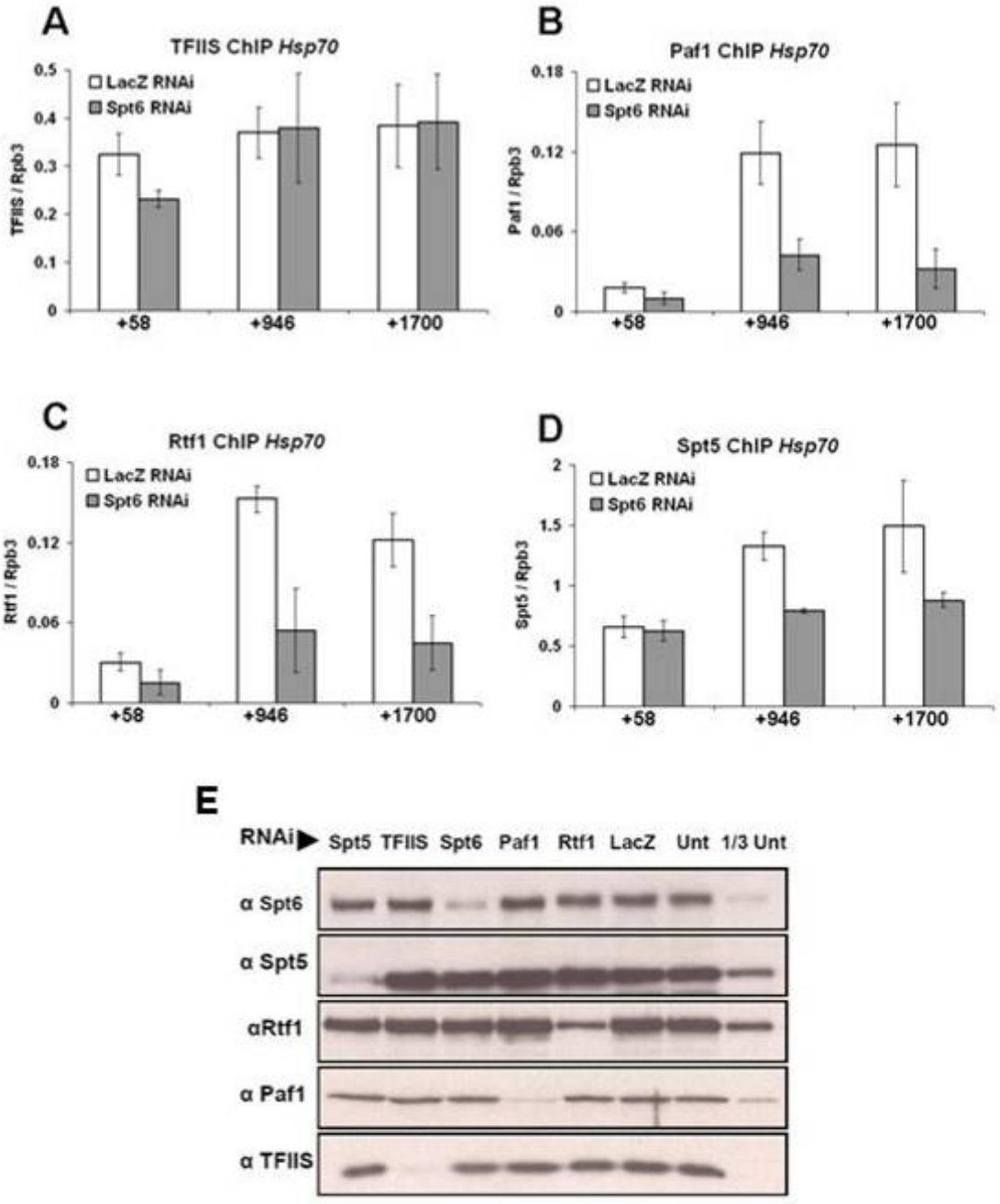
A
TFIIS ChIP Hsp70
LacZ RNAi
Spt6 RNAi
TFIIS / Rpb3
0.5
0.4
0.3
0.2
0.1
0
+58
+946
+1700
B
Paf1 ChIP Hsp70
LacZ RNAi
Spt6 RNAi
Paf1 / Rpb3
0.18
0.12
0.06
0
+58
+946
+1700
C
Rtf1 ChIP Hsp70
LacZ RNAi
Spt6 RNAi
Rtf1 / Rpb3
0.18
0.12
0.06
0
+58
+946
+1700
D
Spt5 ChIP Hsp70
LacZ RNAi
Spt6 RNAi
Spt5 / Rpb3
2
1.5
1
0.5
0
+58
+946
+1700
E
RNAi
Spt5
TFIIS
Spt6
Paf1
Rtf1
LacZ
Unt
1/3 Unt
α Spt6
α Spt5
αRtf1
α Paf1
α TFIIS

2.7D). Therefore, it is possible that the accelerated dissociation of Pol II downstream of the PolyA signal that we observe in Spt6 RNAi is partly due to a decrease in the density of Spt5 with the Pol II transcription machinery. We also note that Spt6 RNAi does not lead to a noticeable global decrease in the cellular levels of the tested elongation factors (Figure 2.7E), suggesting that the lower levels of Paf1, Rtf1 and Spt5 on the body of *Hsp70* are due to recruitment defects.

2.2.9 Spt6 is critical for normal fly development throughout the life cycle

Recently, it was shown that Spt6 mutant animals generated by P-element transformation are lethal at the embryonic stage (Peter et al, 2002), highlighting the requirement of this transcription factor for proper development during this stage. Here, we report that requirement for Spt6 during *Drosophila* development is not limited to the embryonic stage (Figure 2.8A). We observed that constitutively and ubiquitously–driven expression of the Spt6 RNAi by the tubulin GAL4-driver line causes lethality during the larval stage. Moreover, transcription of Spt6 dsRNA from UAS-Spt6^{RNAi} under the control of the 6983 GAL4-driver line, which has a broad expression pattern during the pupal stage, leads to defects in abdominal cuticle deposition and trichome (hair) formation during metamorphosis (Figure 2.8B). Majority of these flies also fail to eclose and die as pharate adults. These data summarized in a flow chart (Figure 2.8A) demonstrate the critical role that Spt6 plays during different developmental stages of *Drosophila* life cycle, presumably as a consequence of Spt6 being required for efficient transcription from many genes throughout development.

2.2.10 Elongation rate of Pol II at *Hsp70* in FACT knock-down cells

The FACT complex is comprised of the Spt16 and Ssrp1 heterodimer, and it

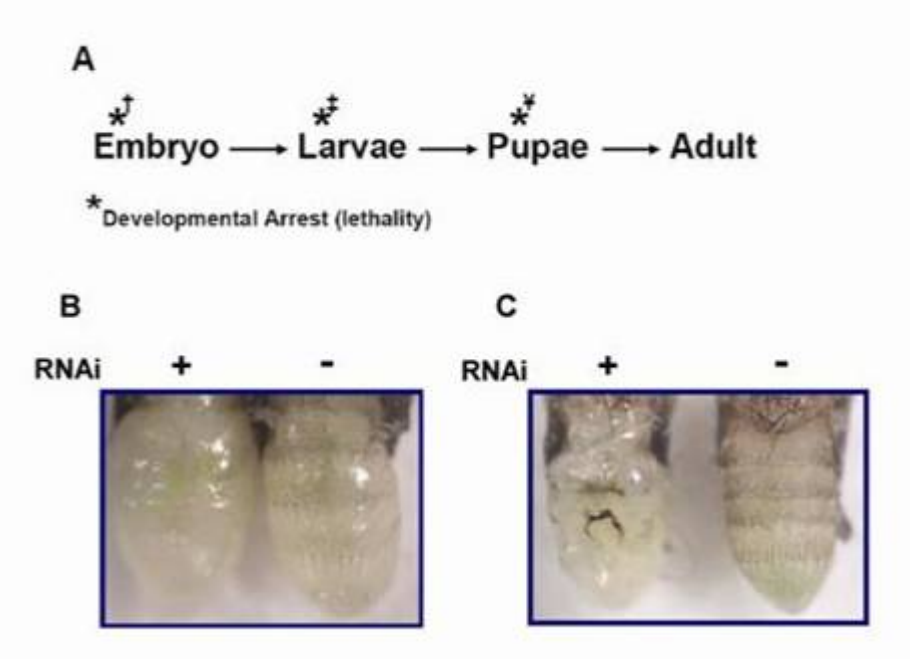

Figure 2.8 Spt6 is critical for normal fly development throughout the life cycle

A) A chart depicting requirement of Spt6 during different stages of development. † Experiments carried out by (Peter et al, 2002) revealed that p-element insertion at the Spt6 gene leads to lethality at the larval stage. ‡ determined by driving expression of UAS-Spt6 ^{RNAi} with the robustly and ubiquitously expressed Tubulin-GAL4 driver line. ¥ crossing the UAS-Spt6 ^{RNAi} to the 6983-GAL4 line which has a broad expression pattern during the pupal stage causes lethality as pharate adults. **B)** Expression of UAS-Spt6^{RNAi} dsRNA during the pupal stage by the 6983-GAL4 driver results in lethality as pharate adults with aberrant abdominal development. Notably defects in cuticle deposition, hair development at around 80 h after puparium formation (APF). **C)** Same as in B, but at later developmental stage prior to eclosion (about 96 APF). What appear to be melanotic lesions were also visible in the abdominal region of the Spt6 RNAi animals at a high frequency. Eclosion frequency of parental lines and 6983-GAL4/ UAS-Spt6^{RNAi} offspring is also displayed as a chart at the bottom of panel C.

has been shown to physically interact with histones and stimulate transcription elongation from chromatin templates *in vitro* by removing an H2A/H2B dimer during the passage of Pol II. The FACT complex has also been shown to possess histone chaperone activity (Belotserkovskaya et al, 2003, Orphanides et al, 1998)and it also prevents transcription initiation from cryptic sites within coding regions by restoring the normal chromatin structure upon passage of Pol II (Kaplan et al, 2003). The fact that numerous research papers have attributed elongation-facilitating activity to the FACT complex and that we detect this complex on the body of the *Hsp70* gene I sought to examine the effect that absence of this factor will have on elongation properties of Pol II at *Hsp70*. I tested the effects of Spt16 RNAi (a subunit of FACT) on the elongation rate of the pioneering Pol II molecules at the *Hsp70* gene 2 min after HS induction and failed to detect any difference in the density (elongation rate) of Pol II throughout *Hsp70* in comparison to control cells (Figure 2.9A). However, depletion of Ssrp1 the other subunit of FACT (Figure 2.9C), resulted in a marked decrease in the density of Pol II immediately after HS induction at the 3'-end of *Hsp70* gene (Figure 2.9A) to an extent similar (partially less) to Spt6 RNAi samples.

In addition to the FACT complex, I also tested the effect of Asf1 chaperone/elongation factor Knock down on elongation. Recently it was shown that the yeast Asf1 is recruited to the body of transcriptionally active genes and that it is required for eviction and deposition of histone H3 at these genes (Schwabish & Struhl, 2006). I also note that RNAi KD of Asf1 as confirmed by looking at Asf1 mRNA level (Figure 2.9D), does not alter the elongation properties of Pol II at *Hsp70* 2 min after HS induction (Figure 2.9A).

2.3 Summary and Discussion

In this chapter, using the native major *Drosophila* heat shock gene, *Hsp70*, I demonstrate that Spt6 is a genuine transcription elongation factor that is critical for normal transcription elongation rate by Pol II *in vivo*. A combination of biochemical (ChIP) and imaging techniques (MPM-based FRAP) allows for rigorous testing of the kinetics of transcription elongation both early after heat shock induction as well as during the steady state of transcription. Therefore, here I also promote the use of native *Hsp70* gene as an attractive gene system for studying the elongation properties of Pol II *in vivo*, in different elongation factor-mutant/RNAi backgrounds.

Immediately after HS induction, the chromatin landscape of the *Hsp70* gene undergoes dramatic modifications by disassembly of the canonical nucleosome structure that lead to a ~3-fold decrease in the nucleosome (micrococcal nuclease protection) and a corresponding depletion in core histone H3 (ChIP) (Petesch & Lis, 2008, Wu, 1980, Wu et al, 1979). While initial phase of nucleosome disassembly is rapid and independent of transcription, a second phase of the nucleosome disruption appears to be contingent on the elongating Pol II machinery and, intrerestingly, does not lead to further loss of H3 (Petesch & Lis, 2008). I demonstrate that Spt6 is critical for Pol II to elongate at its normal rate during this first burst of transcription immediately after heat shock induction (Figure 2.2). A 'snapshot' of Pol II at the 3'-end of the *Hsp70* gene indicates that the density of Pol II is at least 5-fold less in the Spt6-depleted cells at this short time point after induction. This deficiency in transcription elongation during the early stages of heat shock in Spt6-depleted cells

Figure 2.9: Density of the pioneering Pol II molecules at *Hsp70* in FACT and ASF1 RNAi treated cells.
A) Rpb3 ChIP data showing distribution and density of Rpb3 at 5'-end (+58), middle (+946) and 3'-end (+2210) of the Hsp70 gene 2 min after heat shock induction in Asf1, Spt16, Ssrp1 and Spt6 RNAi samples. Each experiment was repeated at least 3 times. Error bars represent SEM. **B-C)** Western Blot analysis to check knock-down of Spt16 **(B)** and Ssrp1**(C)** the two different subunits of FACT transcription elongation complex in Control (LacZ) and Ssrp1 and FACT RNAi treated samples. **D)** Quantitative Real-time reverse transcription-PCR (Q RT-PCR) was performed to check knock-down of Asf1 in control (LacZ RNAi) and Asf1 RNAi treated cells.

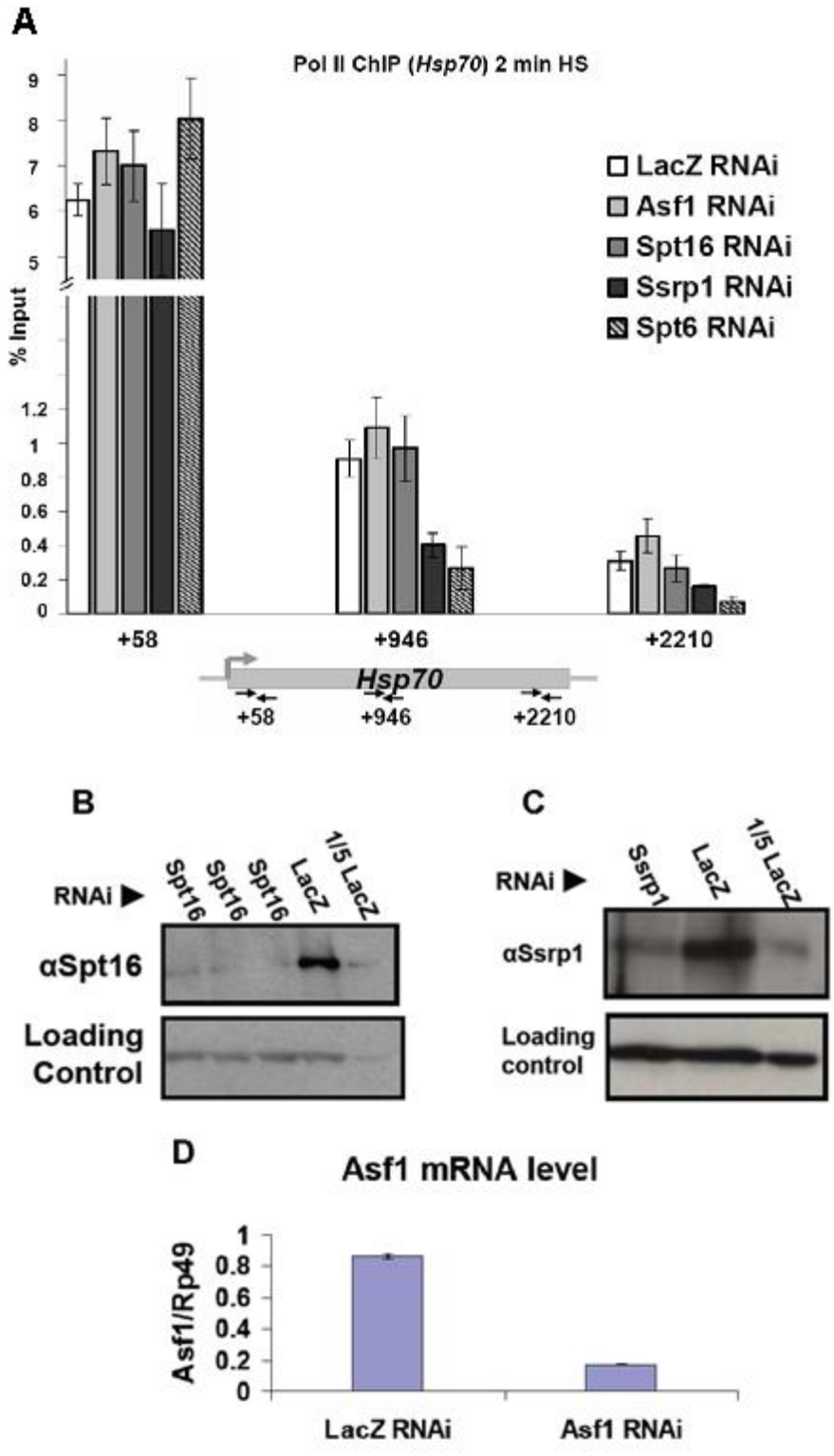
A
Pol II ChIP (Hsp70) 2 min HS
% Input
LacZ RNAi
Asf1 RNAi
Spt16 RNAi
Ssrp1 RNAi
Spt6 RNAi
+58
+946
+2210
Hsp70
B
RNAi
Spt16
Spt16
Spt16
LacZ
1/5 LacZ
αSpt16
Loading Control
C
RNAi
Ssrp1
LacZ
1/5 LacZ
αSsrp1
Loading control
D
Asf1 mRNA level
Asf1/Rp49
LacZ RNAi
Asf1 RNAi

correlates nicely with the inability of these cells to efficiently perform the second stage of more complete nucleosome disruption from the body of *hsp70* as observed by MNase protection assay (Petesch & Lis, 2008). This suggests that Spt6 may be critical for this second transition in disrupting the nucleosome architecture, which does not require additional loss of histone (Petesch & Lis, 2008). In support of this idea, I observed that even during the steady state of HS induction histone H3 density is slightly higher on the body of *Hsp70* in Spt6 KD cells (Figure 2.4A).

Similar to what has been observed at other genes and in other systems (Bell et al, 2007, Li et al, 2007, Pokholok et al, 2005), I note that the middle and 3'-end of the *Hsp70* gene are the main sites of H3-K36 trimethylation (Figure 2.4B) and that depletion of Spt6 results in a small decrease in the density of H3-K36 trimethylation over the *Hsp70* gene (Figure 2.4B). However, depletion of dHypb does not cause any defect in the elongation rate of first wave of Pol II after HS induction. This allowed us to tease apart two different functions of Spt6: its role as a stimulator of transcription elongation rate and its function as a factor contributing to the trimethylation of H3-K36 at actively transcribed genes.

After establishment of the heat shock response the density of Pol II slightly increases within the body of *Hsp70* gene in the Spt6 KD samples (Figure 2.2), similar to an increase reported for Spt6 and FACT mutants in yeast (Mason & Struhl, 2003, Mason & Struhl, 2005). Since we have not detected any apparent cryptic transcription from upstream of the +1700 region (the region that the Northern Blot probe hybridizes to), it is unlikely that this increase in Pol II density emanates from cryptic initiation sites within the gene. One plausible explanation for this Pol II density increase in the

Spt6 KD cells is a slower elongation rate even during the steady state of heat shock transcription (18 min HS). Thus, it is possible that slower movement of the transcription machinery leads to an increase in the density of Pol II at this gene, resulting in a higher density for Pol II as detected by ChIP assay 18min after HS induction. Indeed, results showing slower movement of Pol II at steady state in the FRAP assay at the heat shock loci (Figure 2.3) support this hypothesis.

I also show that RNAi knockdown of Spt6 results in an almost 2-fold reduction in the cellular levels of Ser2-P CTD. Interestingly, a similar decrease was not observed on the body of *Hsp70* during the steady state of heat shock induction. In fact the density of Ser2-P was even slightly higher at the tested regions on *Hsp70*. It is possible that loss of Spt6 exposes those phosphorylated Ser2 residues that are otherwise masked by Spt6 leading to better recognition by Ser2-P antibody. While I do not detect notable processivity defect on the body of *Hsp70* during the steady state of transcription elongation, it is possible that absence of Spt6 causes processivity defects at much larger genes and the dissociated polymerase molecules are likely to get dephosphorylated leading to a lower global Ser2-P level as observed by Western Blot (Figure 2.6A).

The accelerated dissociation of Pol II that we observe downstream of the polyadenylation signal at both *Hsp70* and *Hsp83* genes in Spt6 KD cells is similar to other reports in organisms as diverse as yeast and human (Kaplan et al, 2005, Yoh et al, 2007). In yeast, Spt6 mutation diminishes read-through transcription and formation of a bicistronic transcript at the tandemly arrayed GAL10 and GAL7 genes (Kaplan et al, 2005). Furthermore, Spt6-depleted human HeLa cells preferentially utilize the

premature upstream polyadenylation site at an engineered HIV:LacZ reporter construct (Yoh et al, 2007). A slower elongation rate by Pol II might simply give the termination factors a larger window of opportunity to dismantle the transcription machinery at the 3'-end of the gene (Zhang & Gilmour, 2006). Another non-mutually exclusive explanation for this Pol II density drop at the termination site is loss of factors such as Spt5 (Figure 2.7D) that could potentially enhance the stability of transcribing polymerase. Spt5 has a high degree of homology to the prokaryotic elongation factor NusG, a factor that has been implicated in stabilization of elongating Pol II (Greenblatt et al, 1993).

Spt6 was identified as an essential gene that causes lethality at the embryonic stage in screens to identify X-chromosome genes that affect viability (Bourbon et al, 2002, Peter et al, 2002). However, as expected for a factor implicated in transcription of many Pol II transcribed genes (Kaplan et al, 2000), requirement for Spt6 was not limited to the embryonic stage, and we show that expression of this factor is also critical for normal development during the larval stage as well as metamorphosis and transition to adulthood during pupariation (Figure 2.8B, 2.8C). This finding is in line with developmental studies in zebrafish showing that absence of this elongation factor results in widespread developmental defects (Keegan et al, 2002, Kok et al, 2007). The abdominal-cuticle defect during pupariation is similar to the phenotype observed in the mutants of the histone acetyltransferase Gcn5, another factor implicated in chromatin modulation and transcription (Carre et al, 2005).

In summary, I have tried to show that the *Drosophila Hsp70* gene provides a convenient model system for analyzing the role of suspected transcription elongation

factors in transcription elongation. First, the rapid and relatively synchronous induction of *Hsp70* allows the rate of progression of the first wave of induced Pol II to be tracked by simple kinetic ChIP assays. Additionally, the steady-state transcription rate of these highly-induced genes can be examined optically by FRAP studies at *Hsp70* polytene loci in cultured salivary glands. My results reveal that in addition to the previously reported functions for Spt6 *in vivo* (Adkins & Tyler, 2006, Andrulis et al, 2002, Kaplan et al, 2003, Yoh et al, 2007), this factor is also a *bona fide* transcription elongation factor that positively stimulates the elongation rate of the elongating Pol II. This requirement for Spt6 to positively stimulate elongation is not limited to when Pol II has to negotiate with the nucleosome barrier during the early stage of HS, but also applies to the steady-state of transcription when the chromatin landscape of the gene is in a more transcriptionally-permissive state (Petesch & Lis, 2008)during the steady state of gene activation.

2.4 Materials and Methods

2.4.1 Drosophila S2 cell line maintenance and RNA interference

Drosophila melanogaster S2 cells were grown at 25^{o}C in Shields and Sang M3 medium (Sigma) supplemented with bactopeptone, yeast extract and 10% FBS. For RNAi treatment, exponentially growing S2 cells were diluted to 1×10^{6} cells/ml with serum-free medium (presence of serum interferes with the uptake of dsRNA) (Ramadan et al, 2007) and 1ml of the diluted cells was seeded in a 6-well plate dish. Ten microgram of dsRNA was added to the cells and the plate was gently rocked for a few times to distribute the dsRNA. After 45 to 60 min of incubation at 25^{o}C, 2ml of

20% FBS-containing medium was added to each well, raising the total volume of each sample to 3ml. After 84-96 hrs of incubation at 25°C, cells were harvested. For large scale RNAi experiments designed for ChIP assay, 50µg of dsRNA was added to either 5ml of 1×10^6 cells in a 75cm^2 flask, or 2.5ml of 2×10^6 cells in a 25cm^2 flask. After treatment with dsRNA, equal volume of 20%-FBS containing medium was added to the cells and cells were incubated at 25°C. For the RNAi screen, 250µl of cells at 1×10^6 cells/ml were seeded in each well of a 24-well plate and treated with 2.5µg of dsRNA. After 45 to 60 min of incubation at 25°C the volume was raised to 500µl with 20% FBS-containing medium. An additional 250µl of 10% FBS-containing medium was added to each well 2 days later to compensate for evaporation. Cells were harvested 96 hours after RNAi treatment. For instantaneous heat shock treatment of cells, equal volume of 48 °C medium was added to the cells and cells were incubated at 37 °C for the indicated time.

2.4.2 Generation of dsRNA for RNA interference

The dsRNAs targeting LacZ (β-galactosidase) and other transcription factors described in this chapter were generated using a T7-RNA polymerase based MEGAscript kit (Ambion). 1µg of DNA generated by PCR amplification was used as template for each in vitro transcription reaction. The DNA template targeted a region within one of the exons of the targeted factors, a region with no significant sequence homology to other off-target sites within the genome. After O/N incubation at 37 °C, the reactions were stopped by addition of ammonium acetate and the RNA was phenol: chloroform extracted, precipitated with equal volume of 100% isopropanol and air-dried. The pellet was resuspended in H_2O and heated to 90 °C for 3 min and

gradually cooled down to allow hybridization of complementary strands. The primers sequence used for generation of the PCR template are as follows:

LacZ T7F: 5’GAATTAATACGACTCACTATAGGGA

GAGATATCCTGCTGATGAAGC.LacZT7R:5’GAATTAATACGACTCACTATAG

GGAGAGCAGGAGCTCGTTATCGCAsf1T7F:5’GAATTAATACGACTCACTAT

AGGGATTTGTGCGAAGACAAGCGGAAsf1T7R:GAATTAATACGACTCACTA

TAGGGATAAAGAGGCTTTGTTGGCGGGTTdHypbT7F:5’GAATTAATACGAC

TCACTATAGGGAACGCGCAGGTGAAATGGAAAdHypbT7R:5’GAATTAATAC

GACTCACTATAGGGATGGGCGTTTGCCAAATCCATdPaf1T7F:GAATTAATA

CGACTCACTATAGGGACGTAACTTCAAGTATGACGTGCTGACGGdPaf1 T7R:

GAATTAATACGACTCACTATAGGGAGTTGTACTCTCGAGCGATCTTGTACT

CGRtf1T7F:5’GAATTAATACGACTCACTATAGGGATTCCGACTGGGCCAACA

ACRtf1T7R:5’GAATTAATACGACTCACTATAGGGAGTAATCAGAGACGCCA

GCGGSpt5T7F:5’GAATTAATACGACTCACTATAGGGAATTTACGACTGTCCA

CCACTGGCSpt5T7R:5’GAATTAATACGACTCACTATAGGGAGCAAGAATGC

ATATACAATTAGGAGCACCCSpt6T7F:5’GAATTAATACGACTCACTATAGGG

ACCGTAACCCCGGTGCCCGAGGSpt6T7R:5’GAATTAATACGACTCACTATA

GGGAGGCTCTTGTGCCAGCTGTCGG3’Spt16T7F:GAATTAATACGACTCACT

ATAGGGAGCTGCGAGGCTGCCATTGGCGSpt16T7R:GAATTAATACGACTCA

CTATAGGGACAGCTCGCGCTGTGCTCCTTGCSsrp1T7F:5’GAATTAATACGA

CTCACTATAGGGAGAACATCATCTTCAAGAACACCSsrp1T7R:5’GAATTAAT

ACGACTCACTATAGGGAGTGGTAACGCGTTTGTCCCTGCTFIIST7F:5’GAAT

TAATACGACTCACTATAGGGAGAGAGCAAGATGGCCAGCGACGGCTFIIS T7R:5'GAATTAATACGACTCACTATAGGGAGACCGCACTCGTTGCACATGA CG

2.4.3 RNA isolation and Northern Blot assay

Total RNA was isolated from cells using Trizol reagent (Invitrogen). Radiolabeled antisense RNA probes were used for detection of RNA species. The following primer pairs were used for making the probe templates: Hsp70 F:(5')-ACTTGGACGCCAATGGAATCCTGA -3' and Hsp70 T7R: (5')-GAATTAATACGACTCACTATAGGGA AAGACGTAGCTCTCCAGGGCATTT Hsp83 F: (5')- TGCTGCATTGTCACTTCGCAGTTC-3', Hsp83 T7R: (5')-GAATTAATACGACTCACTATAGGGAACAGCAGGATGACCAGATCCTTGA-3', U6 F:(5')-TCTTGCTTCGGCAGAACATATAC-3', U6 T7R:(5')-GAATTAATACGACTCACTATAGGGATGTGGAACGCTTCACGAT-3'. RNA probes were generated by incorporation of [α-^{32}P] UTP using Maxiscript *in vitro* transcription kit (Ambion). The quality of the probe was checked by running the generated probes on a denaturing urea-PAGE gel. For separation of cellular RNA, 1-2 µg of total RNA was run on a 1% denaturing agarose/formaldehyde gel. RNA species were transferred to Protran nitrocellulose membranes (Whatman) and baked at 80^{o}C for 60 min. Membrane prehybridization and blocking was carried out at 68^{o}C in 20ml of prehybridization buffer [6x SSC, 5x Denhardt's reagent, 0.5% SDS; 100µg/ml sheared salmon sperm DNA] for 60-120 min. Probes were added to the prehybridization buffer and hybridization was carried out at 68^{o}C O/N. Membranes

were then washed once in 2x SSC, 0.5% SDS at room temperature for 5 min followed by another wash in 2x SSC & 0.1% SDS for 15 min on the rotating wheel at room temperature. For the third wash the membrane was incubated in 0.1x SSC, 0.5% SDS at 37^{o}C for 30-60 min. The same wash repeated this time at 68^{o}C. The membrane was left in 0.1x SSC for about a minute, air-dried and sealed in a plastic seal meal bag and exposed to a phosphoimager screen (Fuji). Signals were analyzed using ImageQuant software (Molecular Dynamics).

2.4.4 Tandem RNAi-ChIP assay and real-time DNA quantification

After 84 hrs of RNAi treatment, S2 cells were harvested, instantaneously heat shocked, cross-linked with 1% formaldehyde for 2min and quenched with glycine at a final concentration of 0.125M. Cross-linked chromatin was resuspended at 1×10^{8}cells/ml in sonication buffer [0.5% SDS, 20mM Tris PH 8.0, 2mM EDTA, 0.5mM EGTA, 0.5mM PMSF and 1 tablet of protease inhibitor (Roche)/10ml of sonication buffer] and sonicated with Bioruptor (Diagenode) in 1.5ml eppendorf tubes for 15 min (22sec on, 60sec off) at the high setting. Pre-clearing of the chromatin material was done by a 60 min incubation with 30µl of 50% Agarose protein A slurry (Upstate) in a final 1ml volume of IP buffer[0.5% Triton X-100, 2mM EDTA, 20mM Tris PH 8.0, 150mM NaCl, 10% glycerol]. 1ml of the precleared sonicated chromatin was incubated with 4µl of G. pig Spt6 (Andrulis et al, 2000),4µl of in-house rabbit Rpb3, 4µl of Paf1, 15µl of Rtf1, 2µl of TFIIS, Spt5 antibodies (Adelman et al, 2005, Adelman et al, 2006)and 10µl of polyclonal rabbit H3-K36 trimethylation (Abcam 9050) per Immunoprecipitation. For immunoprecipitation of histone H3, 2µl of polyclonal rabbit antibody (Abcam 1791) was used with 1/5 of cross-linked chromatin

immunoprecipitation material (5×10^5 cells). After O/N incubation at 4 ^oC with antibodies, 60µl of equilibrated protein A-Agarose slurry was added to each IP and samples were incubated for an additional 60-120 min at 4 ^oC on a rotisserie. Beads were precipitated by spinning at 2.6rpm on a table-top centrifuge. Samples were washed once with a low salt wash buffer [0.1% SDS, 1% Triton X-100, 2mM EDTA, 20mM Tris PH 8.0, 150mM NaCl], three times with high salt wash buffer [0.1% SDS, 1% Triton X-100, 2mM EDTA, 20mM Tris PH 8.0, 500mM NaCl], once with LiCl wash buffer [10mM Tris PH 8, 1mM EDTA, 250mM LiCl, 1% NP40, 1% NaDeoxycholate] and twice with 1xTE PH 8.0. All washes were carried out at Room temperature for 3-5min. Beads were then eluted by adding 500µl of elution buffer [1% SDS, 100mM $NaHCO_3$] and rotation at RT for 25 min. 20µl of 5M NaCl was added to each tube and samples were incubated at 65 ^oC for 4 hours to reverse the cross-link. Input material was also reverse cross-linked at this stage without going through the Immunoprecipitation step. After that proteinase K mix [2 µl(4µg) proteinase K (Invitrogen), 1µg Glycoblue (Ambion) 15µl of 1M Tris PH8.0] was added to each tube and samples were further incubated for 30-60 min. Equal volume of Phenol:chloroform was added to tubes, samples were vortexed at max speed for 15 sec and spun down at max speed for 10min. 420µl of the aqueous was added to1ml of ethanol and after at least a 3hrs incubation, DNA was precipitated by centrifugation at max speed for 20min. the pellet was washed once with 70% EtOH and air dried. The IP materials were resuspended in 100 µl water and the Inputs in 1ml (10% input).

The amount of immunoprecipitated DNA was quantified using real-time PCR. 4µl of the IP material from each sample was used for each PCR reaction and the

amount of precipitated DNA for each region was quantified by comparison of IP value to a standard curve generated from the serial dilution (10-0.01% input range) of the same sample's input material. SYBR green Taq mix was used for quantification of DNA in a final 20µl reaction volume. Primer pairs used for real-time PCR are provided.

Hsp70 +58 F:5'-CAATTCAAACAAGCAAAGTGAACAC

Hsp70 +58 R:5'-TGATTCACTTTAACTTGCACTTTA

Hsp70 _946 F, 5'-CATCGACGAGGGATCTCTGTTC

Hsp70 +946 R: 5'-GGCGCGAGGGTTGGA;

Hsp70 +1702 F:5'-GGGTGTGCCCCAGATAGAAG,

Hsp70 +1702 R:5'-TGTCGTTCTTGATCGTGATGTTC;

*Hsp70*Ab+2261F:5'-TGTTCATCAATGGGTTATAACATATGG

GTT, *Hsp70*Ab +2261 R: 5'-AAGACTTGGTAATTAGGTAATACTATT

GTT; *Hsp70*Ab +2669 F: 5'-TCGCAGACACCGCATTTGT, and *Hsp70*Ab

+2669 R: 5'-ACCAATTGCAACAGAGACTGGAA. Hsp83+19F: 5'-

TTTGAATTCGCCCGCACAGGTT, Hsp83+114R: 5'-

TTCTGGATGCCAGGGATGCAACTT, Hsp83 +3628F:5'-

GCGACCAGTCGAAACAAACAACCA, Hsp83 +3732R: 5'-

AACTCGGCCGTAGTAAACTCAG

2.4.5 Western Blot analysis

S2 cells were lyzed in 1x SDS loading buffer and equivalent of 4×10^5 cells (=1) was loaded in each well of an 8% SDS-PAGE gel for visualization of Spt6. Serial dilutions of the control RNAi treatment sample or untreated sample was also loaded to

access the extent of knock-down. The gel was transferred to a nitrocellulose membrane by wet transfer for 1 hour at 100 volts. Equal loading in each well was checked by Staining with 0.1% w/v of Ponceau S dye (Roche). Membrane were washed with 1xTBS, 0.1% Triton x-100 (TTBS) and blocked in 5% milk-TTBS for 1 hour at room temperature. The membranes were incubated in 1%TTBS with antibodies at the following concentrations for 4 hrs: α guinea pig Spt6: 1:2000, α guinea pig TFIIS: 1:2000, α guinea pig Spt5: 1:1000, α rabbit Paf1: 1:2000, α rabbit Rtf1: 1:2000, α Rabbit histone H3(Abcam 1791): 1:2000, α rabbit histone H3-K36 trimethylation(Abcam 9050): 1:2000. After primary antibody incubation, membranes were washed 3×, 10 min each with 1% milk-TTBS. For secondary incubation 1:10,000 concentration of the Horseradish peroxidase(HRP) conjugated secondary antibody was incubated with the membrane for 1 hr. Membrane was washed three times in 1% milk TTBS and visualized by adding ECL reagent and exposure to X-ray film.

2.4.6 Generation of Spt6 RNAi fly line

A 670bp region within the 6th exon of *Drosophila* Spt6 was amplified using the following primers: Spt6 F (5')-CTAGTCTAGAGGTGGGTCTGGACATT-3'. Spt6 R (5')- AGCATTCGACTGAGAACCGGTCAA-3' and cloned in a head to head orientation in the pWIZ vector (Sik Lee & Carthew, 2003)in a 2-step cloning process. The $Spt6^{RNAi}$ pWIZ construct was introduced into the germline by p-element transformation (Genetic Services, Inc.). Homozygous transgenic lines were obtained after a series of crosses and, $Spt6^{RNAi\ 41\text{-}3}$, which harbors the construct on the 3rd chromosome, was used for the experiments described in this chapter.

2.4.7 FRAP analysis

Imaging analysis was performed on the animals with the following genotype: Control: UAS-Rpb3-EGFP/CyO; 6983-GAL4/Ubx. $Spt6^{RNAi}$: UAS-Rpb3-EGFP/+; 6983-GAL4/UAS-$Spt6^{RNAi\text{-}41\text{-}3}$. FRAP analysis was done as described previously (Yao et al, 2006, Yao et al, 2007).

2.4.7 Quantitative real-time reverse transcription-PCR (q RT-PCR):

Total RNA was isolated from cells using Trizol (invitrogen) or RNaesy RNA isolation kit (Qiagen). 200 ng of total RNA was used for reverse transcription using the Superscript III reverse transcriptase (Invitrogen) in a final volume of 20 µl. After 60 min incubation at 37^{o}C, reactions were treated with a 5µl mixture of RNase H (Ambion) and RNase cocktail (Ambion), which contained 0.3µl of each. After 30 min incubation at 37^{o}C, the total volume of the reaction was raised to 400µl with water and 5µl of this was used as template in a real time PCR assay. For real time PCR, SYBR green I (Cambrex) PCR mix (0.8% glycerol, 0.006 M Tris [pH 8], 25 mM KCl, 2.5 mM MgCl2, 75 mM trehalose, 0.1% Tween, 0.1 mg of nonacetylated ultrapure bovine serum albumin/ml, 0.067×SYBR green I, 0.1 mM deoxynucleoside triphosphates, 50 U of *Taq* DNA polymerase/ml) was used and the PCR reaction was carried out on an Opticon thermocycler (MJ Research).

The primer sequences used for detection of RP49 and Asf1 are as follows: Asf1 F: 5'-GCAGTCCGAACAATGACCACACTA and Asf1-R: 5' GGACCAGGAGTGCTAAGTTATCCA. RP49 +204R:

CHAPTER 3

CHARACTERIZATION OF CG40351 (dSet1) A NOVEL SET-DOMAIN CONTAINING NUCLEAR PROTEIN AS THE MAJOR HISTONE H3 LYSINE 4 TRI-METHYLTRANSFERASE IN DROSOPHILA

3.1 Introduction:

3.1.1 Histone H3 Lysine 4 trimethylation is a hallmark of active transcription:

Covalent modifications of histones at conserved residues modulate the structure and compactness of the chromatin and can influence the transcriptional output of associated genes (Workman, 2006). Extensive studies in various eukaryotic organisms has shown that, one of these modifications, histone H3 lysine 4 trimethylation (H3K4me3), is a mark associated with nucleosomes at the 5'-end of transcriptionally-active genes (Ruthenburg et al, 2007, Workman, 2006). In general, numerous reports in different organisms have found a strong positive correlation between this modification mark and Pol II occupancy, transcriptional output and histone acetylation (Barski et al, 2007, Pokholok et al, 2005, Schübeler et al, 2004a) It is worth noting that some reports have also associated trimethylation of H3K4 to gene repression (Carvin & Kladde, 2004, Pena et al, 2006, Pinskaya et al, 2009). In yeast, deletion of the sole histone H3K4me3 methyltransferase, *Set1*, increases transcription from a subset of inducible genes (Carvin & Kladde, 2004), and results in suppression of transcription from cryptic promoters within genes (Pinskaya et al, 2009). In higher eukaryotes, H3K4me3 interaction with the inhibitor of growth 2 protein (ING2), a

subunit of HDAC complex, is necessary for repression of Cyclin D gene in mammals (Pena et al, 2006). Despite these findings, the majority of reports have associated H3K4me3 with gene activation.

3.1.2 Functional significance of histone H3 Lysine 4 trimethylation

Recent studies have suggested that H3K4me3 is more than merely a mark that denotes active transcription. Experiments from the Timmers lab, performed on human U2OS cells, have shown that the basal transcription machinery, TFIID recognizes this modification mark through the PHD domain of the TAF3 subunit. They also show that this interaction is critical for proper expression of a class of genes that lack the classical TATA box such as, HMG-CoA, RPL31, RPL34 and RPS10 (Vermeulen et al, 2007). The chromatin remodeling protein, CHD1, has also been shown to be associate with the H3K4me3 mark *in vivo* via two tandem chromodomains. Through this interaction CHD1 recruits components of the spliceosome complex and facilitates proper splicing of genes in human HeLa cells (Sims III et al, 2007). In addition to these roles in transcription activation, ING5 a factor known to interact with H3K4me3 and a binding partner of the histone H4 acetyltransferase HBO1 has been reported to be required for normal DNA replication (Champagne et al, 2008, Doyon et al, 2006).

3.1.3 *Drosophila* histone H3 lysine 4 methyltransferases

Similar to what has been shown in other eukaryotic organisms, H3K4me3 is found at the 5'-end of genes and the signal intensity shows a direct correlation with transcription level (Schübeler et al, 2004a). Previous *in vivo* and *in vitro* studies in *Drosophila* have attributed H3K4 methylation activity to 3 different factors: Trithorax (Trx) (Smith et al, 2004b), Trithorax-related (Trr) (Sedkov et al, 2003)and absent,

small,or homeotic discs 1 (Ash1) (Beisel et al, 2002, Byrd & Shearn, 2003b). Emerging evidence suggest that the latter is a H3K36 methyltransferase (Tanaka et al, 2007) (also communication with Thomas Kusch). To date, the widely held consensus among the chromatin and *Drosophila* research community is that Trx and Ash1 are the main factors responsible for deposition of this mark (Martin & Zhang, 2005). Trx and Ash1 are both components of the Trithorax group proteins (trxG). Extensive studies decades has shown that these factors are activators of developmentally regulated Hox genes and counter the function of polycomb group (PcG) repressors that repress Hox gene expression through deposition of the repressive histone H3K27 mark (Schuettengruber et al, 2007). In the case of *Ultrabithorax* (*Ubx*), the txG proteins are required for proper spatial and temporal activation of this gene (Schuettengruber et al, 2007). While trithorax binds to the upstream regulatory regions of *Ubx* regardless of the transcriptional status of *Ubx*(Papp & Müller, 2006), Ash1 is only found to associate to downstream regions of only transcriptionally active *Ubx* genes (Papp & Müller, 2006, Sanchez-Elsner et al, 2006). The observation that Ash1 associates with the downstream regions of *Ubx* is consistent with recent reports indicating Ash1 is a histone H3K36 methyltransferase (Tanaka et al, 2007). A single study has also reported recruitment of Trx to active *Hsp70* gene as part of the TAC1 complex (Smith et al, 2004a). The authors also show that Trx is required for expression of Hsp70 gene and histone H3K4 dimethylation at the 5'-end of this gene. In our targeted RNAi screen, we also tested the effects of Trx KD on *Hsp70* transcription and failed to see any effect (Chapter 2, table 2). Unlike the abovementioned study, which was done in

mutant flies, our screen was carried out in S2 cells. It is also possible that the lack of effect in our study was a result of inadequate RNAi KD.

Absent, small,or homeotic discs 2 (Ash2) a nuclear protein, which lacks the SET domain, has been shown to be a component of the core complex of H3K4 methyltransferase complexes in mammals (Ruthenburg et al, 2007, Steward et al, 2006). In *Drosophila* Ash2 shows colocalization with H3K4me3 on polytene chromosomes and absence of this protein leads to reduction in the levels of bulk histone H3 K4me3 (Beltran et al, 2007). However, the evidence linking the *Drosophila* SET-domain containing methyltransferases Ash1, Trr and Trx to H3K4me3 at the global level is less than convincing. Evidence linking these factors to H3K4 methylation comes from *in vitro* methyltransferase assays and in some cases ChIP experiments that have examined the methylation status of H3K4 at a limited number of genes (Beisel et al, 2002, Byrd & Shearn, 2003a, Sedkov et al, 2003, Smith et al, 2004a). In addition, RNAi KD of these methyltransferases in S2 cells shows no effect on the bulk histone H3K4me3 levels (Figure 3.2).

In a search for other possible H3K4 methyltransferase factors in *Drosophila* and through sequence homology analysis I identified CG40351, a SET domain-containing *Drosophila* gene as the closest homolog of *S. cerevisiae* and *S. Pombe* histone H3-K4methyltransferase, Set1. Besides a report in which RNAi KD of this factor was shown to decrease H3K4me3 levels (Yokoyama et al, 2007), CG40351 has not been characterized. The result section of this chapter describes my efforts on further identification and characterization of this factor and the role that it plays in transcription in *Drosophila.*

3.2 Results:

3.2.1 CG40351 is the Drosophila ortholog of Yeast *SET1*

Sequence homology search results identify CG40351 (dSet1) as the closest ortholog of *Schizosaccharomyces pombe* (fission yeast) SET1. A PROSITE database domain comparison between all the putative H3K4 methyltransferases and the *Schizosaccharomyces pombe* SET1 is shown in figure 3.1. Beside presence of the catalytic SET domain and the postSET domain at the C-terminal of yeast and *Drosophila* Set1, both factors contain an RNA recognition motif (RRM) proximal to the N-terminal region (Figure 3.1).

3.2.2 dSet1 is the major H3K4 trimethyltransferase in *Drosophila*

First, I examined the effect of RNAi knock-down (KD) of all putative histone H3K4 methyltransferases, as well as dSet1 on cellular levels of histone H3K4 methylation (figure 3.2A). As a positive control, I also included Ash2, which lacks histone methyltransferase activity but is an essential core component of H3K4 methyltransferase complexes in mammals and a factor required for H3K4me3 in *Drosophila*. Interestingly, only depletion of dSet1 and Ash2 resulted in marked decrease in the levels of both bulk histone H3K4me2 and H3K4me3 (Figure 3.2A), while RNAi KD of Trr methyltransferase and Ash2 resulted in detectable reduction of histone H3K3me1 levels (Figure 3.2A). The fact that other putative H3K4 methyltransferases fail to compensate the H3K4me3 and H3K4me1 levels of bulk histones in absence of dSet1 and Trr, respectively, is indicative of the non-redundant *in vivo* function of these factors. Given that H3K4me3 is predominantly associated

with the 5'-end of active genes, I decided to also examine the status of this modification by ChIP at a subset of randomly selected transcriptionally-active genes in S2 cells (Figure 3.2C). At most of the tested genes, only depletion of dSet1 methyltransferase (along with the core component Ash2) resulted in about a 2-fold or more decrease in H3K4me3 levels, indicating that dSet1 has a role in writing the histone H3K4me3 mark at many active genes *in vivo*. It is worth mentioning that despite this observed decrease in histone H3K4me3 levels, I did not see any detectable changes in the RNA level of these tested genes in dSet1-depleted cells by reverse transcription real-time PCR (rt RT-PCR). I also confirmed knock-down of all the tested methyltransferases by Western Blot or rt RT-PCR, in the case of factors that I did not have antibodies against (Figure 3.2B).

3.3.2 dSet1 widely associates with transcriptionally active loci

The observation that dSet1 is responsible for H3K4me3 at many transcriptionally active loci *in vivo* (Figure 3.2C), led me to examine the genomic distribution pattern of dSet1 on chromatin. I cloned *dSET1* by RT-PCR and a two step Splicing by overlapping extension PCR (SOE –PCR) and generated a GAL4-inducible transgenic GFP-dSet1 fly line by p-element transformation. I confirmed expression of EGFP-Set1 as a band of the right size in the salivary glands of 3rd instar larvae of the lines that had the GFP-dSet1 insert on the 2nd and 3rd chromosome by Western Blot (Figure 3.3A).

To examine localization of GFP-dSet1 within the salivary gland cells, Katie Zobeck, a graduate student in our lab performed confocal reflection microscopy coupled with GFP microscopy and the results from this imaging experiment revealed

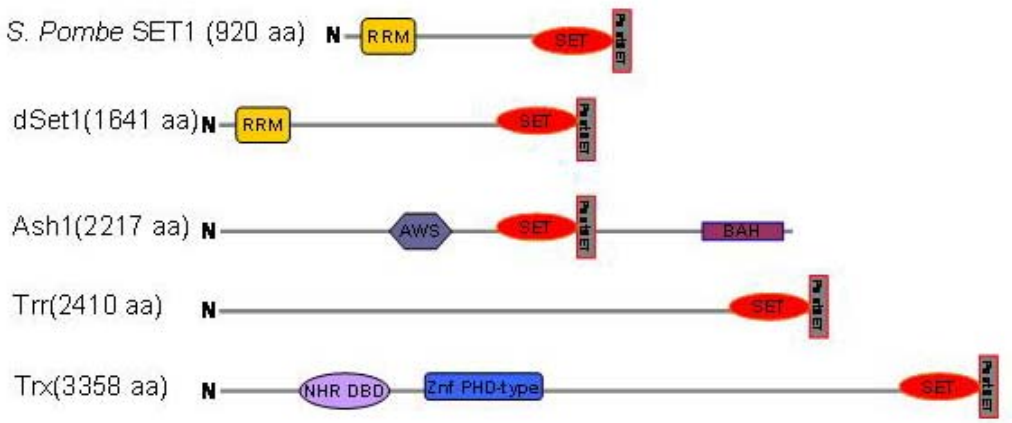

Figure 3.1 PROSITE domain comparison of *Drosophila* H3K4 methyltransferases and *Schizosaccharomyces pombe* SET1.
Among all putative *Drosophila* H3K4 methyltransferases, dSet1 is the only factor that possesses an RNA recognition motif domain (RRM), making it the closest ortholog of yeast SET1. The vertical gray rectangles represent the post set domain.

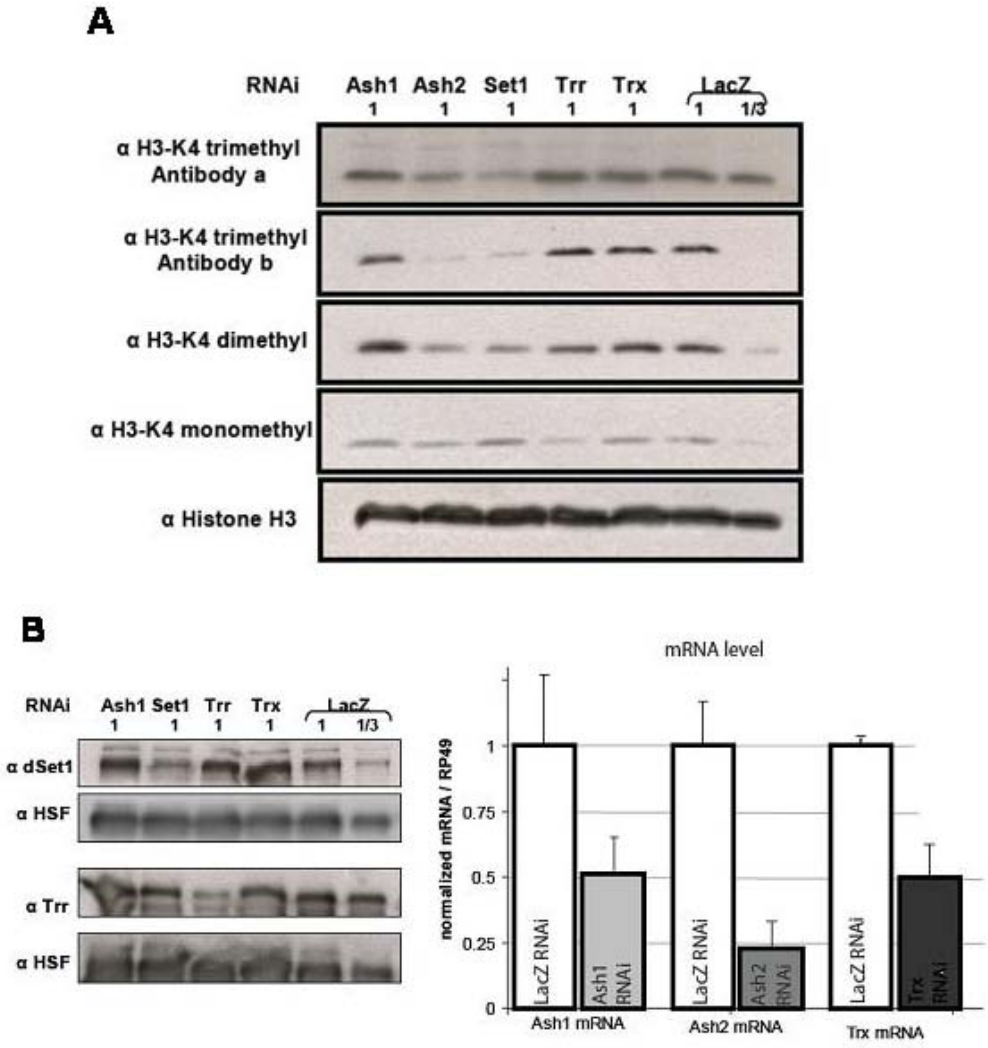

Figure 3.2 RNAi knock-down of dSet1 decreases the bulk and active promoter-associated histone H3K4me3 levels.
A) Western Blot on bulk histone from RNAi-treated cells using two different αH3K4me3 antibodies as well as αH3K4me1, αH3K4me2 and unmodified histone H3.**B)** Examining RNAi KD of methyltransferases by Western Blot (dSet1; Trr) or RT-qPCR (Ash1, Ash2;Trx). **C)** ChIP results showing histone H3K4me3 levels at the 5'-end region of a number of transcriptionally-active genes in RNAi-treated cells.

Figure 3.2(continued)

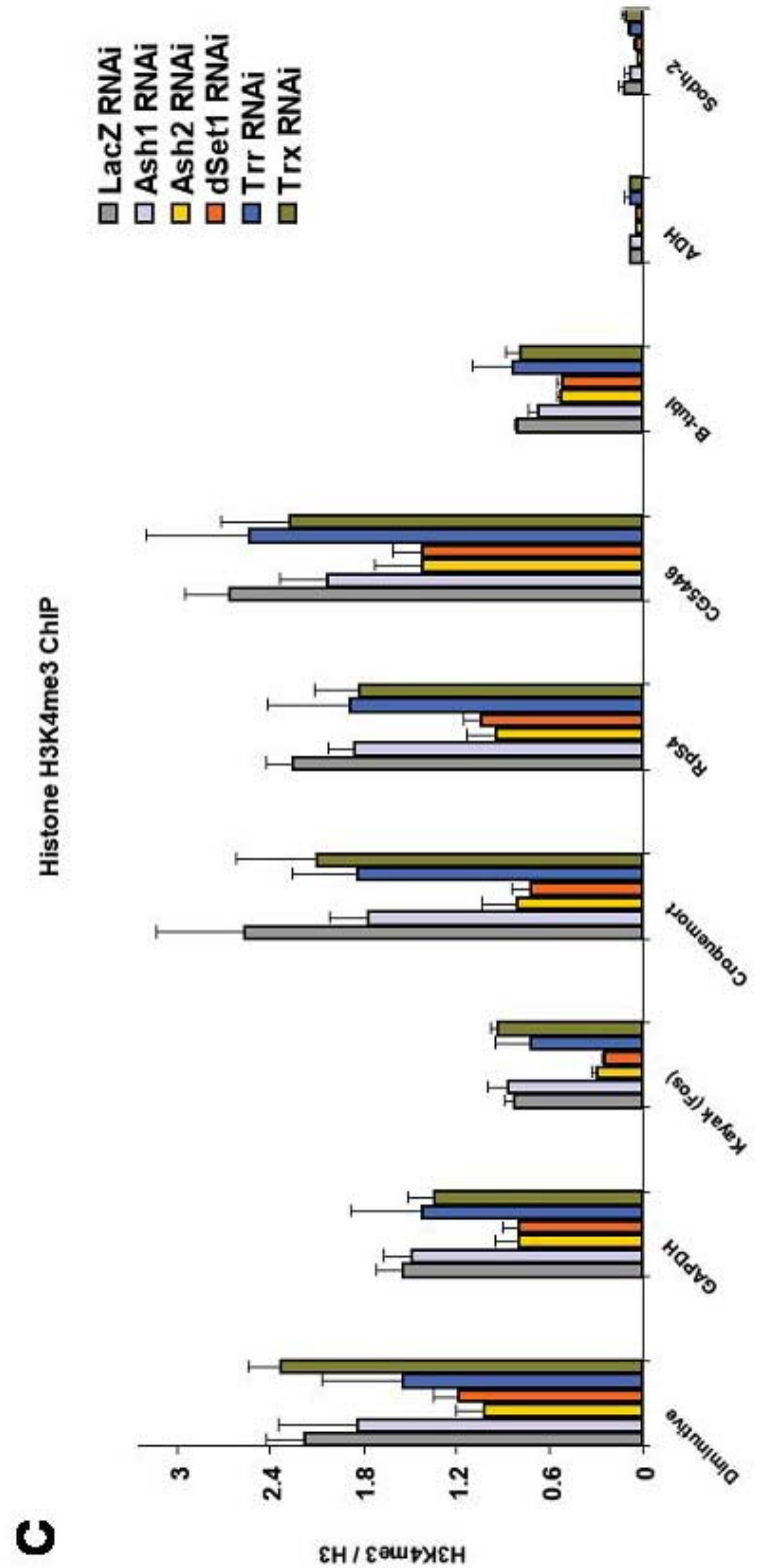

that dSet1 is predominantly a nuclear protein (Figure 3.3B). To verify specificity of GFP-Set1 association with normal sites on the chromatin, Janis Werner performed polytene co-immunostaining with antibodies against both GFP and dSet1 (kind gift of Dr. Thomas Kusch), on the progenies of a cross between GFP-dSet1 3rd-chromsome insert and salivary gland specific 6983-GAL4 driver line. Polytene staining results revealed that GFP and dSet1 show an almost indistinguishable pattern, indicating that GFP-dSet1 localizes to the loci on chromatin occupied by native Set1 (Figure 3.4A). In addition GFP-dSet1 mostly localized with decondensed regions of the polytene chromosome (Figure 3.4A). Unlike Trx, which has been reported to associate with about 20 loci on polytene chromomosome (Kuzin et al, 1994), we observe association of dSet1 with different intensity to more than 120 specific loci, including many interbands and puffs across the polytene chromatin (Figure 3.4A). Two of the notable loci associated with dSet1 include the ecdysone-induced developmental puffs and the 63B heat shock locus, as identified by John T. Lis. This widespread distribution on chromatin and the fact that dSet1 is required for H3K4me3, a mark associated with active transcription, led us to examine dSet1 colocalization with the transcriptionally-active Ser5-P form of RNA polymerase II. The two show a great degree of overlap on chromatin of fixed polytene chromosome (Figure 3.4B), providing evidence for possible involvement of dSet1 in transcription at many Pol II transcriptionally-active sites. As a control we also examined distribution of GFP signal on a line that does not express GFP-dSet1, as expected the signal intensity for the background line was much lower than what detected in the GFP-dSet1 line (Figure 3.4C). We also compared the genomic colocalization of dSet1 with both histone H3K4me3 and H3K4me1

modification marks. Both marks show a good degree of overlap with H3K4me3 and H3K4me1 marks (Figure 3.4D&E), with H3K4me3 showing a greater degree of colocalization with GFP-dSet1.

3.3.3 dSet1 is recruited to the heat shock loci shortly after induction

In addition to performing polytene immunostaining, we also examined the localization and distribution of dSet1 by live cell 2-photon laser scanning microscopy. Image acquisition and analysis for these experiments was carried out by Katie Zobeck. Prior to heat shock induction, maximum intensity projection of GFP-dSet1 and RFP-Rpb3 shows strong colocalization between these two confirming our previous observation by polytene coimmunostaining showing colocalization of dSet1 with Pol II (Figure 3.5A). We also see recruitment of GFP-dSet1 to the *Hsp70* heat shock-induced puffs (Figure 3.5A bottom panel). Analysis of the FRAP recovery profile of multiple random loci revealed that dSet1 shows intermediate levels of recovery suggesting that dSet1 association with bound loci is not completely stable (Figure 3.5B).

3.3.4 dSet1 is Required for maximal accumulation of mRNA from heat shock genes upon induction

To examine the functional role of dSet1 in transcription from *Hsp70* and other heat shock genes I treated S2 cells with dsRNA targeting LacZ (control), dSet1, Ash2, as well a combinatorial treatment with dSet1 and Ash2 dsRNA for maximal depletion of the H3K4me3 complex. Following a 5-day treatment, I harvested and heat shocked the cells, and carried out reverse transcription real-time PCR (RT-rtPCR) analysis on total RNA isolated from samples during a time course of heat shock induction.

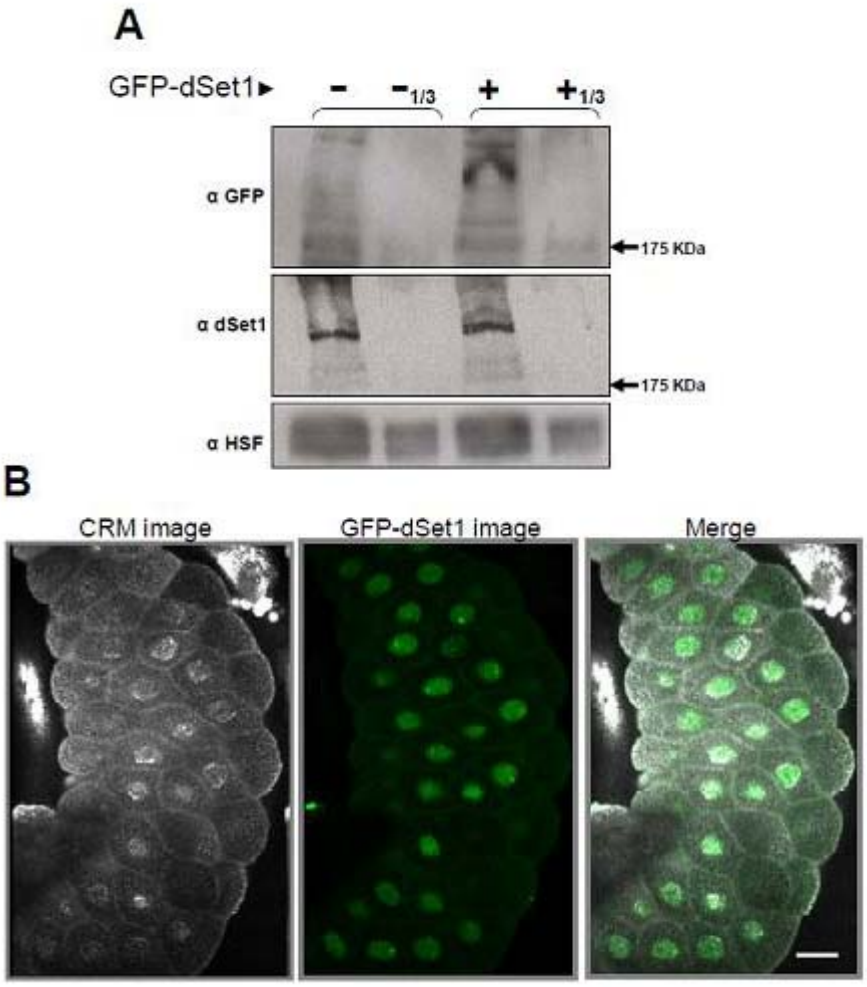

Figure 3.3 Verification of GFP-dSet1 expression and examining its cellular localization

A) GFP and dSet1 western blots performed on the salivary glands of the third instar 6983-GAL4 driver line (-) or the GFP-dSet1/6983-GAL4 line (+), HSF staining was used as a loading control. **B)** Confocal reflection microscopy (CRM) and GFP imaging showing nuclear localization of GFP-dSet1 in the salivary gland nuclei of GFP-dSet1;6983-GAL4 lines. The scale bar on the lower right corner of the merge image represents 100 μM.

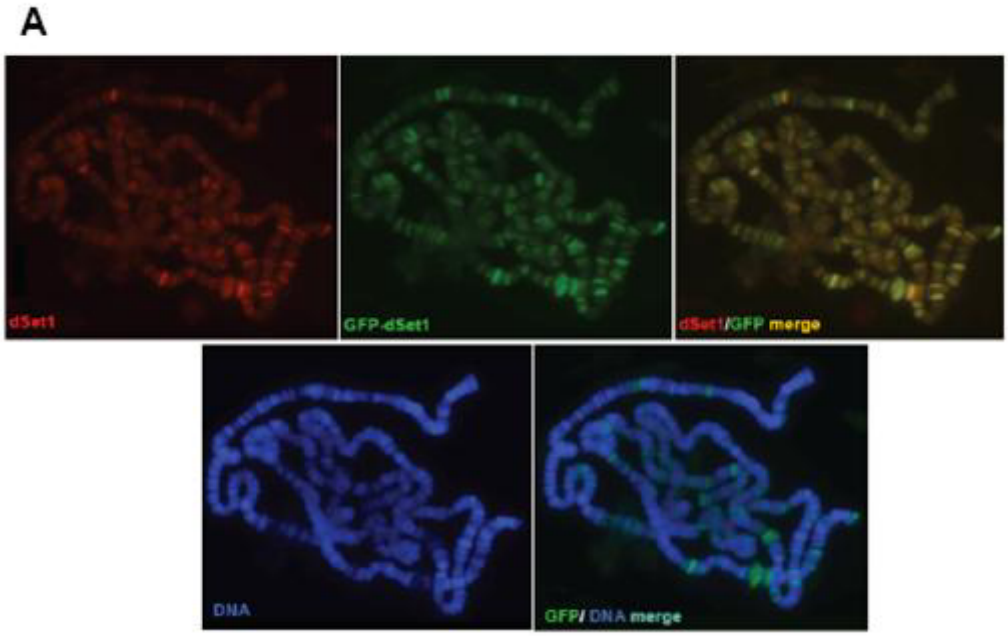

Figure 3.4 dSet1 is widely associated with transcriptionally active loci
A) Polytene immunostaining showing colocalization of Set1 and GFP signals and anticolocalization of GFP-Set1 with dense regions of chromatin as detected by DNA stain (Blue). **B)** Polytene stain showing overlap between transcriptionally engaged Pol II (Ser5-P Pol II) and GFP-dSet1. **C)** Control experiment showing specificity of the GFP signal for GP-dSet1 line, a fly line that lacks GFP-dSet1, does not show specific and robust staining with the GFP antibody. **D)** dSet1 shows a great degree of overlap with histone H3K4me3 mark and to a lesser extent with H3K4me1 **(E)**.

Figure 3.4 (continued)

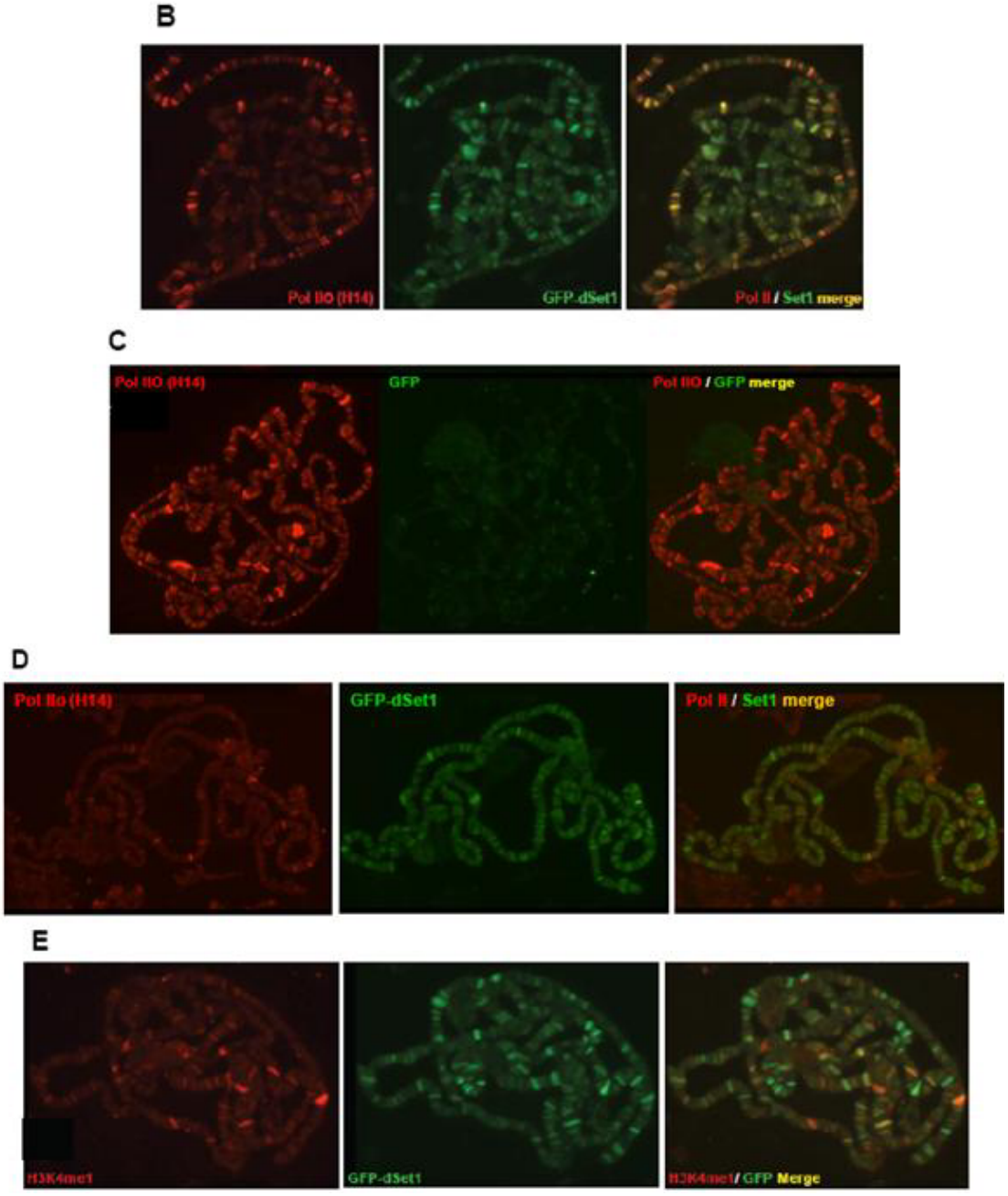

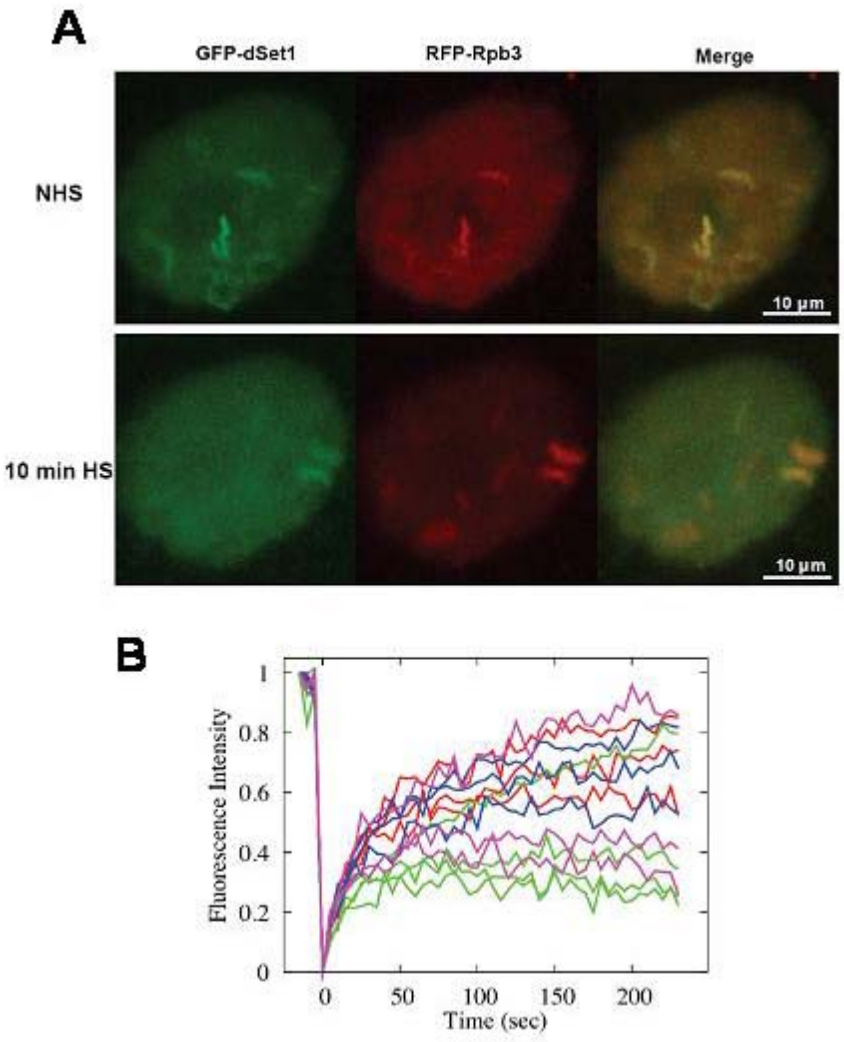

Figure 3.5 dSet1 is recruited to heat shock loci in living salivary-gland cells upon heat stress.
A) laser-scanning microscopy results showing maximum intensity projections reveal co-localization of dSet1 and Pol II prior and after a 10 min HS in living salivary gland cells. Arrows denote 87A & C heat shock loci. **B)** FRAP recovery plot showing recovery at multiple random loci (different recovery curves) in different nuclei (each color represents loci within a cell).

Analysis of mRNA levels revealed no difference between the control and other RNAi treatments before HS and 2.5 and 5 min after HS treatment (Figure 3.6A). However, dSet1 RNAi-treated cells had less mature *Hsp70* mRNA at 10 min after heat shock induction and this deficiency was also noticeable at 20 and 30 min after HS induction. Double knock-down of Ash2 and dSet1 showed a trend similar to dSet1 RNAi, where RNAi treatment affected mRNA production starting 10 min after HS induction (Figure 3.6A). Interestingly, the combinatorial knock-down of Ash2 and dSet1 resulted in even a greater decrease in the level of *Hsp70* mRNA to an extent that the mRNA levels were 1/3 of LacZ control samples 30 min after HS induction. Moreover, while in the LacZ RNAi control sample the *Hsp70* mRNA levels increased by 1/3 from 20 to 30 min after HS induction, the levels of *Hsp70* mRNA was slightly lower in the 30 min samples from dSet1 RNAi in comparison to the 20 min mRNA levels. dSet1 knock-down as well a Ash2 and dSet1 combinatorial knock-down also had a similar effect on *Hsp26* mRNA accumulation (Figure 3.6B), whereas *Hsp83*, which is not induced as robustly as *Hsp70* and *Hsp26* did not show much dependence on dSet1 for transcription (Figure 3.6C).

3.3 *Discussion and Perspectives:*

In this chapter I have presented evidence that the candidate gene CG40351 (dSet1), the closest ortholog of *S. Pombe* SET1, is required for tri and di methylation of bulk histone H3K4. RNAi KD of none of the other putative H3K4 methyltransferases results in as large as a loss in the bulk histone H3K4 trimethylation level. In addition, I show that at almost all tested active genes, depletion of only dSet1

and the methyltransferase core component Ash2, results in reduction of H3K4me3 of nucleosomes at the 5'-end of these genes. The fact that dSet1 KD decreases the global levels of H3K4me3 and the H3K4me3 levels at the promoter region of at all the tested active genes suggest that dSet1 may be required for trimethylation at many transcriptionally active loci. In fact our polytene immunostaining results provide further support for this notion, as we detect dSet1 at more than 120 different genomic loci and it also shows a high degree of overlap with transcriptionally engaged Pol II loci. We also report recruitment of dSet1 shortly after heat shock induction to the *Hsp70* heat shock loci and this association is dynamic in nature as determined by kinetic FRAP experiment.

Ash1, Trx and Trr are all essential genes that are critical for proper development in *Drosophila* (Beisel et al, 2002, Kuzin et al, 1994, Sedkov et al, 2003). Trx and Ash1 are part of a complex known as trxG factors that are required for activation and expression of homeotic genes during development (Schuettengruber et al, 2007). The contribution of these factors to expression of homeotic genes is thought to be through countering of the function of polycomb group repressors rather than acting as coactivators (Klymenko & Muller, 2004). In addition, different reports have demonstrated that these factors posses *in vitro* or *in vivo* H3K4 methyltransferase activity (Li et al, 2007). While trimethylation of histone H3K4 is known to be a hallmark of many transcriptionally active *Drosophila* genes (Schübeler et al, 2004a), it is not clear which one of the factors mentioned above is mainly responsible for H3K4me3 of histones associated with the 5'-end of active genes. A recent paper has reported presence of the N-terminal domain of Trx (termed TRX- N) at 4868

Figure 3.6 dSet1 is required for maximal accumulation of Hsp70 and Hsp26 mRNA upon thermal induction

A) Time course of *Hsp70* mRNA accumulation after heat shock induction in Lac*Z*, dSet1, Ash2 and dSet1 + Ash2 combinatorial dsRNA-treated cells as detected by oligo dT reverse transcription real-time PCR (RT-rtPCR). S2 cells were treated for 5-days with the corresponding dsRNA and instantaneously heat shocked for the indicated time point. **B)** Same as in A, but depicting the time course induction profile of *Hsp26* mRNA. **C)** Hsp83 mRNA time course induction profile. In all panels n=3 and error bars denote SEM.

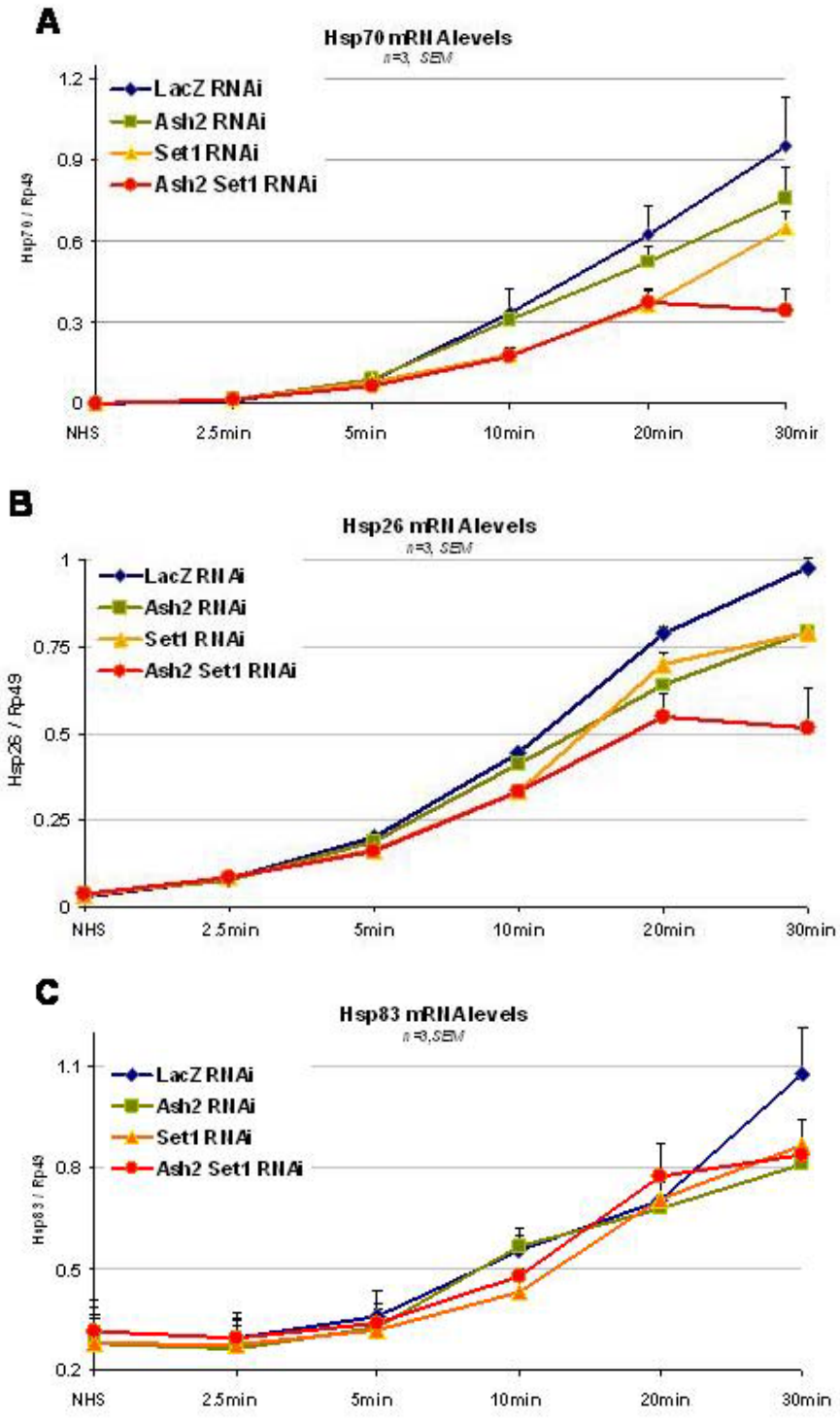
A
Hsp70 mRNA levels
n=3, SEM
LacZ RNAi
Ash2 RNAi
Set1 RNAi
Ash2 Set1 RNAi
Hsp70 / Rp49
1.2
0.9
0.6
0.3
0
NHS
2.5min
5min
10min
20min
30mir
B
Hsp26 mRNA levels
n=3, SEM
LacZ RNAi
Ash2 RNAi
Set1 RNAi
Ash2 Set1 RNAi
Hsp26 / Rp49
1
0.75
0.5
0.25
0
NHS
2.5min
5min
10min
20min
30min
C
Hsp83 mRNA levels
n=3,SEM
LacZ RNAi
Ash2 RNAi
Set1 RNAi
Ash2 Set1 RNAi
Hsp83 / Rp49
1.1
0.8
0.5
0.2
NHS
2.5min
5min
10min
20min
30min

genomic loci out of which, 3130 of these colocalize with H3K4me3 sites. In the same paper they only detect the C-terminal domain of Trx (TRX-C), the segment that contains the catalytic SET domain at only 167 genomic loci (Trx is proteolytically cleaved into two domains *in vivo)*(Schuettengruber et al, 2009). Moreover, the fact that RNAi KD of Trx does not decrease the trimethylation of bulk histone H3K4 suggest that Trx might not be the major methyltransferase responsible for H3K4 trimethylation at the majority of trimethylated sites.

The data presented in this chapter indicate that dSet1 is present at many transcribed loci, and it is recruited to the major heat shock gene, *Hsp70*. Many interesting questions remain to be answered regarding this factor. Future genome-wide analyses (ChIP-seq) could elucidate the genes to which this factor is recruited at high resolution. In human cells genes that lack classical TATA box are more dependent on H3K4me3 methylation for proper mRNA production (Vermeulen et al, 2007). While we did not detect any change in the level of mRNA level at genes that require dSet1 for H3K4me3 (including some TATA-less genes), future global transcriptome analyses could help shed light on the potential genes that require dSet1 for expression. The dSet1 also contains a RRM domain, which is known generally to associate with RNA in other molecules. In other organisms this domain has been shown to be critical for methylation (Schlichter & Cairns, 2005). It would be interesting to see how critical this domain is for H3K4me4 in *Drosophila*, and whether it interacts with any RNA molecule. In addition, it would be of great interest to understand how distribution of function among all these different H3K4 methyltransferases on chromatin is achieved and whether their essential function is mediated through their catalytic activity.

3.4 Materials and Methods

3.4.1 Cell culture and RNAi treatment

Cell culture and RNAi treatment was carried out as described in chapter 2. Double stranded RNA (dsRNA) was generated by in vitro transcription using T7 RNA polymerase. The following primer pairs were used for generating DNA templates by PCR:

LacZF:5'GAATTAATACGACTCACTATAGGGAGAGATATCCTGCTGATGAAG
C

LacZR:5'GAATTAATACGACTCACTATAGGGAGAGCAGGAGCTCGTTATCGC

Ash1F:5'GAATTAATACGACTCACTATAGGGAGCAAGAAAGTGAAGGTCAA
GCGCA

Ash1R:5'GAATTAATACGACTCACTATAGGGAATAGTGGTGCTTGCTCCTGT
TCCA

Ash2F:5'GAATTAATACGACTCACTATAGGGAAAAAACAATCGACAGAAAA
GGAAA

Ash2R:5'GAATTAATACGACTCACTATAGGGACTCGCTTATTTTCAGCTGTG
GT

Set1F:5'GAATTAATACGACTCACTATAGGGATCCAAACCGCAGTAGGGATC
GAAA

Set1R:5'GAATTAATACGACTCACTATAGGGAAGTCGCGAAATTCACGTTTG
ACGG

TrrF:5'GAATTAATACGACTCACTATAGGGATTAAGCCGCTCGACAAGAAT

Trr R: 5'GAATTAATACGACTCACTATAGGGACTGAGTTTGGTGGGCGTATT

TrxF: 5'GAATTAATACGACTCACTATAGGGAGCTTTCTCCAACAGGCAGTC

Trx R: 5'GAATTAATACGACTCACTATAGGGACCTTTGTCGTTTGAGGGTGT

3.4.2 Western Blot

For Western Blot cells were pelleted and lyzed in 1x SDS lysis buffer and the equivalent of $5x10^5$ cells (designated as 1) was loaded in each well (on 15% gel for histone H3 and its modifications, and 8% gel for detection of methyltransferases). The following antibodies were used at the following concentrations for detection: Abcam polyclonal rabbit antibody against histone H3 (ab1791) at 1:2000, Active motif rabbit anti histone H3K4me1 (cat#: 39298) at 1:4000, Active motif rabbit anti histone H3K4me2 (cat#: 39142) at 1:4000, Upstate rabbit polyclonal anti histone H3K4me3 (cat#:07-473) at 1:3000 (Figure 1 b, antibody b), Abcam mouse monoclonal anti histone H3K4me3 (ab1012) at 1:1000 (Figure 1b, antibody a). Rockland anti GFP antibody was used at 1:3000 for detection of GFP-dSet1 expression by Western Blot. In house polyclonal rabbit anti HSF antibody was used at 1:2000.

3.4.3 Indirect immunofluorescence:

Salivary glands were isolated from 6983-GAL4 third instar larvae (control) or 6983-GAL4/EGFP-dSet1. Glands were spread, fixed as described elsewhere (Schwartz et al, 2004)and stained with the following antibodies at the following concentrations: Abcam chicken polyclonal anti GFP (ab13970) at 1:50 dilution, guinea pig anti dSet1 at 1:50 dilution, anti H14 antibody (Covance) at 1:50 dilution. Rabbit polyclonal anti histone H3K4me3 (Upstate cat#:07-473) at 1:20, anti histone H3K4me1 (Active motif cat#: 39298) at 1:50. Image acquisition and data analysis was carried out using a Zeiss Axioplan 2 microscope and velocity imaging software.

3.4.4 Cloning of dSet1 and generation of EGFP-Set1

dSet1 cDNA was generated by performing oligo-dT reverse transcription PCR using superscript reverse transcriptase (invitrogen) on total RNA isolated from S2 cells using the RNaesy kit (Qiagen) followed by a 2 step SOE PCR using the following primer pairs:

SetI +1 F:

5'-ATGCAGGACGTTCGGAATATCAACCTGGTCAACAATTCCAGCAACAGCC

Set1 +5200 R:

5'-TTA GTT AAG TGT ACC CCG ACA TCC TTG GGC GCC GCATAGACAAGG

SetI +2600 F:

5'-CCAACCAAAAGAAATTTTTTGGAAAGAGATTTAAGTGACCAAGAGG

SetI +2600 R:

5'CCAAAAAATTTCTTTTGGTTGGTATAGGGCTAGGATGTTTTCTTATACGC

CG

3.4.5 Chromatin Immunoprecipitation

Chromatin IP was performed as described in (Adelman et al, 2005). For histone H3 IP, 2µl of Abcam rabbit polyclonal against histone H3 was used (ab1791) to pull down sonicated chromatin from $5x10^5$ cells and for histone H3K4me3, 10 µl of rabbit polyclonal anti histone H3K4me3 (Upstate cat#:07-473) to pull down H3K4me3 from $2.5x10^6$ cells from sonicated chromatin. SYBR-green Real time PCR experiments were done using on Roche LightCycler 480. The following primer pairs were used for ChIP signal detection.

Kayak-RA (D-Fos) -81F: 5'-AGTGGATAGCGGGAGAGACAGA

Kayak-RA (D-Fos) +51R: 5’-CTGCAGTCGCGTTTCAATAAGTT

GAPDH -57F: 5’-ATCGCCAGCGCCATTCT

GAPDH +13R: 5’-GCTATTACGACTGCCGCTTTTT

ADH -99F: 5’-CCCCCACGAGAGAACAGTATTTAA

ADH 1R: 5’-CGTTAGCCCGTCTGCTGAA

B-TUB56D -70F: 5’-CACTAAAACGGGATTTGCGTTT

B-TUB56D +11R: 5’-GGAGAGCGCGGGCTTT

Diminutive +190F: 5’-AAGTGCTAAATCCCAGAAATAACCTAA

Diminutive +274R: 5’-TTGTTTCTGCTTTGGAGAAGATTTTT

CG5446 F: 5’-CAGTGCCACAAAGAAGCCACAGAA

CG5446 R: 5’-CGCATTGCTGTTCAGGGAGTAGTT

Croquemort-RB F+38: 5’-GCACCAAAGGTAAAGGGACTAAGC

Croquemort-RB R+169: 5’-AGCATTAGCTTCTGATGGCTCTGT

Sodh-2 F +4: 5’-GCTAAATCGGCGTTCAAAGCGAAC

Sodh-2 R +83: 5’-GTCTGTTGCCATGATTACGCTTGGT

3.4.6 Reverse transcription real time PCR

Total RNA isolated using RNeasy kit (Qiagen) and 200ng was used for reverse transcription using superscript III reverse transcriptase (Invitrogen) and 50 pmol of oligo-dT. Realtime PCR detection was done using SYBR-green reagent on a Roche LightCycler 480 machine. The following primer pairs were used for detection of transcripts:

Ash1 F: 5’-ATGTGGATCCGTCGTTGCTGAAGA

Ash1 R: 5’-CAACCATCTTGGCCTGATGCTGTT

Ash2 F: 5’-TGGAGGAGCTGATCACAGAGCAAT

Ash2 R: 5’-ATTATCCAAGCGCAGACGTCCATC

Trr F: 5’-TCTTGAGTTCCCGCTAGCCATCAA

TrrR: 5’-CTTCGAATGCACGAACTGCTTGCT

Set1F: 5’-TAAGACTGGATGTGCGCGAACTGA

Set1R: 5’-GCTTCGCGGGAAATTCCTTGCATT

TrxF: 5’-AGCACATCATCATCTTTGCGCTGC

TrxR: 5’-TTTCGACGCCCAGCGTCATACTTA

For analysis of heat shock gene mRNA levels oligo dT was used for reverse transcription and +2210 and +3680 primer pairs (described in the previous chapter) were used for real time PCR analysis of *Hsp70* and *Hsp83* genes respectively. For real time PCR analysis of *Hsp26* mRNA levels, the following primer pairs were used:

Hsp26+580F: 5’-CAAGGTTCCCGATGGCTACA,

Hsp26+667R: 5’-CTGCGGCTTGGGAATACTGA,

CHAPTER 4

EXAMINNING PRESENCE OF PHYSICAL INTERACTION BETWEEN THE 5' AND 3'-ENDS OF *DROSOPHILA* HSP70 GENE BEFORE AND AFTER ACTIVATION

4.1 Introduction[3]*:*

Regulatory and enhancer elements are known to interact with regions of DNA that are sometimes several kilobases away (Murrell et al, 2004, Tolhuis et al, 2002). For instance, transcriptionally-active adult β-globin genes physically interact with enhancer elements that are 40-60 kb away in the locus control region (LCR) (Tolhuis et al, 2002, Vakoc et al, 2005). Emerging evidence from multiple model organisms has also provided evidence for physical interaction between the 5'and 3'-ends of genes (O'Sullivan et al, 2004). This type of interaction has been documented for a number of yeast genes including *BUD3* and *SEN1*. This interaction has been shown to require Ssu72 and Pta1, which are components of the CPF 3'-end processing complex, and is dependent on the phosphatase activity of Ssu72 (Ansari & Hampsey, 2005, O'Sullivan et al, 2004). In addition, a point mutation in the B finger domain of TFIIB (E62K) that genetically interacts with *Ssu72*, also disrupts loop formation between the 5' and 3'-end of the genes. Physical interaction between both ends of gene has also been

[3] Sections of this chapter have been published in Yao et al., 2007

reported for some genes in higher eukaryotes, including between the 5′-LTR promoter region and the 3′-LTR poly (A) of the HIV-1 provirus (Perkins et al, 2008)and also the relatively long human BRCA1 gene (Tan-Wong et al, 2008). It has been proposed that gene looping provides a platform for recycling Pol II molecules and factors involved in transcription. More recently, it was reported that during periods of transcription repression, gene loops serve as a memory mark, which allow for a more rapid transcription initiation once transcription resumes (Tan-Wong et al, 2009).

To examine the exchange dynamics of Pol II at the major heat shock genes in living salivary gland cells, Jie Yao a former graduate student in our lab performed FRAP analysis on GFP-Pol II at the heat shock loci (Yao et al, 2007). Photobleaching of EGFP-Pol II 5 min after heat shock induction revealed full recovery of the GFP-Pol II signal within 100 sec. Interestingly, when the experiment was performed at later time points after heat shock, a decrease was observed in the recruitment of unbleached Pol II molecules to the loci, to an extent that almost no recruitment could be detected after Photobleaching the loci 40 min after heat shock induction. Incorporation of 5'-bromouridine-5'-triphosphate (BrUTP) into nascent *Hsp70* mRNA chain at different time points after heat shock revealed that the heat shock loci of the polytene chromosome are transcriptionally active even 40 min after heat shock induction, ruling out the possibility that stalled Pol II molecules across the gene at 40 min post HS induction are preventing entry and elongation by unbleached Pol II molecules. One other possibility that could explain lack of recruitment of new Pol II molecules to the photobleached heat shock loci at later time points, is recycling of the photobleached Pol II molecules and their reentry into active transcription. Recent studies have

reported that the promoter and 3'-end of transcriptionally active genes are physically associated at certain genes (O'Sullivan et al, 2004). This association has been proposed to facilitate initiation of successive rounds of transcription. Therefore, I sought to determine if lack of recruitment of unbleached EGFP-Pol II molecules to the heat shock loci at later time points after heat shock is due to physical association between 5' and 3' ends of the *Hsp70* gene and recycling of photobleached Pol II molecules. The experiments described in the following sections were designed and performed to test presence of physical interaction between the two ends of *Hsp70* gene. This would help us determine whether the lack of Pol II recovery in FRAP experiments after a prolonged HS that has been observed at the Hsp70 loci of polytene chromosomes is a result of gene looping.

4.2 Results

4.2.1 Examining the association profile of HSF and dPcf11 at activated *Hsp70*

If a loop does indeed form between both ends of the activated *Hsp70* gene at later time points after heat shock, factors that normally associate with one end of gene should be detected at the other end of the gene by virtue of formaldehyde crosslinking of chromatin (Ansari & Hampsey, 2005). To address this question and examine existence of a physical association between both ends of *Hsp70* gene, I performed ChIP assays to check for presence of the HSF activator at the 3'-end of *Hsp70*. Likewise, I also checked for presence of dPcf11, a termination factor that is recruited to the 3'-end of the Hsp70 gene, at the promoter region of Hsp70 40 min after HS induction (Zhang & Gilmour, 2006). Results from these ChIP experiment in S2 cells

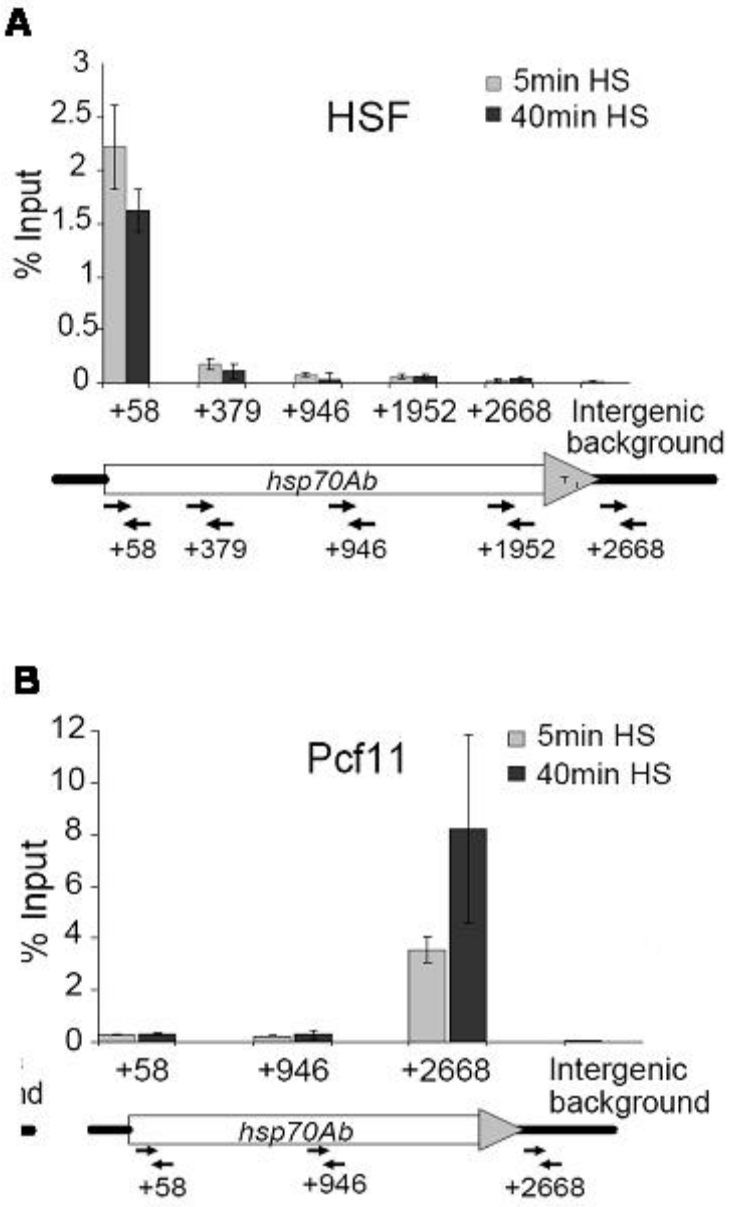

Figure 4.1: HSF activator and Pcf11 termination factor association with *Hsp70* 40min after heat shock induction in S2 cells.
A) HSF does not associate with the 3'-end of Hsp70 at later time points after heat shock. **B)** ChIP results showing association of the termination factor Pcf11 mainly with the 3'-end of the *Hsp70* gene.

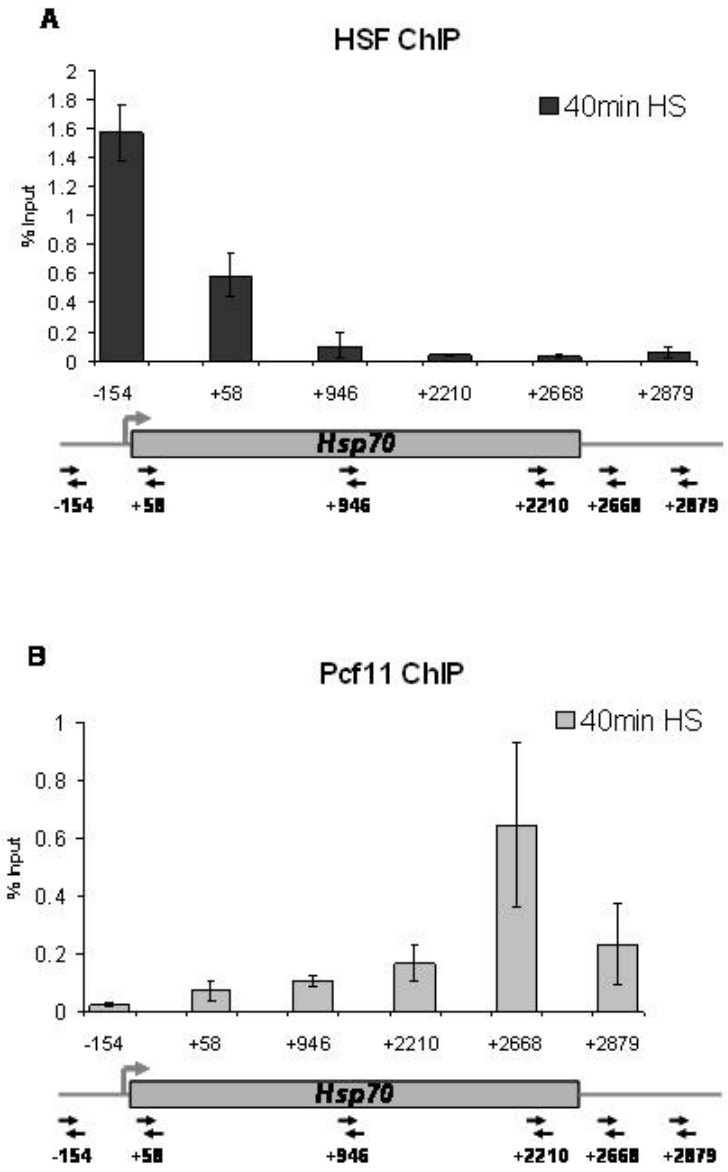

Figure 4.2: HSF and Pcf11 association profile with *Hsp70* 40min after heat shock induction in salivary gland cells.
A) HSF does not associate with the 3'-end of Hsp70 at later time points after heat shock. **B)** ChIP results showing association of the termination factor Pcf11 mainly with the 3'-end of the *Hsp70* gene.

showed no significant enrichment for HSF and dPcf11 at the 3'and 5'-end of the *Hsp70* gene respectively (Figure 4.1). Given that the FRAP experiment was performed on salivary gland cells, I also carried out this experiment in chromatin isolated from salivary gland, in which the chromatin has a dramatically different structure compared do normal diploid cells. Similar to what I observed in S2 cells, no significant enrichment was observed at the 3' end and the promoter region of *Hsp70* for HSF and dPcf11, respectively. These ChIP results suggest that the lack of recovery observed at later time points in the FRAP assay is not due to recycling of Pol II via a physical loop between both ends of the *Hsp70* gene.

4.2.2 Testing physical association between the promoter and 3'-end of the *Hsp70* by chromosome conformation capture (3C)

I also examined presence of physical association between both ends of the *Hsp70* gene by Chromosome (chromatin) Conformation Capture assay (3C). In this technique, the three dimensional architecture of chromatin is preserved by formaldehyde crosslinking. In the next Step, crosslinked chromatin is digested with a specific restriction enzyme, and the resulting chromatin fragments are diluted (to favor intramolecular ligation) and ligated. The newly ligated DNA is isolated and physical interaction between different regions is tested by PCR. An outline for this technique is illustrated in figure 4.3.

To test physical interaction between both ends of the *Hsp70* gene, I designed multiple primers flanking *MboI* cleavage sites throughout the body of *Hsp70Ab* gene. As depicted in Figure 4.4. Several controls were also included in the experiment to ensure accurate quantification and meaningful interpretation of the data.

a) To demonstrate that formation of each PCR product upon 3C processing is dependent on formaldehyde crosslinknig we tested amplification of PCR products in presence and absence of formaldehyde (figure 4.5).

b) I used radioactively-labeled primers to minimize PCR cycles (~ 30 cycles) and to ensure the PCR products are within the linear range of amplification.

c) I also normalized for PCR amplification efficiency between different primer pairs. For this purpose, a PCR product spanning the *Hsp70Ab* gene (from -836F to +2706R) was digested with *MboI* and ligated to generate an equimolar mixture of all possible intermolecular ligation products. Serial dilution of this randomly ligated DNA template was used to quantify and compare absolute interaction frequency between different regions of the *Hsp70Ab* gene (Figure 4.6). The interaction frequency of these fragments is not expected to be different before and after HS induction

d) Also, to control for cross-linking, cleavage and ligation efficiency, as well as any general modifications that may be caused in chromatin by thermal stress, I tested the interaction frequency between two neighboring *MboI* fragments from an intergenic region of cytological band 102B (fourth chromosome), using two forward primers (PA& PC) that were separated by one *MboI* cleavage site (Figure 4.6)

e) To confirm amplification of the right PCR fragment, the PCR products were also sequenced.

f) Physical interaction has been reported for the scs and scs' insulator elements, which flank the 87A loci. These insulators are about15kb apart. Therefore as a positive control for the 3C assay, I also checked interaction between these regions by 3C and verified amplification of the correct PCR product by sequencing.

I tested the frequency of interaction between the 5'-end with both the middle and also the 3' end of *Hsp70* using primer pairs described in figure 4.4 under three different conditions: NHS, 5'HS and 40'after HS induction. A serial dilution of control template was also used along with the experimental samples to control for the amplification efficiency of the primer pairs.

4.2.3 Prolonged heat shock results in a minute increase in the interaction frequency between the 5' and 3'-ends of *Hsp70*

Figure 4.6 shows results from the 3C assay. Compared to NHS, we detect an almost 2-fold increase in the interaction frequency between P2&P4 as well as P3&P7 after 5'and 40' heat shock induction (Figure 4.6). The values obtained from P3+P7 and P2+P4 PCR products were normalized to the PA+PC PCR products to control for crosslinknig, cleavage and ligation efficiency. This increase in interaction after HS, is likely to be due to recruitment of transcription factors to the heat shock loci (Fuda et al, 2009), which could enhance the crosslinknig efficiency between different regions of the DNA. We also detect a very small increase in the frequency of interaction between the 5' and middle of the *Hsp70* from 5 to 40 min (Figure 4.6). This interaction frequency increases to about 1.5-fold when we compare the P3&P7 PCR products between the 5 and 40 min samples. In addition, the frequency of interaction between the 5'-end and middle of *Hsp70* (P2&P4) is about 5-fold more than the interaction between both ends (P3&P7) of the gene. These observations along with the fact that after a prolonged heat shock there is no significant enrichment in association of dPcf11 and HSF with 5' and 3'-end of *Hsp70*, respectively, suggest that formation of a physical loop between the 5' and 3' of *Hsp70* genes is not likely to be a major

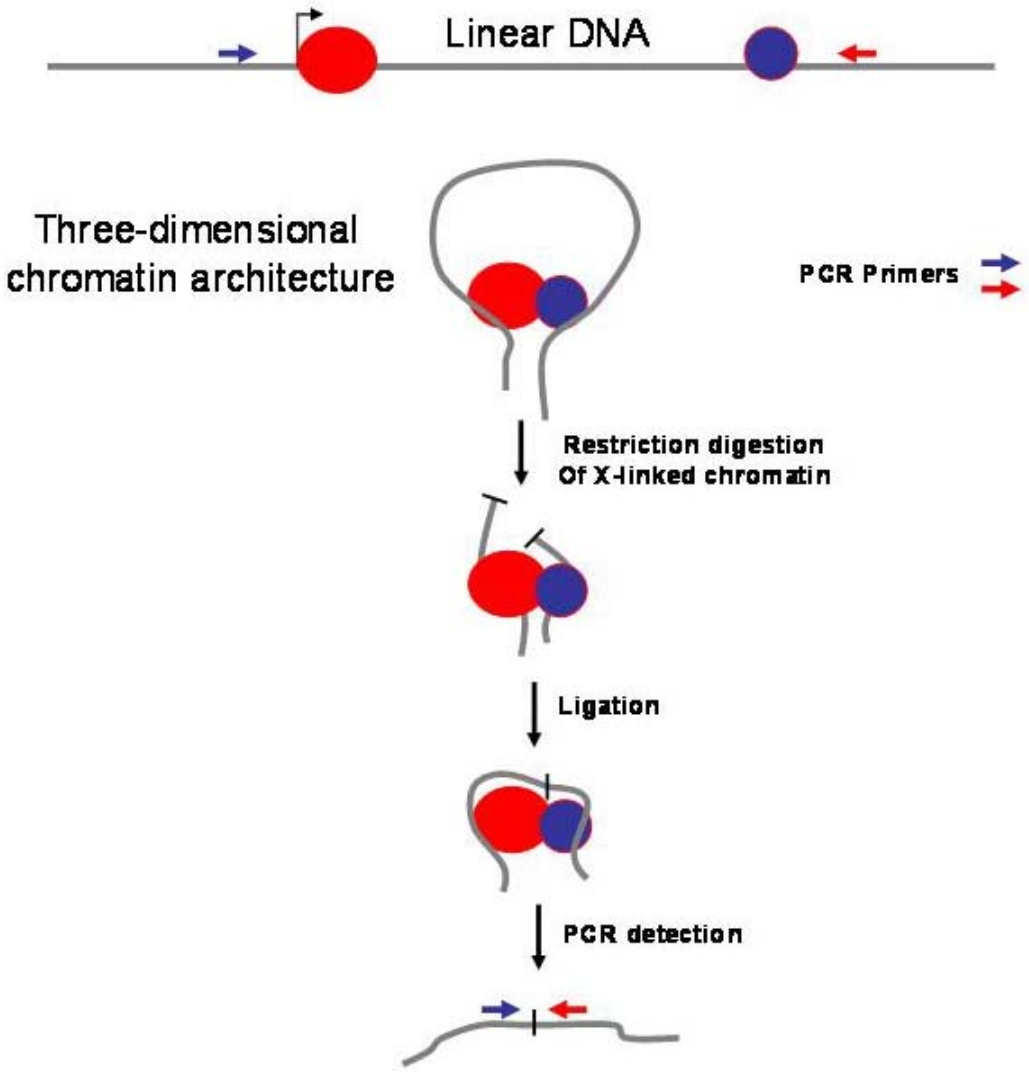

Figure 4.3 Graphic illustration of chromosome conformation capture assay

In this technique, crosslinked chromatin is restriction digested and the resulting fragments are diluted and ligated. To test physical proximity of different regions of the chromatin, the collection of newly formed ligation products are then interrogated using specific PCR primers that would not yield the correct PCR product if a non-processed DNA is used as a template. Colored circles represent chromatin bound proteins.

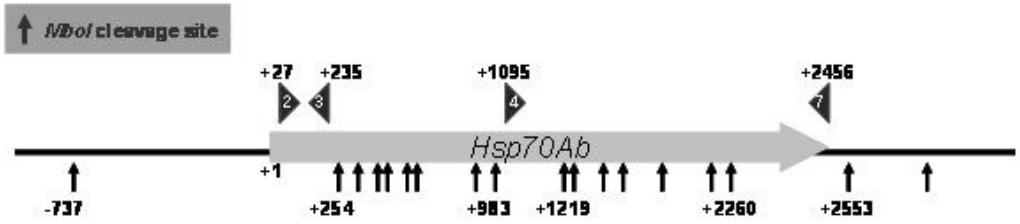

Figure 4.4: Illustration of *MboI* cleavage sites at *Hsp70Ab* and 3C primer pairs. Black vertical arrows represent cleavage sites across the *Hsp70Ab*. The position of those that flank the primers is shown relative to the transcription start site. Triangles represent 3C primers and their orientation. The numbers within the triangles represents their location relative to transcription start site.

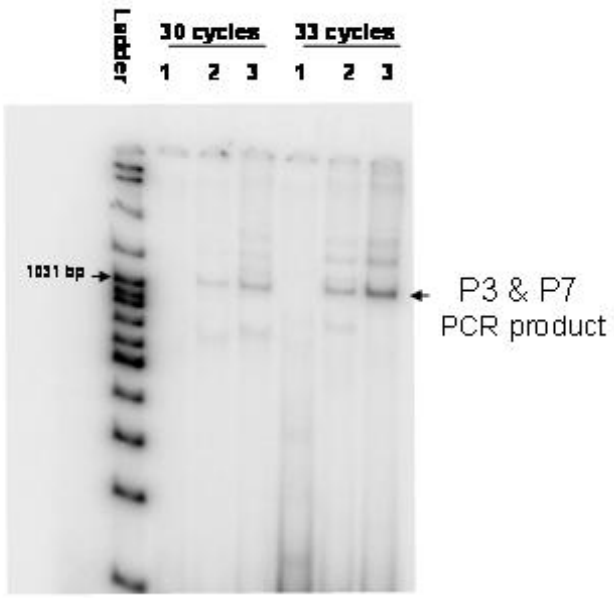

Figure 4.5 3C assay signal is dependent on formaldehyde crosslinknig. Non-crosslinked NHS templates were used for amplification for 30 or 33 cycles in lanes 1. Lane 2 and 3 are from crosslinked NHS and 40' HS samples respectively. Black arrow denotes a 1168bp PCR product amplified by primers P3 and P7.

mechanism that leads to efficient recycling of Pol II molecules at the *Hsp70* genes.

4.2.4 Recruitment kinetics of Pol II to the *Hsp70* gene in salivary gland cells

Two-photon laser scanning microscopy coupled with time series quantification of GFP-Pol II recruitment to the 87A and 87C heat shock loci, which harbor the *Hsp70* genes has revealed that Pol II recruitment to these sites increases after 5 min and reaches plateau at around 20 min after heat shock in salivary gland cells (Yao et al, 2007). This is in contrast with the observed intensity of Pol II signal on the body of *Hsp70* gene in S2 cells as detected by ChIP (Boehm et al, 2003). The ChIP results showed that the signal intensity of Pol II and the Ser-2P and Ser-5P forms of Pol II reaches peak at around 5 min after heat shock induction. While Pol II ChIP detects recruitment and association of chromatin bound Pol II molecules, 2-photon laser scanning microscopy imaging detects recruitment of molecules to a large locus and not all the detected molecules in these loci are necessarily bound to the chromatin. It is also possible that the Pol II molecules observed by imaging are chromatin bound and the difference in the recruitment kinetics could be due to the unique architecture of the polytene chromosomes or a property of salivary gland cells.

To discern between these possibilities, I performed ChIP analysis on crosslinked chromatin isolated from salivary gland nuclei. Isolated intact salivary glands were instantaneously heat shocked for the indicated time point and crosslinked. As expected, prior to heat shock the paused Pol II could be detected at the +58 region and no detectable signal could be seen on the body of the *Hsp70* gene. Interestingly, 5, 10 and 20 min heat shock induction experiments revealed that Pol II recruitment doesn't increase significantly beyond 5 min. For most tested regions, the 5 min signal

Figure 4.6 prolonged heat shock results in only a small increase in interaction between the 5' and 3' of *Hsp70* gene.

A) PCR products showing interaction between the 5' and 3'-ends of *Hsp70* (P3+P7) and 5'-end and middle of *Hsp70* (P2+P4) and a control region on the fourth chromosmes which was used for normalization of crosslinknig, cleavage and ligation efficiency (PA+PC). The serial dilution PCR products were amplified using a template pool that contained all possible *MboI*-cleaved ligation products at the *Hsp70* gene at equimolar amounts. **B)** Quantitation of interaction frequency by normalizing the P3+P7 and P2+P4 PCR products to the PA+PC PCR products. PCR products were quantified with imageJ and analyzed by Origin 7.0 (OriginLab).

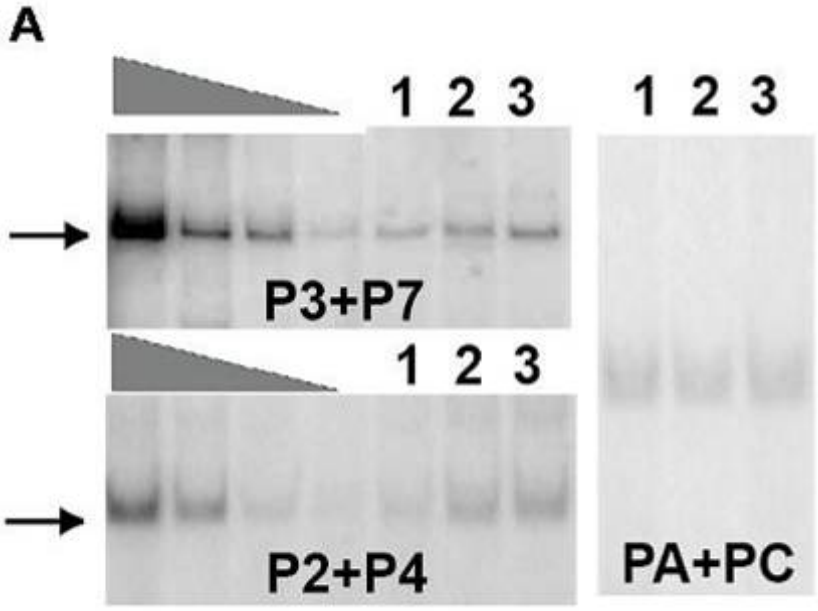
A
1 2 3
1 2 3
P3+P7
1 2 3
P2+P4
PA+PC

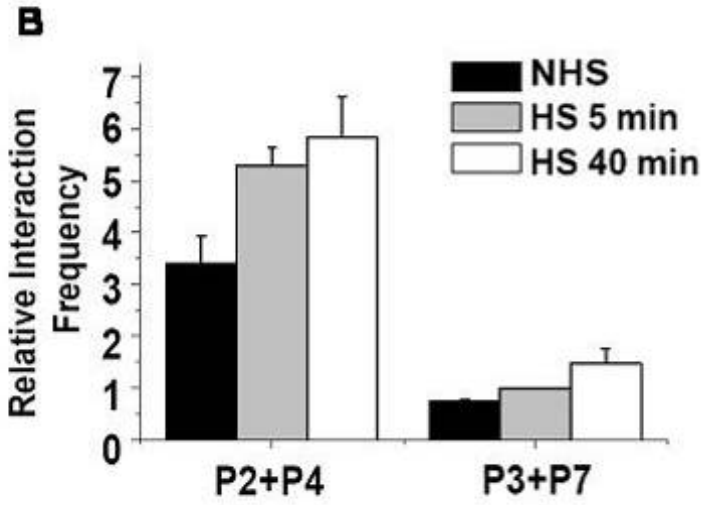
B
Relative Interaction Frequency
0
1
2
3
4
5
6
7
NHS
HS 5 min
HS 40 min
P2+P4
P3+P7

is higher or equal to what is detected after a 20 min heat shock induction. Therefore, similar to what was detected in S2 cells, in salivary glands the maximum intensity of Pol II is also detected at about 5 min after heat shock induction. Result from the salivary gland Pol II ChIP experiment suggest that the additional Pol II molecules that are recruited to the heat shock loci after 5 min, as detected by two-photon laser scanning microscopy are likely to not be bound to chromatin and are recruited to the heat shock puff loci.

4.3 Summary and Discussion:

In this chapter I presented experiments that were designed to determine the spatial organization of the *Drosophila Hsp70* gene. Formation of physical loop between the 5' and 3'-end of genes has been reported in different systems (Ansari & Hampsey, 2005, O'Sullivan et al, 2004, Singh & Hampsey, 2007, Tan-Wong et al, 2008). It has been proposed that this three-dimensional structure facilitates recycling of Pol II machinery, so that they could initiate additional rounds of replication (Ansari & Hampsey, 2005). More recent results suggest that this looping mechanism serves as a memory sign for inactive genes. Through this mechanism, inactive genes could reactivate more rapidly upon reinduction (Tan-Wong et al, 2009).

FRAP analysis of GFP-Pol II at the *Drosophila* heat shock loci 87A and 87C in revealed that Pol II molecules are recycled at the loci after prolonged heat shock induction (Yao et al, 2007). An attractive explanation for this recycling phenomenon is existence of a physical loop between the two ends of *Hsp70* gene. Therefore I tested

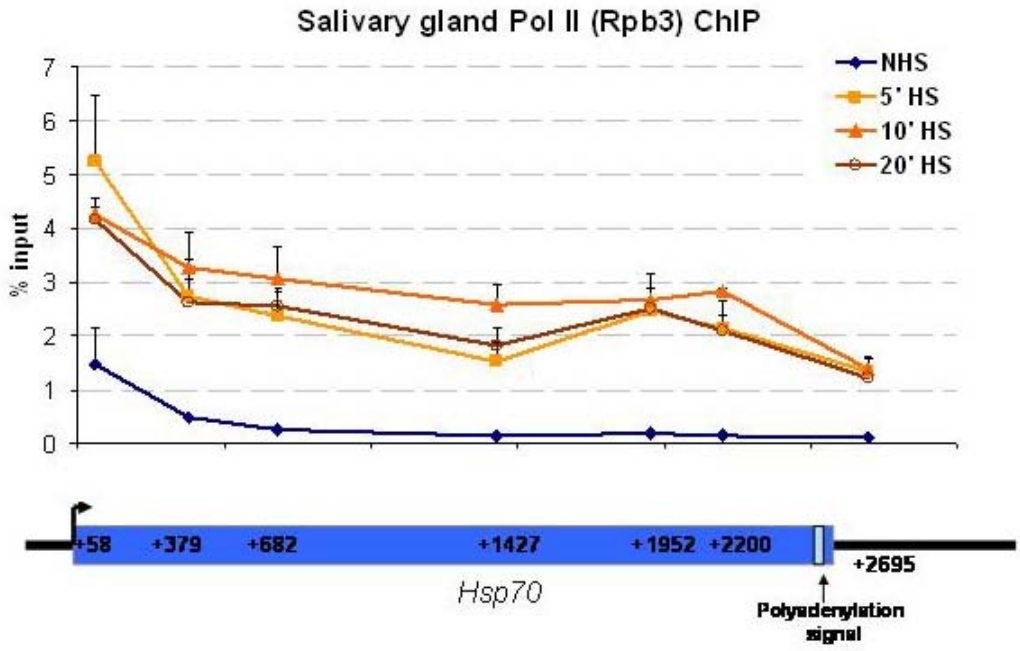

Figure 4.7 Kinetic ChIP analysis of Pol II distribution on *Hsp70* in polytene nuclei of salivary gland cells.

Intact glands were instantaneously heat shocked for the indicated time and processed for ChIP as described in the materials and method section. Different segments of *Hsp70* that were probed for presence of Pol II are aligned at the bottom directly below each graph point on the Hsp70 gene cartoon of the graph. N=4 for 5' and 20' HS samples and N=2 for NHS and 10 min HS samples. Error bars represent S.E.M.

this possibility by performing 3C and ChIP experiments. Using ChIP assay in both S2 cells and salivary gland tissue, I did not detect a significant signal (compared to adjacent regions) for HSF and dPcf11 at the 3' and 5'-end of the genes respectively. I also tested the physical interaction between both ends of the DNA by 3C assay. While a small increase was observed in the interaction frequency of both ends of Hsp70 gene after 40 min (Figure 4.6), this increase is likely not a result of loop formation between both ends. In instances where the two ends of a gene are physically linked, a much higher interaction frequency than the ~1.5-fold increase that we observe has been detected (Ansari & Hampsey, 2005, Singh & Hampsey, 2007). While it would also be informative to perform the 3C assay in salivary gland cells, our ChIP results in both salivary gland and S2 cells as well as our 3C assay in S2 cells indicate that physical interaction between the two ends of the *Hsp70* gene is not causal for recycling of Pol II molecules after prolonged heat shock inductions. Based on these results, it has been proposed that a "transcription compartment" is formed after prolonged heat shock, which ensnares Pol II and transcription factor molecules that are present at a high local concentration (Yao et al, 2007). The affinity of these transcription factors for polymerase and regulatory elements may also contribute to this compartment structure. The observation that Pol II molecules are continuously recruited to the heat shock loci up to 20 min after HS induction, while the Pol II ChIP signal on the body of Hsp70 gene saturates at 5 min is supportive of a compartment-like structure that could possibly accommodate non-chromatin bound Pol II molecules.

4.4 Materials and Method

4.4.1 Salivary gland and S2 cell Chromatin Immunoprecipitation

Salivary gland ChIP was carried out according to the following protocol: glands were first dissected in 50% Grace's medium and fat bodies were detached from the gland without damaging the salivary gland tissue. Salivary glands from 10 animals were transferred to a 1.5ml eppendorf tube containing 375λ of 50% Grace's medium. This yields enough material for 2 IPs (1 antibody and 1 no antibody control [3.5 larvae glands/IP]). Equal volume (375µl) of 48^{o}C medium was added to the heat shock samples for instantaneous heat shock, and after completion of heat shock, 50µl of 16% paraformaldehyde from the ampoules was added to each sample (1% final concentration of formaldehyde) and crosslink for 1 or 2min. samples were then quenched with 42.5λ of 2.5M glycine (0.125M final concentration) for 3min and samples were next placed on ice for a few more minutes (The glands tend to stick to the inner wall of the pipette tips, I tried to avoid pippeting up the glands while mixing the formaldehyde or glycine). Quenched samples were spun-down at 4000rpm for 3min in a tabletop centrifuge in the cold room. The supernatant was discarded and 100µl of the sonication buffer (described in previous chapters) was added to the samples. Contents were pipetted up and down multiple times to disintegrate the gland tissue and samples were left on ice for 10min. Sonication was carried out using the Bioruptor with the 1.5ml tube adaptors on high setting with 22sec On time and 60sec rest intervals for 15min. this yielded chromatin fragments with an average size of 300bp. Samples were spun down in the cold room for 5min at max speed, and the supernatants were used for IP. 35µl of the X-linked chromatin material (7 glands) was

used for each IP with the antibody of interest and another 35µl for the no antibody control. Also half of the volume (17.5µl) was stored to be used as input material. The preclearing, IP, washes, elution crosslink reversal, DNA precipitation and real time PCR analysis of the DNA was performed as described in the previous chapters.

ChIP assay was carried out as described in the previous chapters with the following modifications: to maximize crosslinknig efficiency of interacting regions of chromatin, heat shocked cells were not cooled down to room temperature prior to crosslinking and crosslinking was carried out for 10 min. Two µl of the HSF antibody and 3.5µl of the dPcf11 antibody were used for each IP. Tthe guinea pig dPcf11 antibody was the kind gift of Dr. David Gilmour that has been described previously (Zhang & Gilmour, 2006). The HSF antibody was a lab stock that has been described Previously (Saunders et al, 2003).

The following PCR primers were used for PCR detection of immunoprecipitated DNA

Hsp70 +334F 5'-CACCACGCCGTCCTACGT,

Hsp70Ab +423R 5'-GGTTCATGGCCACCTGGTT,

Hsp70Ab +645F 5'-ATATCTGGGCGAGAGCATCACA

Hsp70Ab +718R 5'-GTAGCCTGGCGCTGGGAGTC

Hsp70Ab +1363F 5'-CTGTGCAGGCCGCTATCC,

Hsp70Ab +1490R 5'-GCGCTCGATCAGCTTGGT,

hsp70Ab, +1925F: 5'-TGGACGAGGCTGACAAGAACT,

hsp70Ab,+1978R: 5'-ACCGGATAGTGTCGTTGCACTT,

hsp70Ab, +2631: 5'-TCGCAGACACCGCATTTGT;

hsp70Ab, +2706: 5'-ACCAATTGCAACAGAGACTGGAA;

hsp70Ab, +2796F:5'-CATTGCCCGGAATCACAGCAATCA;

hsp70Ab, +2961R:5'-AGCAAGAGCTTTGTGCAGTCCAAC

Other primers have been described in previous chapters.

4.4.2 Chromosome conformation capture (3C):

Heat shocked or non heat shocked S2 cells were spun down and the pellet was resuspended in 1ml of lysis buffer (10mM Tris [PH 8.0], 10 mM NaCl, 0.2% NP-40 and protease inhibitors) and placed on ice for 10 min and dounced 15 times. The dounced material was spun down at 3000 rpm for 5 min in a tabletop centrifuge in cold room. The nuclei pellet was washed once in 500µl of 1x restriction digestion buffer and the pellet was resuspended again in 1ml of 1x *MboI* digestion buffer (NEB buffer 3), which contained 0.1% SDS. Materials were incubated at 37^{o}C for 30 min and the SDS was then sequestered by addition of Triton X-100 to a final concentration of 1%. Digestion was performed O/N at 37^{o}C on 2.5x10^{6} nuclei in presence of 112.5U of *MboI* (NEB). The restriction enzyme was inactivated by adding SDS to a final concentration of 1.6% and incubating the reactions at 65^{o}C for 20 min. Samples were diluted 12 times in T4 DNA ligase reaction buffer (50mM Tris-HCl [pH 7.5], 10mM $MgCl_2$, 10mM DTT, 1mM ATP, 25µg/ml BSA) containing 1% Triton X-100. For ligation 1000U of T4 DNA ligase (NEB) was added to each reaction and samples were incubated at 17^{o}C for 8 hr.

To normalize for PCR efficiency between different primer sets for the purpose of comparative quantification, a PCR product spanning the *Hsp70Ab* gene (from -836F to +2706R) was digested with *MboI* and ligated to generate an equimolar

mixture of all possible intermolecular ligation products. Serial dilution of this randomly-ligated DNA template was used to quantify and compare absolute interaction frequency between different regions of the *Hsp70Ab* gene (Figure 4.6).

PCR primers were end-labeled with T4 Polynucleotide kinase (NEB) in presence of [γ-^{32}P] ATP and amplification was done for 30 cycles (94^{o}C at 60 s, 60 ^{o}C at 60 s, 72 ^{o}C at 90 s). The PCR products were separated by native PAGE (6%) and visualized using a phosphoimager. Signal intensity of the PCR products was analyzed by Jie Yao using the ImageQuant software (Molecular Dynamics). The following primers were used in the 3C assay:

Hsp70Ab +27F (P2) (5'GCTAAGCAAACAAACAAGCGCAGC),

Hsp70Ab +235R (P3) (5'GTGTGTGAGTTCTTCTTCCTCGGT),

Hsp70Ab +1095F (P4) (5'TGAGGGCCAAGACTTCTACACCAA),

Hsp70Ab +2456R (P7) (5'AGAATGTAGAATGAACCCATGT),

102B C F (5'AGCTGGTCCAAGTGAGACCGATAA),

102B A F (5'GTGAACGCAAATAGTTTGTATGGCT).

The same primer pairs that were described in Blanton et al., 2003, were used for detection of scs and scs' interaction.

APPENDIX A

TESTING THE RNAi KNOCK-DOWN EFFECT OF A SUBSET OF TRANSCRIPTION FACTORS ON INDUCED HSP70 RNA LEVELS BY NORTHERN BLOT

A.1 Introduction:

With the goal of furthering our understanding of transcription from heat shock genes, and in order to find the transcription factors that play role in production of *Hsp70* transcript upon induction, our lab embarked on performing a functional RNAi screen, in which we targeted more than 141 different putative transcription factors (Ardehali et al, 2009). These candidate genes were selected either based on presence of direct evidence for their recruitment to the *Hsp70*, or existing results from other gene systems or organisms indicating that these factors or their ortholog are implicated in transcription by Pol II. This RNAi screen was performed in two phases, the first part was a collaborative effort between Karen Adelman, Nick Fuda and me, and the second phase was performed by Steven Petesch, Nick Fuda and me. While we mainly used reverse transcription real time PCR (rt RT-PCR) assay as our readout for measuring the levels of *Hsp70* mRNA, I also performed Northern Blot analysis for the first phase of the screen. This was done to a) detect potential cryptic transcription from within the *Hsp70* gene in absence of specific factors, which would normally go

undetected in our rt RT-PCR assay b) identify potential transcription processing defects which would possibly manifest itself as a smear instead of a band c) in addition to the aforementioned notes, Northern Blot would also provide an independent means of confirming the rt RT-PCR results and measuring the *Hsp70* mRNA levels.

A.2 Results

RNAi treatment and Northern Blot assay was performed as described in the materials and method section of chapter 2. Prior to starting the screen and to ensure that the signals detected from the *Hsp70* RNA and U6 snRNA probes are in the quantitative linear range, I performed two control experiments. A serial dilution of total RNA was loaded on gel and transferred to the nitrocellulose membrane and RNA levels were quantified using radiolabeled RNA probes against Hsp70 and U6 snRNA. As shown in Figure A.1, *Hsp70* mRNA signals are within the linear range from 0.5 to 8 μg of total RNA and the U6 snRNA signal is within the linear range between 0.25 to 4 μg of total RNA. It is also worth noting that no detectable nonspecific signal could be observed when the membrane was incubated with either one of the probes, which allowed me to simultaneously probe for Hsp70 and U6 on each membrane.

For the RNAi screen, untreated and LacZ RNAi treated cells served as control for comparison of the *Hsp70* mRNA signal and HSF, CycT and Paf1 RNAi treatments were used as positive control for factors that are known to decrease the levels of induced Hsp70 mRNA to various degrees. Cells were heat shocked for 20 or 30 min. Representative Northern Blot membranes are shown in figure A.2, and the normalized

Figure A.1 **Testing the linear range of *Hsp70* and U6 RNA Northern Blot signals with different amounts of total RNA.**

A) The indicated amount of total RNA was loaded on a denaturing formaldehyde agarose gel and transferred to nitrocellulose membrane, the linear range of *Hsp70* mRNA detection, as detected with radiolabeled RNA probe was determined by analyzing the signal intensity of by ImageQuant software (table on right). The numbers on the left side of the gel denote the size of RNA ladder (single stranded RNA ladder, NEB). **B)** Same as in A, the membrane was probed for U6.

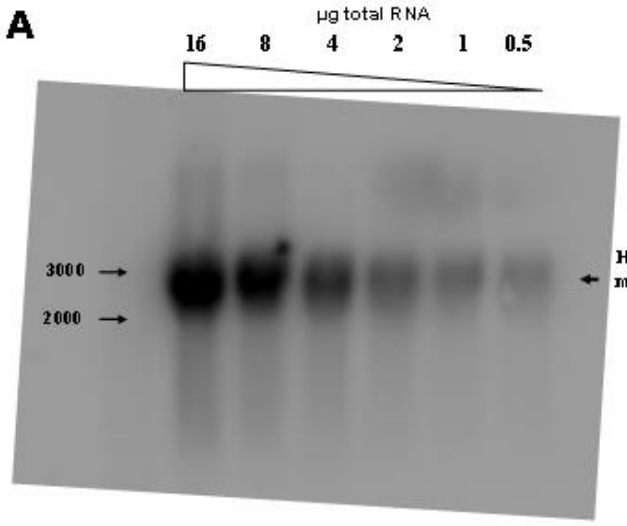

µg total RNA	Hsp70 mRNA signal intensity
16	29392780
8	20807019
4	10990440
2	5428880
1	2999532
0.5	1873466

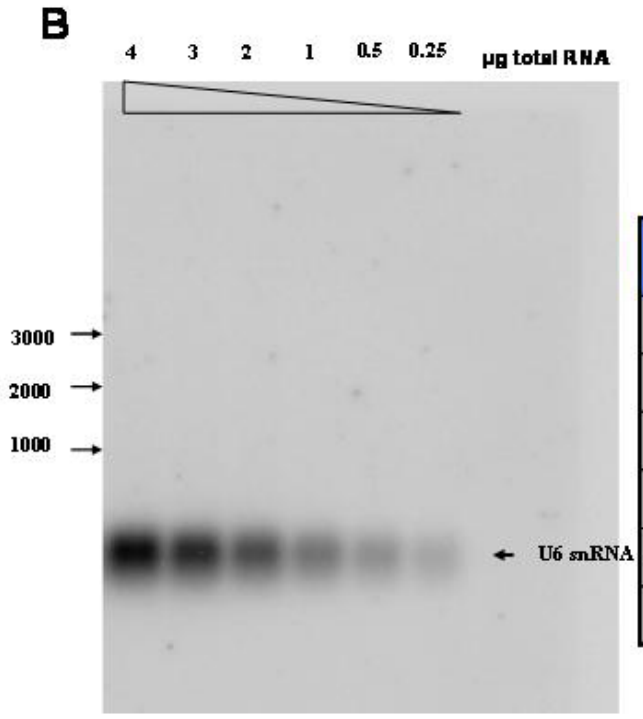

µg total RNA	U6 snRNA signal intensity
4	4614178
3	3406109
2	2131127
1	1029309
0.5	500354.8
0.25	212960.2

Figure A.2 **Induced *Hsp70* mRNA level of RNAi treated samples from the targeted screen, as detected by Northern Blot.**
(A-F) Northern Blot membranes from the RNAi screen experiment. Cells were heat shocked for 20 min (**A,B, E; F**) or 30 min (**C; D**) and 1-2 μg of total RNA from each RNAi treated sample was loaded in each well and the ratio of *Hsp70* to U6 was determined by quantification of the phosphoimager screen signal intensity by ImageQuant. The *Hsp70* mRNA level (ratio of *Hsp70* over U6 snRNA, a Pol III transcript) is shown directly below each lane. Factors, which their knock-down resulted in ~ 1/3 or more decrease in the levels of *Hsp70* mRNA are highlighted in red.

A

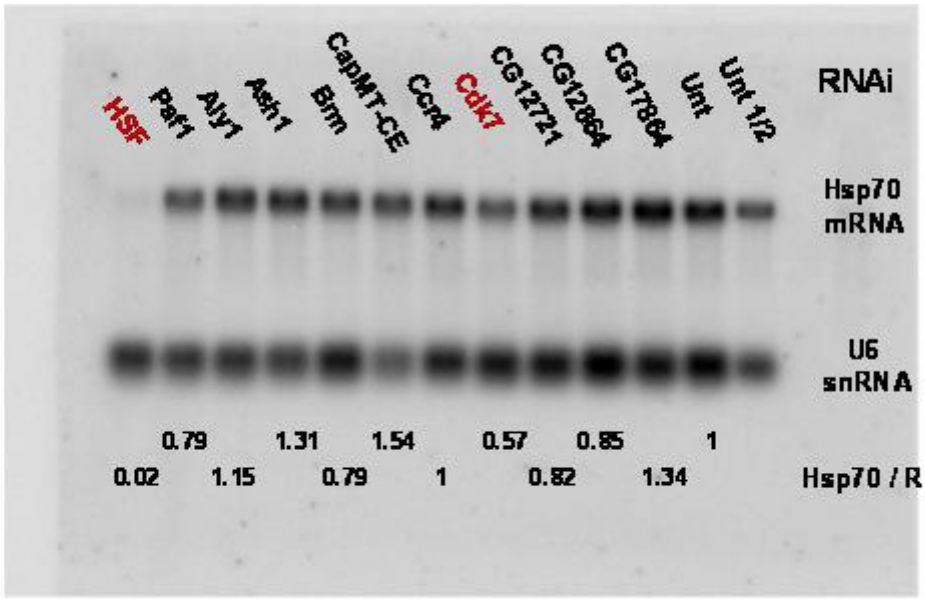
HSF
Paf1
Aly1
Ash1
Brm
CapMT-CE
CcrA
Cdk7
CG12721
CG12864
CG17864
Unt
Unt 1/2
RNAi
Hsp70 mRNA
U6 snRNA
0.79
1.31
1.54
0.57
0.85
1
0.02
1.15
0.79
1
0.82
1.34
Hsp70 / Rp49

B

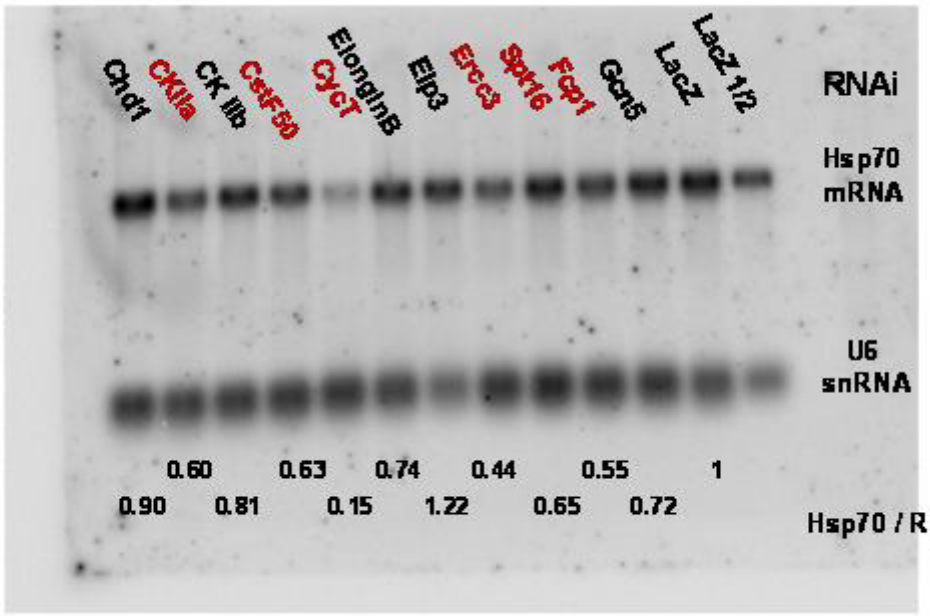
Chd1
CKIIa
CK IIb
CstF50
CycT
ElongInB
Elp3
Ercc3
Spt16
Fcp1
Gcn5
LacZ
LacZ 1/2
RNAi
Hsp70 mRNA
U6 snRNA
0.60
0.63
0.74
0.44
0.55
1
0.90
0.81
0.15
1.22
0.65
0.72
Hsp70 / Rp49

C

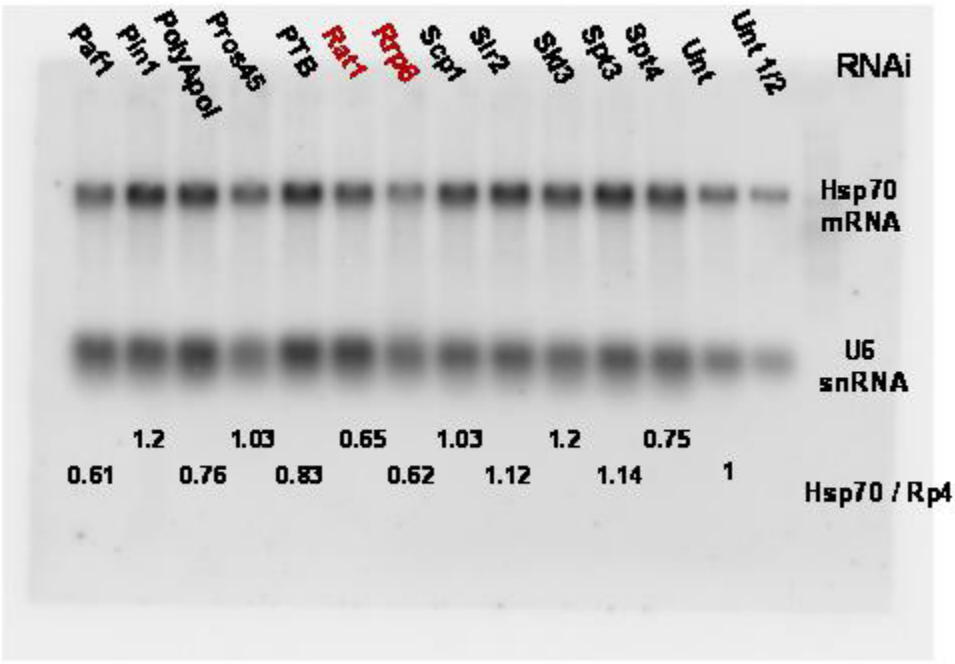
Paf1
Pin1
PolyApol
ProsA5
PTB
Rat1
Rrp6
Scp1
Slr2
SM3
Spt3
Spt4
Unt
Unt 1/2
RNAi
Hsp70 mRNA
U6 snRNA
1.2
1.03
0.65
1.03
1.2
0.75
0.61
0.76
0.83
0.62
1.12
1.14
1
Hsp70 / Rp49

D

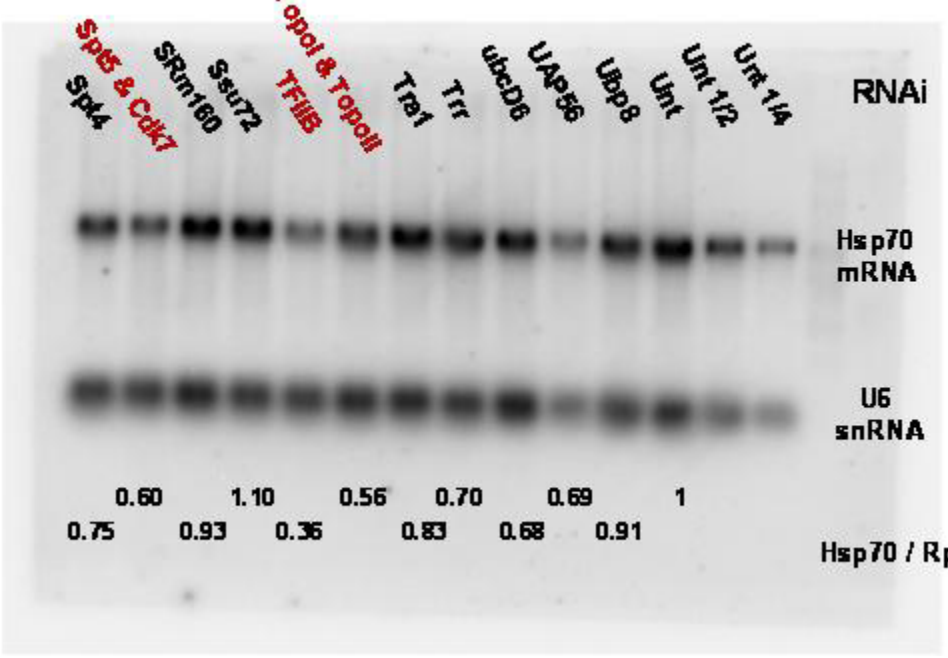
Spt4
Spt5 & Cdk7
SRm160
Ssu72
TFIIB
Topoi & Topoii
Tra1
Trr
ubcD6
UAP56
Ubp8
Unt
Unt 1/2
Unt 1/4
RNAi
Hsp70 mRNA
U6 snRNA
0.60
1.10
0.56
0.70
0.69
1
0.75
0.93
0.36
0.83
0.68
0.91
Hsp70 / Rp49

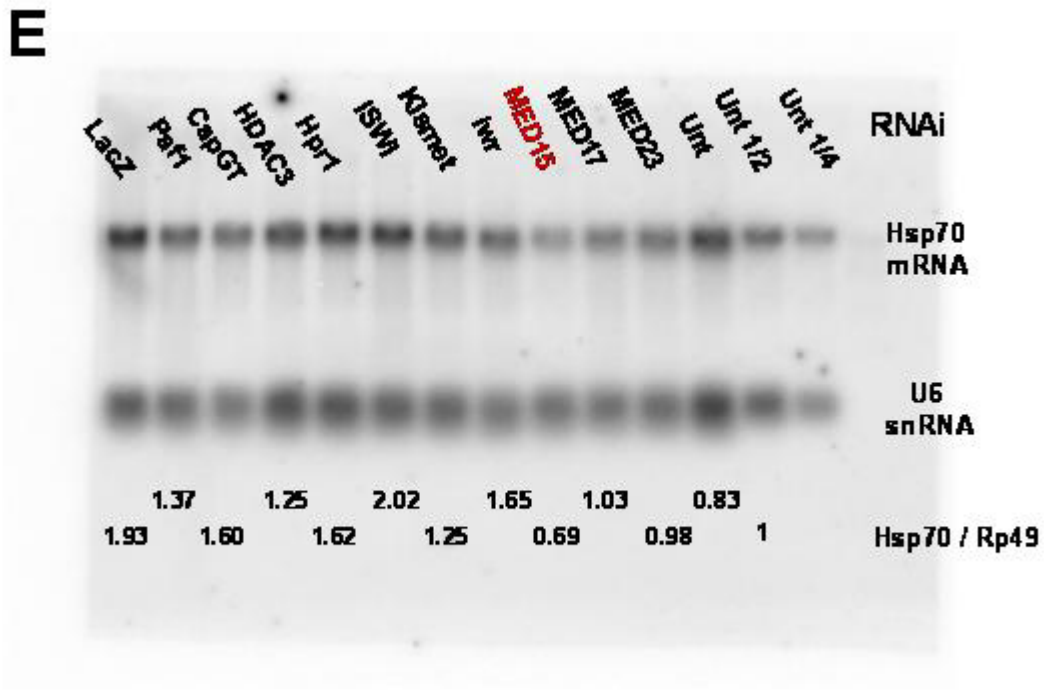
E
LacZ
Paf1
CapGT
HDAC3
Hpr1
ISWI
Ktenet
Int
MED15
MED17
MED23
Unt
Unt 1/2
Unt 1/4
RNAi
Hsp70 mRNA
U6 snRNA
1.37
1.25
2.02
1.65
1.03
0.83
1.93
1.60
1.62
1.25
0.69
0.98
1
Hsp70 / Rp49

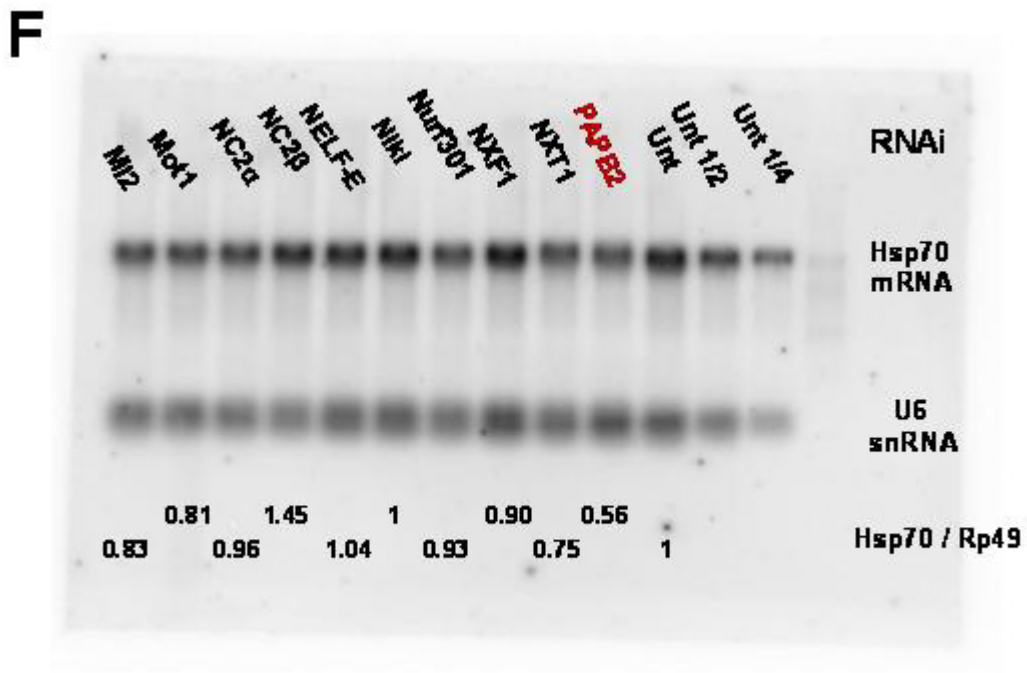
F
Mi2
Mot1
NC2α
NC2β
NELF-E
NiM
Nurf301
NXF1
NXT1
PAPB2
Unt
Unt 1/2
Unt 1/4
RNAi
Hsp70 mRNA
U6 snRNA
0.81
1.45
1
0.90
0.56
0.83
0.96
1.04
0.93
0.75
1
Hsp70 / Rp49

Hsp70 mRNA levels are depicted below each lane. For each membrane, normalized *Hsp70* mRNA levels for untreated or LacZ treatment were set to 1 (Figure A.2).

A.3 Discussions

While knock-down of several of the factors in the screen resulted in a decrease in accumulation of mature *Hsp70* mRNA (Figure B.2, highlighted in red), I did not detect formation of cryptic transcripts in any of the knocked-down samples from the upstream of the Hsp70 probe (~ +1700). In addition, judging from absence of smear in the *Hsp70* signal, no apparent processing defect could be detected.

All together, the Northern Blot experiment provided another means for measuring the *Hsp70* mRNA level of the RNAi-treated samples and in most part the results from this experiment corroborated the results obtained from the reverse transcription real time PCR assay (table 2.1). Some factors such as PAPB2 and Rat1 were identified as factors that positively stimulate transcription from *Hsp70* by Northern Blot, but not by rt RT-PCR. While a factor like HDAC3 was identified by rt RT-PCR as a positive hit, but not with Northern Blot. It is possible that the differences between the assays are within the error range. However, given that the loading control genes are Pol II and Pol III transcribed for rt RT-PCR and Northern Blot, respectively, it is also likely that RNAi KD of a certain factor also modulates the RNA level of Rp49 or U6 snRNA but not both, which leads to variation in mRNA readout.

APPENDIX B

EXAMINING THE DISTRIBUTION PATTERN AND ROLE OF HISTONE H3 LYSINE 79 METHYLATION IN TRANSCRIPTION FROM DROSOPHILA HSP70 GENE IN S2 CELLS

B.1 Introduction:

Covalent histone modification at specific residues has been shown to facilitate modulation of chromatin structure. Some of these modifications are associated with active transcription whereas others are linked to repressed chromatin marks (Campos & Reinberg, 2009). Genome-wide experiments in different organisms have revealed that one of these marks, histone H3K79 methylation, is associated with the body of actively transcribed genes. A global analysis in yeast has shown that H3K79me3 is enriched on the body of transcriptionally active gene. While, another ChIP on chip study carried out in *Drosophila*, revealed that H3K79me2 is present on the body of transcriptionally active gene and the extent of methylation is positively correlated with gene expression (Schübeler et al, 2004a). It must also be noted that a separate global ChIP-Seq analysis did not find enrichment of H3K79 methylation on the body of transcriptionally active genes in human T cells. This discrepancy could partly be due to utilization of different antibodies in these separate experiments. Grappa is the *Drosophila* ortholog of yeast H3K79 methyltransferase, DOT1. Interestingly, mutation

in *Grappa* results in phenotypes similar to both Trithorax and polycomb group factors, which have opposing functions.

Given that a ChIP on chip analysis in *Drosophila* Kc cells had revealed association of H3K79me2 with transcriptionally active genes, I sought to check the H3K79me2 status at the transcriptionally active *Hsp70* gene and also examine requirement of Grappa, the H3K79 methyltransferase for efficient expression of the Hsp70 gene.

B.2 Results:

B.2.1 Grappa decrease the cellular levels of H3K79me2

I first checked the cellular levels of H3K79me2 in LacZ control and Grappa RNAi treated samples. As shown in figure B.1., RNAi KD of Grappa results in greater than 70% decrease in the global levels of H3K79me2, given that I did not have any antibody against this factor, I could not verify KD of Grappa by Western Blot. The decrease in H3K79me2 was therefore used as an indirect measurement of Grappa KD. In yeast it has been reported that H3K79 methylation is dependent on presence of Paf1 and Rtf1, components of the Paf1 Complex (Krogan et al, 2003). To test and see if loss of Paf1 in S2 cells results in a decrease in H3K79me2, I checked the global level of this mark in S2 cells that were depleted of Paf1 and Rtf1. Interestingly, no detectable decrease was observed in the levels of histone H3K79me2 (Figure B.1B).

Next I sought to look at the distribution of H3K79 methylation mark on the body of *Hsp70* and at the scs and scs' boundary elements. The antibody was first

titrated for ChIP and I performed ChIP with primer pairs that recognized different regions of *Hsp70Ab*, scs and scs' boundary elements. Prior to heat shock, the highest K79 methylation signal was observed for a region within the scs' boundary elements, higher than the signal detected for the +946 region of *Hsp70Ab* gene. While heat shock resulted in about a 2-fold increase in the density of H3K79me2 within the body of Hsp70 gene, the density of H3K79me2 was still at least 4-fold higher at the scs' *BamHI* primer pair region. In addition, RNAi knockdown of Grappa resulted in about a 10-fold decrease in the density of H3K79me2 at all tested regions, indicating that Grappa is responsible for H3K79 methylation at the 87A heat shock locus. It must be noted that the non-heat shock results are untreated samples, whereas the 10 min HS samples are LacZ RNAi control.

Hsp70Ab, scs and scs' boundary elements. Prior to heat shock, the highest K79 methylation signal was observed for a region within the scs' boundary elements, higher than the signal detected for the +946 region of *Hsp70Ab* gene. While heat shock resulted in about a 2-fold increase in the density of H3K79me2 within the body of Hsp70 gene, the density of H3K79me2 was still at least 4-fold higher at the scs' *BamHI* primer pair region. In addition, RNAi knockdown of Grappa resulted in about a 10-fold decrease in the density of H3K79me2 at all tested regions, indicating that Grappa is responsible for H3K79 methylation at the 87A heat shock locus. It must be noted that the non-heat shock results are untreated samples, whereas the 10 min HS samples are LacZ RNAi control.

Given that H3K79me2 increases on the body of Hsp70 gene upon heat shock, I sought to test the effect of Grappa KD on production of mature *Hsp70* transcript. I checked

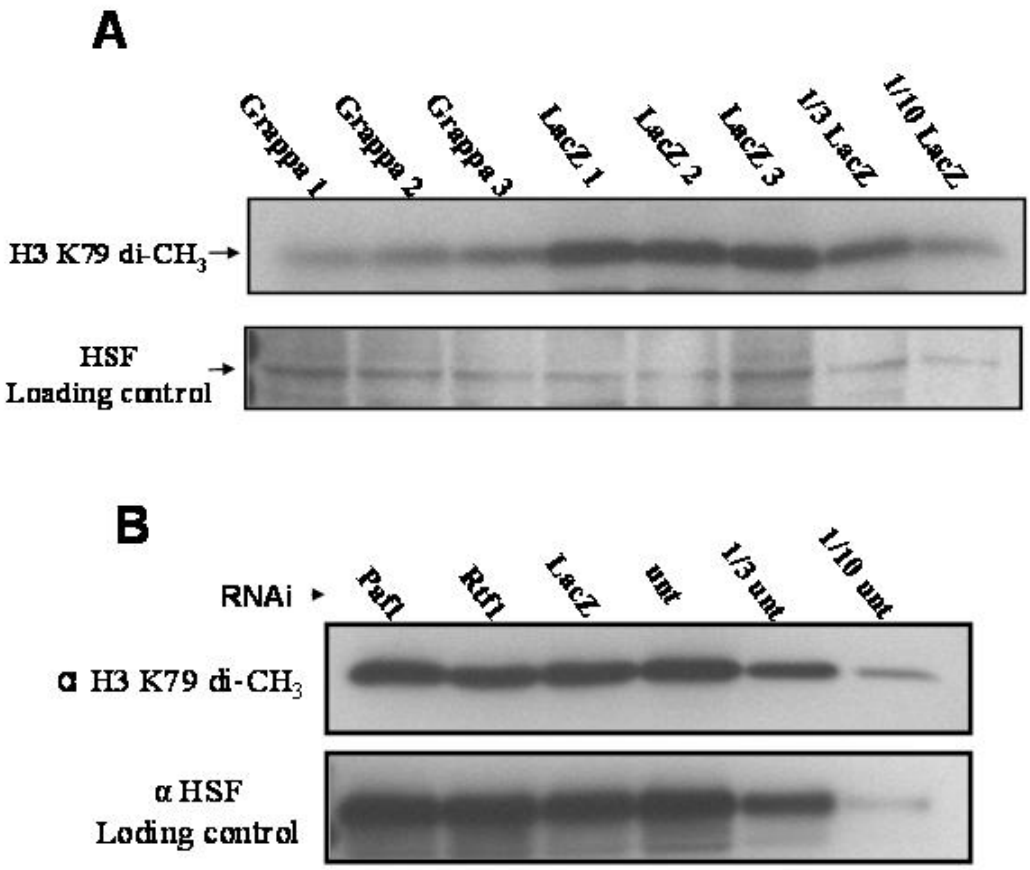

Figure B.1 RNAi KD of grappa decrease the cellular levels of H3K79me2
A) Western Blot experiment showing the cellular levels of histone H3K79me2 in grappa RNAi KD cells. Each lane represents an independent RNAi samples. HSP antibody was used as a loading control. **B)** Western Blot showing the levels of H3K79me2 in Paf1 and Rtf1 RNAi treated cells, KD of Paf1 and Rtf1 are not shown, but are comparable to the knockdown shown in Chapter 2.

Figure B.2 H3K79 predominantly localizes to the scs' boundary element
The density of H3K79me2 was tested by ChIP at the *Hsp70Ab* as well as the scs and scs' boundary elements. A) prior to heat shock the highest density for H3K79me2 was observed at scs' (scs' & scs'-*BamHI* primers), error bars denote standard deviation of 3 independent ChIP experimets . B)values same as in A but normalized to the histone H4 levels at the corresponding loci (n=3 for H3K79me2 levels, n=1 for histone H4 level). C) H3K79me2 ChIP signals at the same regions after heat shock induction in LacZ and Grappa RNAi treated samples (n=1). 87C or (87C 32442) denotes the background region signal.

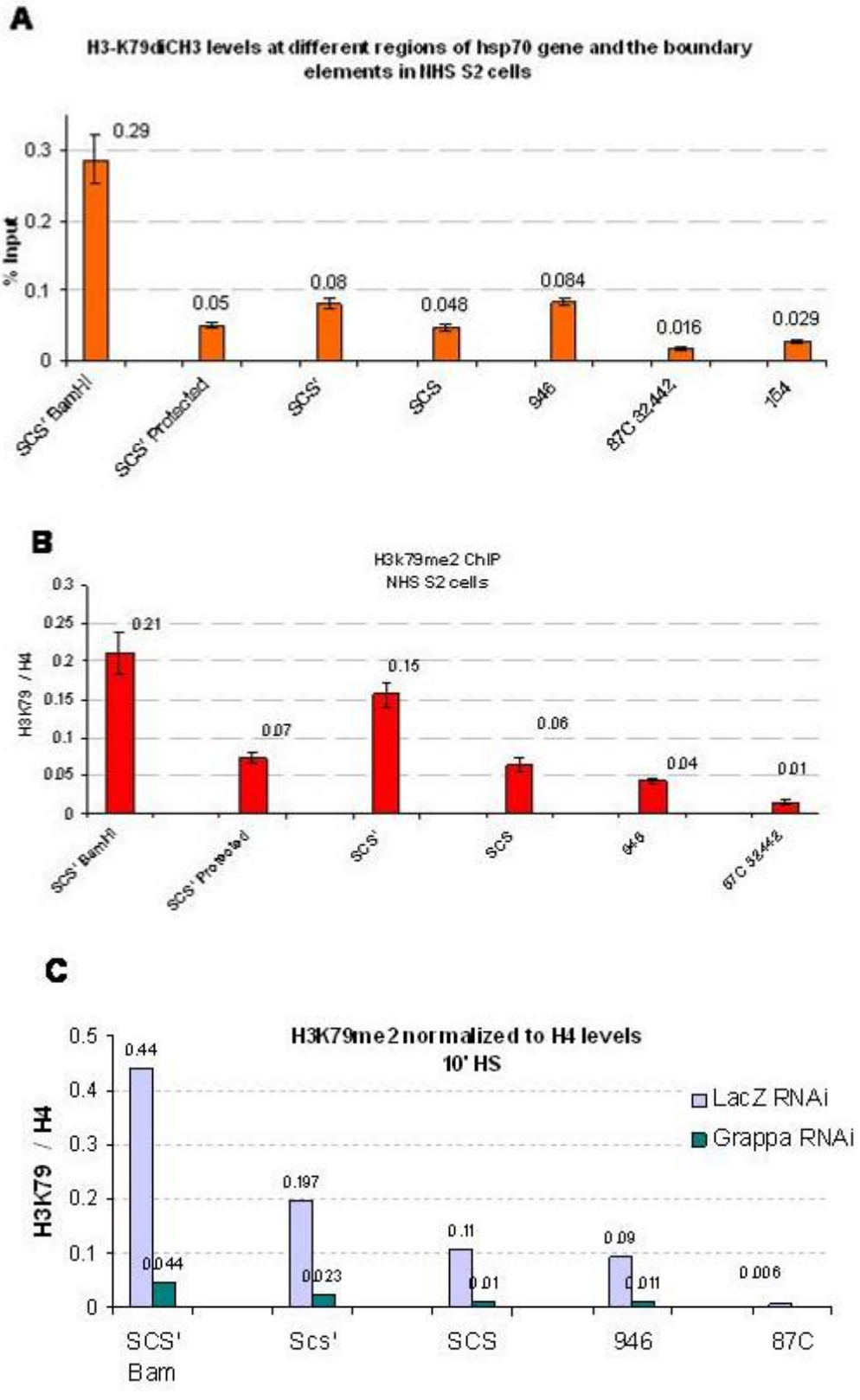
A
H3-K79diCH3 levels at different regions of hsp70 gene and the boundary elements in NHS S2 cells
% Input
0.29
0.05
0.08
0.048
0.084
0.016
0.029
SCS' BamHI
SCS' Protected
SCS'
SCS
946
87C 32442
154
B
H3k79me2 ChIP
NHS S2 cells
H3K79 / H4
0.21
0.07
0.15
0.06
0.04
0.01
SCS' BamHI
SCS' Protected
SCS'
SCS
946
87C 32442
C
H3K79me2 normalized to H4 levels
10' HS
H3K79 / H4
LacZ RNAi
Grappa RNAi
0.44
0.044
0.197
0.023
0.11
0.01
0.09
0.011
0.006
SCS' Bam
Scs'
SCS
946
87C

the level of *Hsp70* mRNA 30 min after heat shock by reverse transcription real-time PCR. RNAi KD of Grappa results in only about a 17% decrease in induced *Hsp70* mRNA level, which is within the error range of the assay (Figure B.3).

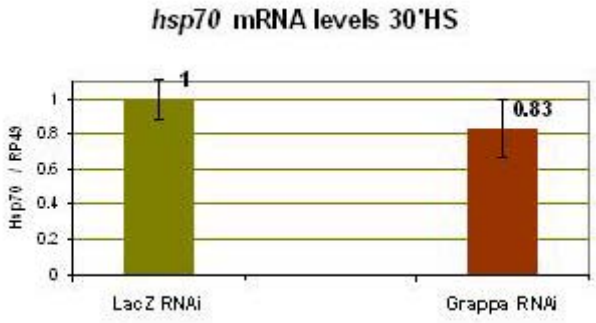

Figure B.3 Grappa KD does not decrease induced Hsp70 mRNA levels
Reverse transcription real-time PCR results showing the relative *Hsp70* mRNA level (normalized to RP49 transcript levels) after a 30 min HS induction (error bars denote standard deviation for Grappa RNAi n=3, and range for LacZ RNAi, n=1).

B.4 Discussion:

Results from these experiments show that Grappa is responsible for bulk H3K79me2. Results from the Schedl lab had shown that Grappa is responsible for H3K79 methylation in wing, eye and CNS imaginal discs of *Drosophila* larvae Shanower et a., 2005). Here we show that the methyltransferase activity of Grappa is also responsible for histone H3k79 dimethylation in S2 cells. Moreover I also detected an almost 2-fold increase in the density of histone H3K79me2 at the middle of Hsp70 gene after induction. This is consistent with reports where H3K79 methylation was mainly detected on the body of transcriptionally active genes (Schübeler et al., 2004). Grappa is also mainly responsible for H3K79 methylation at the *Hsp70* gene as RNAi

KD of this factor results in about a 10-fold decrease in the levels of this modification. The highest levels of H3K79me2 signal was detected at the boundary element scs' region. In yeast H3K79 methylation has been implicated in prevention of silencing spread from heterochromatic regions (van Leeuwen 2002), therefore it is tempting to speculate that high levels of H3K79 methylation at the scs' boundary element may have something to do with the function of scs' element as an insulator.

B.1 materials and methods

For Western Blot, anti rabbit histone dimethyl-H3K79 monoclonal IgG (Upstate, cat# 05-835) was used at 1:2000 dilution, house made rabbit anti HSF was used as described in the pervious chapters. For ChIP, 10µl of the antidimethyl H3K79 antibody as well as rabbit polyclonal anti histone H4 from Abcam were used per IP. The following primer pairs were used for the real-time PCR detection by ChIP.

scs' protected F: 5'-AGACGCTTTGATAGATGTATTTGTATAG

scs' protected R: 5'-TTGAATAGTGCTCTAAACTTTGGCATTT

scs BamHI F: 5'-AAATGCTCCGCACAGAATGCCAGAAA

scs BamHI R: 5'-AACTTACCTTCTTTCCCAATAGCAAGTT

scs' F: 5'-TTGTTGATAACACCTGATGTTCAGAGAT

scs' R: 5'-ATCGTTAATTGTGTACATCTCAATTCCA

scs F: 5'-ACGCAGCACAAATTTATTATAACACGTAAAC

scs R: 5'-TTTCAACAACTTCTCTCTGCGGAACTTA

Other primer pairs have been described in the previous chapters.

Reverse transcription real time PCR was carried out as described in the previous chapters.

For productin of grappa dsRNA the following primers were used for making the template:

Grappa T7F:

5’-GAATTAATACGACTCACTATAGGGATGCCAGCACCCAAACAACAA

Grappa T7R:

5’-GAATTAATACGACTCACTATAGGGAATGCTGATGCTGCACATGCT

APPENDIX C

A NEW APPROACH FOR IMMUNOPRECIPITATION OF PRIMARY MOUSE IgM ANTIBODIES IN ChIP ASSAYS USING A NON-CONJUGATED SECONDARY ANTIBODY AGAINST THE MOUSE IgM

C.1 Introduction

In ChIP assays the primary antibody that recognizes the antigen of interest associated with chromatin is often pulled-down efficiently with recombinant staphylococcal protein A or streptococcal Protein G that are conjugated to beads. Protein A and G are both bacterially expressed proteins that have high affinity and different specificity for most IgGs originating from a wide range of organisms. Some antibodies, in particular IgM monoclonal antibodies generated in mouse cells do not bind efficiently to the aforementioned proteins. IgM antibodies are usually pulled down with a secondary antibody against the mouse IgM (μ-chain specific) that is conjugated to beads (Boehm et al, 2003). The pull-down efficiency and percent input values that are obtained from two widely used antibodies that recognize the Ser2 and Ser5 phosphorylated CTD, H5 and H14 (Covance), are usually in the lower limits of an acceptable range(Boehm et al, 2003), and recently we have had problem obtaining meaningful percent input values that are higher than the no antibody background control samples using the anti mouse IgM antibodies conjugated to agarose for pull-down. To overcome this problem, I decided to use a secondary rabbit IgG antibody against the μ-chain of mouse IgM antibody and pull-down the interaction with protein A-agarose beads that recognize the rabbit IgG antibody. This modification in the

protocol resulted in successful and specific pull-down of the mouse antibodies, the details of which are described in the following sections.

C.2 Result and Discussion

An illustration of the two different approaches for pulling down mouse IgM antibody in the ChIP assay is shown in Figure C.1. In the traditional approach 10µl of the primary mouse IgM antibody (e.g., α Ser2-P) and the α mouse IgM antibody conjugated to agarose beads (50µl of 50% slurry with a binding capacity of 0.4 mg/ml of packed beads) are added simultaneously to the chromatin material and incubated on a rotisserie at 4^{o}C O/N. On the following day the beads are washed and the crosslink is reversed. The new approach was performed with the following modifications: 3 hours after adding 10µl of the primary mouse IgM antibody (anti Ser2-P) to the sonicated chromatin material, 20µl or 30µl of the rabbit anti mouse IgM,µ-chain specifc (2mg/ml) was added to the IP material (2 and 3-fold molar excess, respectively) and incubated on a rotisserie at 4^{o}C O/N. The beads were washed on the following day and the samples were processed as described in the materials and method section of chapter 2.

The first two columns for each tested regiono in figure C.2 show the percent input of Ser-2 phosphorylated Pol II at the *Hsp70* gene during the steady state of transcription when Ser2-P is detected throughout the body of the Hsp70 gene (Boehm et al, 2003, Ni et al, 2007). The percent input signal of Ser2-P with the old approach is only about 5-fold higher than the no antibody control (second green column in each region, Figure C.2.B) and the percent input material is around 0.1% input. It is also worth noting that the percent input values on the body of the induced Hsp70 gene are merely

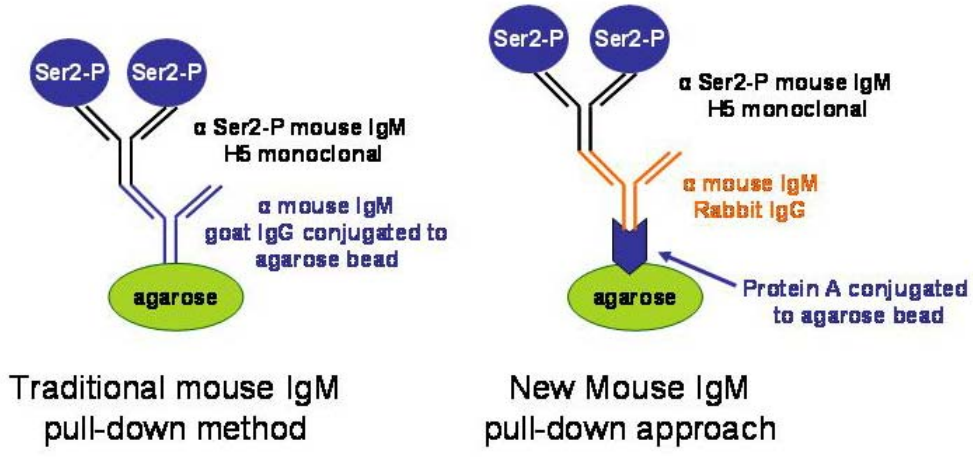

Figure C.1 comparison of the traditional and the new approach for anti mouse IgM (e.g., α Ser2-P) pull-down (for the sake of simplicity, mouse IgM is depicted as a monomer).

Figure C.2 comparison of the old and new ChIP approach for primary mouse IgM antibody pull down (Ser2-P, H5 antibody) at Hsp70 gene 18 min after HS induction

A) Results from the ChIP experiment showing the percent input material that was precipitated under different conditions. The no antibody (NA) plus anti IgM-agarose served as a control for the mouse IgM anti Ser2-P antibody experiment (H5). Protein A agarose bead alone (PA) or PA + rabbit anti IgM served as control for the Rpb3 and the H5 + rabbit α IgM experiments respectively.

B) The same graph as in A, but the y axis maximum scale is set to 1 for better comparison of the efficiency of the old and new approach in terms of percent input material n=1. The 87C and 102D regions are intergenic background regions, where no Pol II is present

A

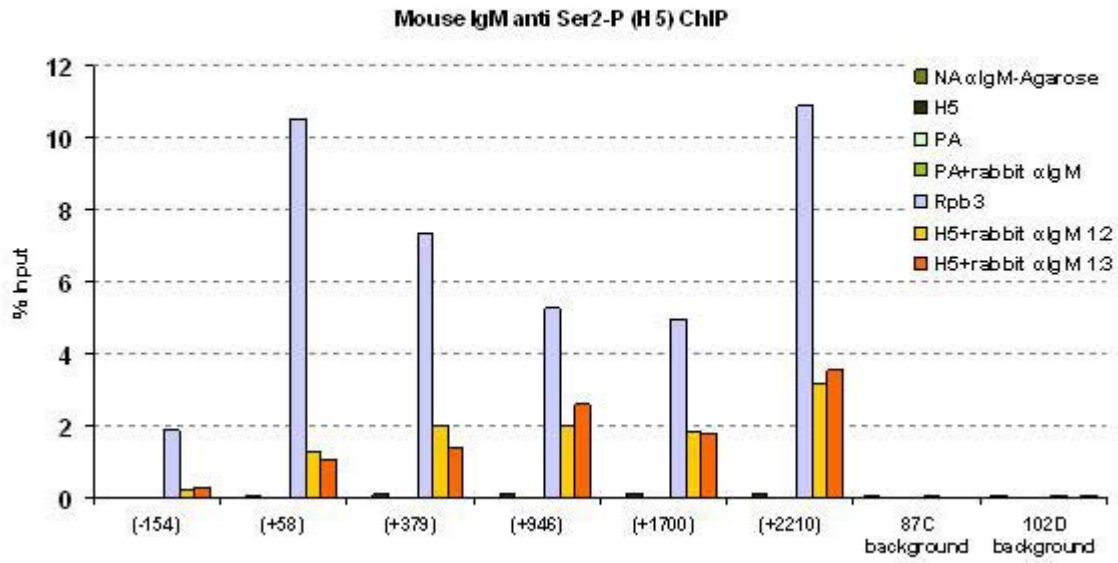
Mouse IgM anti Ser2-P (H5) ChIP
% Input
12
10
8
6
4
2
0
(-154)
(+58)
(+379)
(+946)
(+1700)
(+2210)
87C background
102D background
NA αIgM-Agarose
H5
PA
PA+rabbit αIgM
Rpb3
H5+rabbit αIgM 1:2
H5+rabbit αIgM 1:3

B

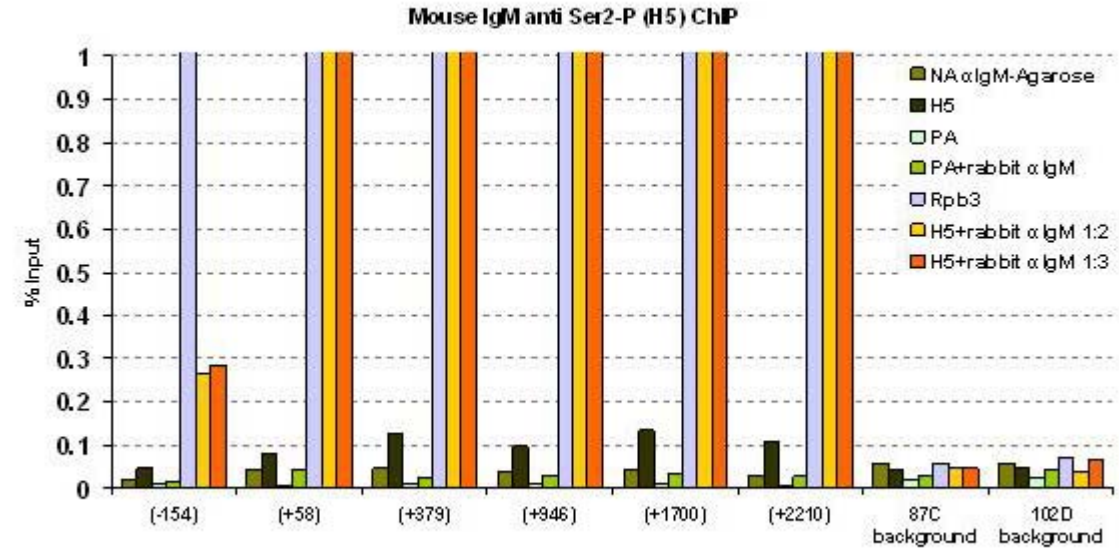
Mouse IgM anti Ser2-P (H5) ChIP
% Input
1
0.9
0.8
0.7
0.6
0.5
0.4
0.3
0.2
0.1
0
(-154)
(+58)
(+379)
(+946)
(+1700)
(+2210)
87C background
102D background
NA αIgM-Agarose
H5
PA
PA+rabbit αIgM
Rpb3
H5+rabbit αIgM 1:2
H5+rabbit αIgM 1:3

2-fold higher than the Ser2-P levels at the background regions (87C, 102D background loci), two regions where we do not expect to detect Pol II signals.

With the new approach, the % inputs are in the range of 1.5 to 3.5% input on the body of the gene (last two columns, figure C.2) .This is 10 to 20 fold higher than the old approach, while the background signals are comparable to the old approach (compare light green and darker green in the first column). With the new approach, Ser2-P signals were also detected at the right place along the body of the gene, with low signal being picked up at the upstream region of *Hsp70*, where we do not expect to detect Ser2-P. In addition, the Ser2-P signal is comparable to the no antibody signal at the 87C and 102D intergenic background region. While the experiment shown in figure C.2 is representative of a single experiment, this approach was utilized multiple times with reproducible results. These results are described in Figure 2.6 in Chapter 2.

In conclusion, I would like to promote this pull-down strategy as a more efficient approach for ChIP experiments where the primary antibody against the chromatin-associated factor of interest is a mouse IgM antibody. The new approach yields superior percent input signal levels for the antibody, without any increase in the level of no antibody signal. This higher percent input value and larger signal to no-antibody control margin would facilitate meaningful interpretation of data from ChIP experiments.

C.3 Materials and Methods

Thermo scientific rabbit α mouse IgM antibody (μ-chain specific) was used at 20 or 30 μl per IP experiment (2 mg/ml). This concentration is similar to the concentration of the mouse IgM Ser2-P antibody (Covance), 10 μl of the mouse IgM antibody is used per IP therfore, 20 and 30 μl of the rabbit anti mouse IgM antibody was used to ensure presence of the secondary antibody at the saturation level. ChIP experiment was carried out as described in Chapter 2 and the modifications written-out in the result and discussion section above.

The following primer pairs were also used in this experiment; the remaining primers are described in the previous chapters.

Chr4 102D +1100F: GTGAACGCAAATAGTTTGTATGGCT

Chr4 102D +1301R: TTAATAGCTGCCAAGAACCCAAAGGG

Hsp70 –200F 5'-TGCCAGAAAGAAAACTCGAGAAA,

Hsp70 –108R 5'-GACAGAGTGAGAGAGCAATAGTACAGAGA,

REFERENCES

Adams MD, Celniker SE, Holt RA, Evans CA, Gocayne JD, Amanatides PG, Scherer SE, Li PW, Hoskins RA, Galle RF, George RA, Lewis SE, Richards S, Ashburner M, Henderson SN, Sutton GG, Wortman JR, Yandell MD, Zhang Q, Chen LX et al (2000) The Genome Sequence of Drosophila melanogaster. *Science* **287**: 2185-2195

Adelman K, Marr MT, Werner J, Saunders A, Ni Z, Andrulis ED, & Lis JT (2005) Efficient release from promoter-proximal stall sites requires transcript cleavage factor TFIIS. *Mol Cell* **17**: 103-112

Adelman K, Wei W, Ardehali MB, Werner J, Zhu B, Reinberg D, & Lis JT (2006) Drosophila Paf1 modulates chromatin structure at actively transcribed genes. *Mol Cell Biol* **26**: 250-260

Adkins MW & Tyler JK (2006) Transcriptional activators are dispensable for transcription in the absence of Spt6-mediated chromatin reassembly of promoter regions. *Mol Cell* **21**: 405-416

Andrulis ED, Guzman E, Doring P, Werner J, & Lis JT (2000) High-resolution localization of Drosophila Spt5 and Spt6 at heat shock genes in vivo: roles in promoter proximal pausing and transcription elongation. *Genes Dev* **14**: 2635-2649

Andrulis ED, Werner J, Nazarian A, Erdjument-Bromage H, Tempst P, & Lis JT (2002) The RNA processing exosome is linked to elongating RNA polymerase II in Drosophila. *Nature* **420**: 837-841

Ansari A & Hampsey M (2005) A role for the CPF 3′-end processing machinery in RNAP II-dependent gene looping. *Genes & Development* **19**: 2969-2978

Ardehali MB, Yao J, Adelman K, Fuda NJ, Petesch SJ, Webb WW, & Lis JT (2009) Spt6 enhances the elongation rate of RNA polymerase II in vivo. *EMBO J*

Ardehali MB & Lis JT (2009) Tracking rates of transcription and splicing in vivo. *Nat Struct Mol Biol* 16: 1123-1124

Arndt KM & Kane CM (2003) Running with RNA polymerase: eukaryotic transcript elongation. *Trends in Genetics* **19**: 543-550

Bannister AJ, Schneider R, Myers FA, Thorne AW, Crane-Robinson C, & Kouzarides T (2005) Spatial Distribution of Di- and Tri-methyl Lysine 36 of Histone H3 at Active Genes. *Journal of Biological Chemistry* **280**: 17732-17736

Barski A, Cuddapah S, Cui K, Roh T, Schones DE, Wang Z, Wei G, Chepelev I, & Zhao K (2007) High-Resolution Profiling of Histone Methylations in the Human Genome. *Cell* **129**: 823-837

Beisel C, Imhof A, Greene J, Kremmer E, & Sauer F (2002) Histone methylation by the Drosophila epigenetic transcriptional regulator Ash1. *Nature* **419**: 857-862

Bell O, Wirbelauer C, Hild M, Scharf AN, Schwaiger M, MacAlpine DM, Zilbermann F, van Leeuwen F, Bell SP, Imhof A, Garza D, Peters AH, & Schubeler D (2007) Localized H3K36 methylation states define histone H4K16 acetylation during transcriptional elongation in Drosophila. *EMBO J* **26**: 4974-4984

Belotserkovskaya R & Reinberg D (2004) Facts about FACT and transcript elongation through chromatin. *Curr Opin Genet Dev* **14**: 139-146

Belotserkovskaya R, Oh S, Bondarenko VA, Orphanides G, Studitsky VM, & Reinberg D (2003) FACT Facilitates Transcription-Dependent Nucleosome Alteration. *Science* **301**: 1090-1093

Beltran S, Angulo M, Pignatelli M, Serras F, & Corominas M (2007) Functional dissection of the ash2 and ash1 transcriptomes provides insights into the transcriptional basis of wing phenotypes and reveals conserved protein interactions. *Genome Biol* **8**: R67

Bernstein BE, Kamal M, Lindblad-Toh K, Bekiranov S, Bailey DK, Huebert DJ, McMahon S, Karlsson EK, Kulbokas III EJ, Gingeras TR, Schreiber SL, & Lander ES (2005) Genomic Maps and Comparative Analysis of Histone Modifications in Human and Mouse. *Cell* **120**: 169-181

Birch JL, Tan BC, Panov KI, Panova TB, Andersen JS, Owen-Hughes TA, Russell J, Lee SC, & Zomerdijk JC (2009) FACT facilitates chromatin transcription by RNA polymerases I and III. *EMBO J* **28**: 854-865

Boehm AK, Saunders A, Werner J, & Lis JT (2003) Transcription factor and polymerase recruitment, modification, and movement on dhsp70 in vivo in the minutes following heat shock. *Mol Cell Biol* **23**: 7628-7637

Boettiger AN & Levine M (2009) Synchronous and Stochastic Patterns of Gene Activation in the Drosophila Embryo. *Science* **325**: 471-473

Boireau S, Maiuri P, Basyuk E, de la Mata M, Knezevich A, Pradet-Balade B, Backer V, Kornblihtt A, Marcello A, & Bertrand E (2007) The transcriptional cycle of HIV-1 in real-time and live cells. *J Cell Biol* **179**: 291-304

Bortvin A & Winston F (1996) Evidence that Spt6p controls chromatin structure by a direct interaction with histones. *Science* **272**: 1473-1476

Bourbon HM, Gonzy-Treboul G, Peronnet F, Alin MF, Ardourel C, Benassayag C, Cribbs D, Deutsch J, Ferrer P, Haenlin M, Lepesant JA, Noselli S, & Vincent A (2002) A P-insertion screen identifying novel X-linked essential genes in Drosophila. *Mech Dev* **110**: 71-83

Bourgeois CF, Kim YK, Churcher MJ, West MJ, & Karn J (2002) Spt5 Cooperates with Human Immunodeficiency Virus Type 1 Tat by Preventing Premature RNA Release at Terminator Sequences. *Mol Cell Biol* **22**: 1079-1093

Bushnell DA & Kornberg RD (2003) Complete, 12-subunit RNA polymerase II at 4.1-Å resolution: Implications for the initiation of transcription. *Proceedings of the National Academy of Sciences of the United States of America* **100**: 6969-6973

Byrd KN & Shearn A (2003a) ASH1, a Drosophila trithorax group protein, is required for methylation of lysine 4 residues on histone H3. *Proc Natl Acad Sci USA* **100**: 11535-11540

Byrd KN & Shearn A (2003b) ASH1, a Drosophila trithorax group protein, is required for methylation of lysine 4 residues on histone H3. *Proc Natl Acad Sci U S A ; Proceedings of the National Academy of Sciences of the United States of America* **100**: 11535-11540

Campos EI & Reinberg D (2009) Histones: Annotating Chromatin. *Annu Rev Genet* **43**: 559-599

Carre C, Szymczak D, Pidoux J, & Antoniewski C (2005) The Histone H3 Acetylase dGcn5 Is a Key Player in Drosophila melanogaster Metamorphosis. *Mol Cell Biol* **25**: 8228-8238

Carrozza MJ, Li B, Florens L, Suganuma T, Swanson SK, Lee KK, Shia W, Anderson S, Yates J, Washburn MP, & Workman JL (2005) Histone H3 Methylation by Set2 Directs Deacetylation of Coding Regions by Rpd3S to Suppress Spurious Intragenic Transcription. *Cell,* **123**: 581-592

Carvin CD & Kladde MP (2004) Effectors of Lysine 4 Methylation of Histone H3 in Saccharomyces cerevisiae Are Negative Regulators of PHO5 and GAL1-10. *Journal of Biological Chemistry* **279**: 33057-33062

Champagne KS, Saksouk N, Pena PV, Johnson K, Ullah M, Yang XJ, Cote J, & Kutateladze TG (2008) The crystal structure of the ING5 PHD finger in complex with an H3K4me3 histone peptide. *Proteins* **72**: 1371-1376

Chapman RD, Heidemann M, Hintermair C, & Eick D (2008) Molecular evolution of the RNA polymerase II CTD. *Trends in Genetics* **24**: 289-296

Clark-Adams CD & Winston F (1987) The SPT6 gene is essential for growth and is required for delta-mediated transcription in Saccharomyces cerevisiae. *Mol Cell Biol* **7**: 679-686

Corden JL (1990) Tails of RNA polymerase II. *Trends Biochem Sci* **15**: 383-387

Core LJ, Waterfall JJ, & Lis JT (2008) Nascent RNA Sequencing Reveals Widespread Pausing and Divergent Initiation at Human Promoters. *Science; Science* **322**: 1845-1848

Costa PJ & Arndt KM (2000) Synthetic lethal interactions suggest a role for the Saccharomyces cerevisiae Rtf1 protein in transcription elongation. *Genetics* **156**: 535-547

Cramer P (2004) RNA polymerase II structure: from core to functional complexes. *Curr Opin Genet Dev* **14**: 218-226

Cui Y & Denis CL (2003) In Vivo Evidence that Defects in the Transcriptional Elongation Factors RPB2, TFIIS, and SPT5 Enhance Upstream Poly(A) Site Utilization. *Mol Cell Biol* **23**: 7887-7901

Darzacq X, Shav-Tal Y, de Turris V, Brody Y, Shenoy SM, Phair RD, & Singer RH (2007) In vivo dynamics of RNA polymerase II transcription. *Nat Struct Mol Biol* **14**: 796-806

Deng W & Roberts SG (2007) TFIIB and the regulation of transcription by RNA polymerase II. *Chromosoma* **116**: 417-429

Dieci G, Fiorino G, Castelnuovo M, Teichmann M, & Pagano A (2007) The expanding RNA polymerase III transcriptome. *Trends in Genetics* **23**: 614-622

Doyon Y, Cayrou C, Ullah M, Landry A, Côté V, Selleck W, Lane WS, Tan S, Yang X, & Côté J (2006) ING Tumor Suppressor Proteins Are Critical Regulators of Chromatin Acetylation Required for Genome Expression and Perpetuation. *Mol Cell* **21**: 51-64

Endoh M, Zhu W, Hasegawa J, Watanabe H, Kim DK, Aida M, Inukai N, Narita T, Yamada T, Furuya A, Sato H, Yamaguchi Y, Mandal SS, Reinberg D, Wada T, & Handa H (2004) Human Spt6 stimulates transcription elongation by RNA polymerase II in vitro. *Mol Cell Biol* **24**: 3324-3336

Femino AM, Fay FS, Fogarty K, & Singer RH (1998) Visualization of Single RNA Transcripts in Situ. *Science* **280**: 585-590

Fernandes M, Xiao H, & Lis JT (1995) Binding of heat shock factor to and transcriptional activation of heat shock genes in Drosophila. *Nucl Acids Res* **23**: 4799-4804

Fuda NJ, Ardehali MB, & Lis JT (2009) Defining mechanisms that regulate RNA polymerase II transcription in vivo. *Nature* **461**: 186-192

Geiger JH, Hahn S, Lee S, & Sigler PB (1996) Crystal Structure of the Yeast TFIIA/TBP/DNA Complex. *Science* **272**: 830-836

Gerber M, Ma J, Dean K, Eissenberg JC, & Shilatifard A (2001) Drosophila ELL is associated with actively elongating RNA polymerase II on transcriptionally active sites in vivo. *EMBO J* **20**: 6104-6114

Gerber M, Eissenberg JC, Kong S, Tenney K, Conaway JW, Conaway RC, & Shilatifard A (2004) In Vivo Requirement of the RNA Polymerase II Elongation Factor Elongin A for Proper Gene Expression and Development. *Mol Cell Biol* **24**: 9911-9919

Gilmour DS & Lis JT (1986) RNA polymerase II interacts with the promoter region of the noninduced hsp70 gene in Drosophila melanogaster cells. *Mol Cell Biol* **6**: 3984-3989

Greenblatt J, Nodwell JR, & Mason SW (1993) Transcriptional antitermination. *Nature* **364**: 401-406

Guenther MG, Levine SS, Boyer LA, Jaenisch R, & Young RA (2007) A chromatin landmark and transcription initiation at most promoters in human cells. *Cell* **130**: 77-88

Hartzog GA, Wada T, Handa H, & Winston F (1998) Evidence that Spt4, Spt5, and Spt6 control transcription elongation by RNA polymerase II in Saccharomyces cerevisiae. *Genes Dev* **12**: 357-369

Honda BM, Dixon GH, & Candido EP (1975) Sites of in vivo histone methylation in developing trout testis. *Journal of Biological Chemistry* **250**: 8681-8685

Izban MG & Luse DS (1991) Transcription on nucleosomal templates by RNA polymerase II in vitro: inhibition of elongation with enhancement of sequence-specific pausing. *Genes & Development* **5**: 683-696

Izban M & Luse D (1992) Factor-stimulated RNA polymerase II transcribes at physiological elongation rates on naked DNA but very poorly on chromatin templates. *J Biol Chem* **267**: 13647-13655

Jaehning JA The Paf1 complex: Platform or player in RNA polymerase II transcription? *Biochimica et Biophysica Acta (BBA) - Gene Regulatory Mechanisms* In Press, Corrected Proof

Johnson SJ, Close D, Robinson H, Vallet-Gely I, Dove SL, & Hill CP (2008) Crystal Structure and RNA Binding of the Tex Protein from Pseudomonas aeruginosa. *J Mol Biol* **377**: 1460-1473

Kaplan CD, Holland MJ, & Winston F (2005) Interaction between transcription elongation factors and mRNA 3'-end formation at the Saccharomyces cerevisiae GAL10-GAL7 locus. *J Biol Chem* **280**: 913-922

Kaplan CD, Laprade L, & Winston F (2003) Transcription elongation factors repress transcription initiation from cryptic sites. *Science* **301**: 1096-1099

Kaplan CD, Morris JR, Wu C-, & Winston F (2000) Spt5 and Spt6 are associated with active transcription and have characteristics of general elongation factors in D. melanogaster. *Genes Dev* **14**: 2623-2634

Keegan BR, Feldman JL, Lee DH, Koos DS, Ho RK, Stainier DY, & Yelon D (2002) The elongation factors Pandora/Spt6 and Foggy/Spt5 promote transcription in the zebrafish embryo. *Development* **129**: 1623-1632

Keene MA & Elgin SCR (1981) Micrococcal nuclease as a probe of DNA sequence organization and chromatin structure. *Cell* **27**: 57-64

Kim J, Guermah M, & Roeder RG (2010) The Human PAF1 Complex Acts in Chromatin Transcription Elongation Both Independently and Cooperatively with SII/TFIIS. *Cell* **140**: 491-503

Kim M, Ahn SH, Krogan NJ, Greenblatt JF, & Buratowski S (2004a) Transitions in RNA polymerase II elongation complexes at the 3' ends of genes. *EMBO J* **23**: 354-364

Kim M, Ahn SH, Krogan NJ, Greenblatt JF, & Buratowski S (2004b) Transitions in RNA polymerase II elongation complexes at the 3' ends of genes. *EMBO J* **23**: 354-364

Kireeva ML, Walter W, Tchernajenko V, Bondarenko V, Kashlev M, & Studitsky VM (2002) Nucleosome Remodeling Induced by RNA Polymerase II: Loss of the H2A/H2B Dimer during Transcription. *Molecular Cell,* **9**: 541-552

Kizer KO, Phatnani HP, Shibata Y, Hall H, Greenleaf AL, & Strahl BD (2005) A Novel Domain in Set2 Mediates RNA Polymerase II Interaction and Couples Histone H3 K36 Methylation with Transcript Elongation. *Mol Cell Biol* **25**: 3305-3316

Klymenko T & Muller J (2004) The histone methyltransferases Trithorax and Ash1 prevent transcriptional silencing by Polycomb group proteins. *EMBO Rep* **5**: 373-377

Kok FO, Oster E, Mentzer L, Hsieh JC, Henry CA, & Sirotkin HI (2007) The role of the SPT6 chromatin remodeling factor in zebrafish embryogenesis. *Dev Biol* **307**: 214-226

Kouzarides T (2007) Chromatin Modifications and Their Function. *Cell* **128**: 693-705

Krogan NJ, Kim M, Ahn SH, Zhong G, Kobor MS, Cagney G, Emili A, Shilatifard A, Buratowski S, & Greenblatt JF (2002) RNA polymerase II elongation factors of Saccharomyces cerevisiae: a targeted proteomics approach. *Mol Cell Biol* **22**: 6979-6992

Krogan NJ, Dover J, Wood A, Schneider J, Heidt J, Boateng MA, Dean K, Ryan OW, Golshani A, Johnston M, Greenblatt JF, & Shilatifard A (2003) The Paf1 Complex Is Required for Histone H3 Methylation by COMPASS and Dot1p: Linking Transcriptional Elongation to Histone Methylation. *Mol Cell* **11**: 721-729

Kulaeva OI, Gaykalova DA, & Studitsky VM (2007) Transcription through chromatin by RNA polymerase II: Histone displacement and exchange. *Mutation Research/Fundamental and Molecular Mechanisms of Mutagenesis,* **618**: 116-129

Kuzin B, Tillib S, Sedkov Y, Mizrokhi L, & Mazo A (1994) The Drosophila trithorax gene encodes a chromosomal protein and directly regulates the region-specific homeotic gene fork head. *Genes Dev* **8**: 2478-2490

Larschan E & Winston F (2001) The S. cerevisiae SAGA complex functions in vivo as a coactivator for transcriptional activation by Gal4. *Genes Dev ; Genes & Development* **15**: 1946-1956

Lee CK, Shibata Y, Rao B, Strahl BD, & Lieb JD (2004) Evidence for nucleosome depletion at active regulatory regions genome-wide. *Nat Genet* **36**: 900-905

Li B, Carey M, & Workman JL (2007) The role of chromatin during transcription. *Cell* **128**: 707-719

Li J, Moazed D, & Gygi SP (2002) Association of the Histone Methyltransferase Set2 with RNA Polymerase II Plays a Role in Transcription Elongation. *Journal of Biological Chemistry* **277**: 49383-49388

Lindstrom DL, Squazzo SL, Muster N, Burckin TA, Wachter KC, Emigh CA, McCleery JA, Yates JR,3rd, & Hartzog GA (2003a) Dual roles for Spt5 in pre-mRNA processing and transcription elongation revealed by identification of Spt5-associated proteins. *Mol Cell Biol* **23**: 1368-1378

Lindstrom DL, Squazzo SL, Muster N, Burckin TA, Wachter KC, Emigh CA, McCleery JA, Yates JR,III, & Hartzog GA (2003b) Dual Roles for Spt5 in Pre-mRNA Processing and Transcription Elongation Revealed by Identification of Spt5-Associated Proteins. *Mol Cell Biol* **23**: 1368-1378

Lis JT (2007) Imaging Drosophila gene activation and polymerase pausing in vivo. *Nature* **450**: 198-202

Lis JT, Mason P, Peng J, Price DH, & Werner J (2000) P-TEFb kinase recruitment and function at heat shock loci. *Genes Dev* **14**: 792-803

Liu Y, Kung C, Fishburn J, Ansari AZ, Shokat KM, & Hahn S (2004) Two Cyclin-Dependent Kinases Promote RNA Polymerase II Transcription and Formation of the Scaffold Complex. *Mol Cell Biol* **24**: 1721-1735

Martin C & Zhang Y (2005) The diverse functions of histone lysine methylation. *Nat Rev Mol Cell Biol* **6**: 838-849

Mason PB & Struhl K (2005) Distinction and relationship between elongation rate and processivity of RNA polymerase II in vivo. *Mol Cell* **17**: 831-840

Mason PB & Struhl K (2003) The FACT complex travels with elongating RNA polymerase II and is important for the fidelity of transcriptional initiation in vivo. *Mol Cell Biol* **23**: 8323-8333

Mueller CL, Porter SE, Hoffman MG, & Jaehning JA (2004) The Paf1 Complex Has Functions Independent of Actively Transcribing RNA Polymerase II. *Molecular Cell,* **14**: 447-456

Müller F, Demény MA, & Tora L (2007) New Problems in RNA Polymerase II Transcription Initiation: Matching the Diversity of Core Promoters with a Variety of Promoter Recognition Factors. *Journal of Biological Chemistry* **282**: 14685-14689

Murrell A, Heeson S, & Reik W (2004) Interaction between differentially methylated regions partitions the imprinted genes Igf2 and H19 into parent-specific chromatin loops. *Nat Genet* **36**: 889-893

Muse GW, Gilchrist DA, Nechaev S, Shah R, Parker JS, Grissom SF, Zeitlinger J, & Adelman K (2007) RNA polymerase is poised for activation across the genome. *Nat Genet* **39**: 1507-1511

Ng HH, Robert F, Young RA, & Struhl K (2003) Targeted Recruitment of Set1 Histone Methylase by Elongating Pol II Provides a Localized Mark and Memory of Recent Transcriptional Activity. *Mol Cell* **11**: 709-719

Ni Z, Saunders A, Fuda NJ, Yao J, Suarez JR, Webb WW, & Lis JT (2007) P-TEFb is critical for the maturation of RNA Polymerase II into productive elongation in vivo. *Mol Cell Biol*

Ni Z, Schwartz BE, Werner J, Suarez JR, & Lis JT (2004) Coordination of transcription, RNA processing, and surveillance by P-TEFb kinase on heat shock genes. *Mol Cell* **13**: 55-65

Nishiwaki K, Sano T, & Miwa J (1993) emb-5, a gene required for the correct timing of gut precursor cell division during gastrulation in Caenorhabditis elegans, encodes a protein similar to the yeast nuclear protein SPT6. *Mol Gen Genet* **239**: 313-322

O'Brien T & Lis JT (1993) Rapid changes in Drosophila transcription after an instantaneous heat shock. *Mol Cell Biol* **13**: 3456-3463

Okada Y, Feng Q, Lin Y, Jiang Q, Li Y, Coffield VM, Su L, Xu G, & Zhang Y (2005) hDOT1L Links Histone Methylation to Leukemogenesis. *Cell* **121**: 167-178

Okuhara K, Ohta K, Seo H, Shioda M, Yamada T, Tanaka Y, Dohmae N, Seyama Y, Shibata T, & Murofushi H (1999) A DNA unwinding factor involved in DNA replication in cell-free extracts of Xenopus eggs. *Current Biology* **9**: 341-351

Orphanides G, LeRoy G, Chang C, Luse DS, & Reinberg D (1998) FACT, a Factor that Facilitates Transcript Elongation through Nucleosomes. *Cell,* **92**: 105-116

O'Sullivan JM, Tan-Wong SM, Morillon A, Lee B, Coles J, Mellor J, & Proudfoot NJ (2004) Gene loops juxtapose promoters and terminators in yeast. *Nat Genet* **36**: 1014-1018

Owen-Hughes T & Workman JL (1994) Experimental analysis of chromatin function in transcription control. *Crit Rev Eukaryot Gene Expr* **4**: 403-441

Papp B & Müller J (2006) Histone trimethylation and the maintenance of transcriptional ONand OFF states by trxG and PcG proteins. *Genes & Development* **20**: 2041-2054

Park JM, Werner J, Kim JM, Lis JT, & Kim Y (2001) Mediator, Not Holoenzyme, Is Directly Recruited to the Heat Shock Promoter by HSF upon Heat Shock. *Mol Cell* **8**: 9-19

Pena PV, Davrazou F, Shi X, Walter KL, Verkhusha VV, Gozani O, Zhao R, & Kutateladze TG (2006) Molecular mechanism of histone H3K4me3 recognition by plant homeodomain of ING2. *Nature* **442**: 100-103

Perkins KJ, Lusic M, Mitar I, Giacca M, & Proudfoot NJ (2008) Transcription-Dependent Gene Looping of the HIV-1 Provirus Is Dictated by Recognition of Pre-mRNA Processing Signals. *Mol Cell* **29**: 56-68

Peter A, Schottler P, Werner M, Beinert N, Dowe G, Burkert P, Mourkioti F, Dentzer L, He Y, Deak P, Benos PV, Gatt MK, Murphy L, Harris D, Barrell B, Ferraz C, Vidal

S, Brun C, Demaille J, Cadieu E et al (2002) Mapping and identification of essential gene functions on the X chromosome of Drosophila. *EMBO Rep* **3**: 34-38

Peterson CL & Workman JL (2000) Promoter targeting and chromatin remodeling by the SWI/SNF complex. *Curr Opin Genet Dev* **10**: 187-192

Petesch SJ & Lis JT (2008) Rapid, Transcription-Independent Loss of Nucleosomes over a Large Chromatin Domain at Hsp70 Loci. *Cell,* **134**: 74-84

Pinskaya M, Gourvennec S, & Morillon A (2009) H3 lysine 4 di- and tri-methylation deposited by cryptic transcription attenuates promoter activation. *EMBO J* **28**: 1697-1707

Pokholok DK, Harbison CT, Levine S, Cole M, Hannett NM, Lee TI, Bell GW, Walker K, Rolfe PA, Herbolsheimer E, Zeitlinger J, Lewitter F, Gifford DK, & Young RA (2005) Genome-wide Map of Nucleosome Acetylation and Methylation in Yeast. *Cell* **122**: 517-527

Pray-Grant MG, Daniel JA, Schieltz D, Yates JR,3rd, & Grant PA (2005) Chd1 chromodomain links histone H3 methylation with SAGA- and SLIK-dependent acetylation. *Nature* **433**: 434-438

Ramadan N, Flockhart I, Booker M, Perrimon N, & Mathey-Prevot B (2007) Design and implementation of high-throughput RNAi screens in cultured Drosophila cells. *Nat Protoc* **2**: 2245-2264

Rasmussen E & Lis J (1993) In vivo Transcriptional Pausing and Cap Formation on Three Drosophila Heat Shock Genes. *Proceedings of the National Academy of Sciences* **90**: 7923-7927

Rondon AG, Gallardo M, Garcia-Rubio M, & Aguilera A (2004) Molecular evidence indicating that the yeast PAF complex is required for transcription elongation. *EMBO Rep* **5**: 47-53

Rondon AG, Garcia-Rubio M, Gonzalez-Barrera S, & Aguilera A (2003a) Molecular evidence for a positive role of Spt4 in transcription elongation. *EMBO J* **22**: 612-620

Rondon AG, Jimeno S, Garcia-Rubio M, & Aguilera A (2003b) Molecular evidence that the eukaryotic THO/TREX complex is required for efficient transcription elongation. *J Biol Chem* **278**: 39037-39043

Rougvie AE & Lis JT (1988) The RNA polymerase II molecule at the 5′ end of the uninduced hsp70 gene of D. melanogaster is transcriptionally engaged. *Cell* **54**: 795-804

Ruthenburg AJ, Allis CD, & Wysocka J (2007) Methylation of Lysine 4 on Histone H3: Intricacy of Writing and Reading a Single Epigenetic Mark. *Mol Cell* **25**: 15-30

Sadowski M, Dichtl B, Hubner W, & Keller W (2003) Independent functions of yeast Pcf11p in pre-mRNA 3' end processing and in transcription termination. *EMBO J* **22**: 2167-2177

Sanchez-Elsner T, Gou D, Kremmer E, & Sauer F (2006) Noncoding RNAs of Trithorax Response Elements Recruit Drosophila Ash1 to Ultrabithorax. *Science* **311**: 1118-1123

Saunders A, Core LJ, & Lis JT (2006) Breaking barriers to transcription elongation. *Nat Rev Mol Cell Biol* **7**: 557-567

Saunders A, Werner J, Andrulis ED, Nakayama T, Hirose S, Reinberg D, & Lis JT (2003) Tracking FACT and the RNA polymerase II elongation complex through chromatin in vivo. *Science* **301**: 1094-1096

Schlichter A & Cairns BR (2005) Histone trimethylation by Set1 is coordinated by the RRM, autoinhibitory, and catalytic domains. *EMBO J* **24**: 1222-1231

Schübeler D, MacAlpine DM, Scalzo D, Wirbelauer C, Kooperberg C, van Leeuwen F, Gottschling DE, O'Neill LP, Turner BM, Delrow J, Bell SP, & Groudine M (2004a) The histone modification pattern of active genes revealed through genome-wide chromatin analysis of a higher eukaryote. *Genes & Development* **18**: 1263-1271

Schübeler D, MacAlpine DM, Scalzo D, Wirbelauer C, Kooperberg C, van Leeuwen F, Gottschling DE, O'Neill LP, Turner BM, Delrow J, Bell SP, & Groudine M (2004b) The histone modification pattern of active genes revealed through genome-wide chromatin analysis of a higher eukaryote. *Genes & Development* **18**: 1263-1271

Schuettengruber B, Ganapathi M, Leblanc B, Portoso M, Jaschek R, Tolhuis B, van Lohuizen M, Tanay A, & Cavalli G (2009) Functional anatomy of polycomb and trithorax chromatin landscapes in Drosophila embryos. *PLoS Biol* **7**: e13

Schuettengruber B, Chourrout D, Vervoort M, Leblanc B, & Cavalli G (2007) Genome Regulation by Polycomb and Trithorax Proteins. *Cell* **128**: 735-745

Schwabish MA & Struhl K (2006) Asf1 mediates histone eviction and deposition during elongation by RNA polymerase II. *Mol Cell* **22**: 415-422

Schwabish MA & Struhl K (2007) The Swi/Snf Complex Is Important for Histone Eviction during Transcriptional Activation and RNA Polymerase II Elongation In Vivo. *Mol Cell Biol* **27**: 6987-6995

Schwabish MA & Struhl K (2004) Evidence for Eviction and Rapid Deposition of Histones upon Transcriptional Elongation by RNA Polymerase II. *Mol Cell Biol* **24**: 10111-10117

Schwartz BE, Werner JK, & Lis JT (2004) Indirect immunofluorescent labeling of Drosophila polytene chromosomes: visualizing protein interactions with chromatin in vivo. *Methods Enzymol* **376**: 393-404

Sedkov Y, Cho E, Petruk S, Cherbas L, Smith ST, Jones RS, Cherbas P, Canaani E, Jaynes JB, & Mazo A (2003) Methylation at lysine 4 of histone H3 in ecdysone-dependent development of Drosophila. *Nature* **426**: 78-83

Shanower GA, Muller M, Blanton JL, Honti V, Gyurkovics H, & Schedl P (2005) Characterization of the grappa Gene, the Drosophila Histone H3 Lysine 79 Methyltransferase. *Genetics* **169**: 173-184

Shermoen AW & O'Farrell PH (1981) Progression of the cell cycle through mitosis leads to abortion of nascent transcripts. *Cell* **67**: 303-310

Shilatifard A (2004) Transcriptional elongation control by RNA polymerase II: a new frontier. *Biochim Biophys Acta* **1677**: 79-86

Sik Lee Y & Carthew RW (2003) Making a better RNAi vector for Drosophila: use of intron spacers. *Methods,* **30**: 322-329

Sims III RJ, Millhouse S, Chen C, Lewis BA, Erdjument-Bromage H, Tempst P, Manley JL, & Reinberg D (2007) Recognition of Trimethylated Histone H3 Lysine 4 Facilitates the Recruitment of Transcription Postinitiation Factors and Pre-mRNA Splicing. *Mol Cell* **28**: 665-676

Sims RJ,3rd, Belotserkovskaya R, & Reinberg D (2004) Elongation by RNA polymerase II: the short and long of it. *Genes Dev* **18**: 2437-2468

Singh BN & Hampsey M (2007) A Transcription-Independent Role for TFIIB in Gene Looping. *Mol Cell* **27**: 806-816

Singh J & Padgett RA (2009) Rates of in situ transcription and splicing in large human genes. *Nat Struct Mol Biol* **16**: 1128-1133

Smale ST & Kadonaga JT (2003) THE RNA POLYMERASE II CORE PROMOTER. *Annu Rev Biochem* **72**: 449-479

Smith ST, Petruk S, Sedkov Y, Cho E, Tillib S, Canaani E, & Mazo A (2004a) Modulation of heat shock gene expression by the TAC1 chromatin-modifying complex. *Nat Cell Biol* **6**: 162-167

Smith ST, Petruk S, Sedkov Y, Cho E, Tillib S, Canaani E, & Mazo A (2004b) Modulation of heat shock gene expression by the TAC1 chromatin-modifying complex. *Nat Cell Biol* **6**: 162-167

Squazzo SL, Costa PJ, Lindstrom DL, Kumer KE, Simic R, Jennings JL, Link AJ, Arndt KM, & Hartzog GA (2002) The Paf1 complex physically and functionally associates with transcription elongation factors in vivo. *EMBO J* **21**: 1764-1774

Steward MM, Lee JS, O'Donovan A, Wyatt M, Bernstein BE, & Shilatifard A (2006) Molecular regulation of H3K4 trimethylation by ASH2L, a shared subunit of MLL complexes. *Nat Struct Mol Biol* **13**: 852-854

Struhl K (1989) Molecular Mechanisms of Transcriptional Regulation in Yeast. *Annu Rev Biochem* **58**: 1051-1077

Svejstrup JQ (2004) The RNA polymerase II transcription cycle: cycling through chromatin. *Biochim Biophys Acta* **1677**: 64-73

Tanaka Y, Katagiri Z, Kawahashi K, Kioussis D, & Kitajima S (2007) Trithorax-group protein ASH1 methylates histone H3 lysine 36. *Gene* **397**: 161-168

Tan-Wong SM, French JD, Proudfoot NJ, & Brown MA (2008) Dynamic interactions between the promoter and terminator regions of the mammalian BRCA1 gene. *Proceedings of the National Academy of Sciences* **105**: 5160-5165

Tan-Wong SM, Wijayatilake HD, & Proudfoot NJ (2009) Gene loops function to maintain transcriptional memory through interaction with the nuclear pore complex. *Genes & Development* **23**: 2610-2624

Tennyson CN, Klamut HJ, & Worton RG (1995) The human dystrophin gene requires 16 hours to be transcribed and is cotranscriptionally spliced. *Nat Genet* **9**: 184-190

Thummel CS, Burtis KC, & Hogness DS (1990) Spatial and temporal patterns of E74 transcription during Drosophila development. *Cell* **61**: 101-111

Tolhuis B, Palstra R, Splinter E, Grosveld F, & de Laat W (2002) Looping and Interaction between Hypersensitive Sites in the Active β-globin Locus. *Mol Cell* **10**: 1453-1465

Tsukiyama T & Wu C (1995) Purification and properties of an ATP-dependent nucleosome remodeling factor. *Cell* **83**: 1011-1020

Tupler R, Perini G, & Green MR (2001) Expressing the human genome. *Nature* **409**: 832-833

Ucker DS & Yamamoto KR (1984) Early events in the stimulation of mammary tumor virus RNA synthesis by glucocorticoids. Novel assays of transcription rates. *J Biol Chem* **259**: 7416-7420

Uptain SM, Kane CM, & Chamberlin MJ (1997) BASIC MECHANISMS OF TRANSCRIPT ELONGATION AND ITS REGULATION. *Annu Rev Biochem* **66**: 117-172

Vakoc CR, Letting DL, Gheldof N, Sawado T, Bender MA, Groudine M, Weiss MJ, Dekker J, & Blobel GA (2005) Proximity among Distant Regulatory Elements at the β-Globin Locus Requires GATA-1 and FOG-1. *Mol Cell* **17**: 453-462

Venter JC, Adams MD, Myers EW, Li PW, Mural RJ, Sutton GG, Smith HO, Yandell M, Evans CA, Holt RA, Gocayne JD, Amanatides P, Ballew RM, Huson DH, Wortman JR, Zhang Q, Kodira CD, Zheng XH, Chen L, Skupski M et al (2001) The Sequence of the Human Genome. *Science* **291**: 1304-1351

Vermeulen M, Mulder KW, Denissov S, Pijnappel WWMP, van Schaik FMA, Varier RA, Baltissen MPA, Stunnenberg HG, Mann M, & Timmers HTM (2007) Selective Anchoring of TFIID to Nucleosomes by Trimethylation of Histone H3 Lysine 4. *Cell* **131**: 58-69

Wada T, Takagi T, Yamaguchi Y, Ferdous A, Imai T, Hirose S, Sugimoto S, Yano K, Hartzog GA, Winston F, Buratowski S, & Handa H (1998) DSIF, a novel transcription

elongation factor that regulates RNA polymerase II processivity, is composed of human Spt4 and Spt5 homologs. *Genes Dev* **12**: 343-356

Werner M, Thuriaux P, & Soutourina J (2009) Structure–function analysis of RNA polymerases I and III. *Curr Opin Struct Biol* **19**: 740-745

Winkler M, aus dem Siepen T, & Stamminger T (2000) Functional Interaction between Pleiotropic Transactivator pUL69 of Human Cytomegalovirus and the Human Homolog of Yeast Chromatin Regulatory Protein SPT6. *J Virol* **74**: 8053-8064

Winston F, Chaleff DT, Valent B, & Fink GR (1984) MUTATIONS AFFECTING TY-MEDIATED EXPRESSION OF THE HIS4 GENE OF SACCHAROMYCES CEREVISIAE. *Genetics* **107**: 179-197

Wittmeyer J & Formosa T (1997) The Saccharomyces cerevisiae DNA polymerase alpha catalytic subunit interacts with Cdc68/Spt16 and with Pob3, a protein similar to an HMG1- like protein. *Mol Cell Biol* **17**: 4178-4190

Workman JL (2006b) Nucleosome displacement in transcription. *Genes Dev* **20**: 2009-2017

Wu C (1980) The 5' ends of Drosophila heat shock genes in chromatin are hypersensitive to DNase I. *Nature* **286**: 854-860

Wu C, Wong Y, & Elgin SCR (1979) The chromatin structure of specific genes: II. Disruption of chromatin structure during gene activity. *Cell,* **16**: 807-814

Wu S & Chiang C (2007) The Double Bromodomain-containing Chromatin Adaptor Brd4 and Transcriptional Regulation. *Journal of Biological Chemistry* **282**: 13141-13145

Xiao H & Lis JT (1989) Heat shock and developmental regulation of the Drosophila melanogaster hsp83 gene. *Mol Cell Biol* **9**: 1746-1753

Yao J, Munson KM, Webb WW, & Lis JT (2006) Dynamics of heat shock factor association with native gene loci in living cells. *Nature* **442**: 1050-1053

Yao J, Ardehali MB, Fecko CJ, Webb WW, & Lis JT (2007) Intranuclear Distribution and Local Dynamics of RNA Polymerase II during Transcription Activation. *Molecular Cell*, **28**: 978-990

Yoh SM, Cho H, Pickle L, Evans RM, & Jones KA (2007) The Spt6 SH2 domain binds Ser2-P RNAPII to direct Iws1-dependent mRNA splicing and export. *Genes Dev* **21**: 160-174

Yokoyama R, Pannuti A, Ling H, Smith ER, & Lucchesi JC (2007) A Plasmid Model System Shows that Drosophila Dosage Compensation Depends on the Global Acetylation of Histone H4 at Lysine 16 and Is Not Affected by Depletion of Common Transcription Elongation Chromatin Marks. *Mol Cell Biol* **27**: 7865-7870

Youdell ML, Kizer KO, Kisseleva-Romanova E, Fuchs SM, Duro E, Strahl BD, & Mellor J (2008) Roles for Ctk1 and Spt6 in regulating the different methylation states of histone H3 lysine 36. *Mol Cell Biol* **28**: 4915-4926

Zhang Z & Gilmour DS (2006) Pcf11 Is a Termination Factor in Drosophila that Dismantles the Elongation Complex by Bridging the CTD of RNA Polymerase II to the Nascent Transcript. *Molecular Cell*, **21**: 65-74

Zhao J, Herrera-Diaz J, & Gross DS (2005) Domain-Wide Displacement of Histones by Activated Heat Shock Factor Occurs Independently of Swi/Snf and Is Not Correlated with RNA Polymerase II Density. *Mol Cell Biol* **25**: 8985-8999